INFORMATION TO USERS

University of Alberta

Kinetics of the Catalytic Dehydration of 2-Propanol in an Aqueous Medium

By

Jean-Marc Rivard   ©

A thesis submitted to the Faculty of Graduate Studies and Research in partial fulfillment of the requirements for the degree of **Master of Science**

in

Chemical Engineering

Department of Chemical and Materials Engineering

Edmonton, Alberta

Fall 2000

University of Alberta

Library Release Form

Name of Author: Jean-Marc Rivard
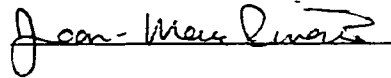
Title of Thesis: Kinetics of the Catalytic Dehydration of 2-Propanol in an Aqueous Medium

Degree: Master of Science

Year this Degree Granted: 2000

Jean-Marc Rivard

Department of Chemical and
         Materials Engineering
University of Alberta
Edmonton, Canada T6G 2G6

Date: Sept 21, 2000

Abstract

The liquid-phase catalytic dehydration of 2-propanol was investigated in a batch slurry reactor. Alumina, zeolite 13X, SAPO-5 and silicalite are all active in the liquid phase dehydration of 2-propanol at 463 K with silicalite being the most active catalyst. Propylene was found to be the major reaction product, with diisopropyl ether and acetone formed in trace amounts. The reaction kinetics over silicalite was determined at a temperature range of 434 – 463 K and at a concentration range of 4 – 10 mol % 2-propanol in water. A single site Langmuir-Hinshelwood-Hougen-Watson type mechanism was found to describe the kinetic data well. The rate equation was determined to be

$$r = k K_A C_A / (1 + K_A C_A + K_W C_W)$$

The activation energy over silicalite was determined to be 226.8 kJ/mol while the heat of adsorption model parameters for 2-propanol and water were -45.5 and -9.6 kJ/mol, respectively.

A simplified first order rate model was also found to describe the kinetic data well at low 2-propanol concentrations. An activation energy of 195.8 kJ/mol was determined over silicalite. For the purpose of designing an appropriate separation process for wastewater purification it is recommended that the simple first order model be used, due to its simplicity and accuracy at low 2-propanol concentrations.
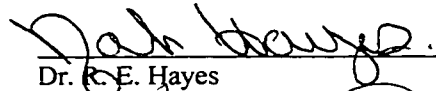
University of Alberta

Faculty of Graduate Studies and Research
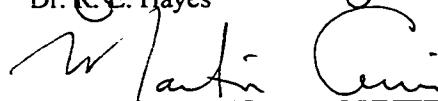
The undersigned certify that they have read, and recommend to the Faculty of Graduate Studies and Research for acceptance, a thesis entitled **Kinetics of the Catalytic Dehydration of 2-Propanol in an Aqueous Medium** submitted by **Jean-Marc Rivard** in partial fulfillment of the requirements for the degree of **Master of Science** in **Chemical Engineering**.

_____
Dr. K. T. Chuang (Supervisor)

_____
Dr. R. E. Hayes

_____
Dr. M. Cowie

Date: _Sept. 18, 2000_

Acknowledgements

The completion of this thesis would not have been possible without the gracious assistance of several fine individuals in this department. I would like to thank my supervisor Dr. Karl Chuang for his patience and encouragement throughout this work and for suggesting this very interesting project.

I would also like to thank Dr. Qinglin Zhang for his many invaluable suggestions, for his assistance in helping me write this thesis and for sharing his knowledge with me through many enlightening discussions.

I would like to thank Andrée Koenig for her assistance in the analytical aspects of this project. The outstanding work done by Walter Boddez and Richard Cooper of the instrument shop and Bob Scott and James McKinnon of the machine shop on the experimental apparatus is greatly appreciated.

I am extremely grateful for the generous financial assistance provided by the University of Alberta and the Natural Science and Engineering Research Council.

I would like to thank my fellow graduate students for providing a stimulating and enjoyable atmosphere during my stay here in Edmonton.

I will always be in debt to my parents, Roch and Lise Rivard for their love and support in whatever I chose to embark upon. They are without a doubt, the finest individuals I have ever met.

Table of Contents

List of Tables

List of Figures

Chapter 1

Introduction

The increased industrial usage of water in recent years has led to an increase in the volume of wastewater effluent [Terzis, 1994]. Wastewater from various industries, such as pharmaceutical, cosmetic, textile, and rubber contain aliphatic organic solvents which are often flammable, malodorous and potentially toxic to aquatic organisms [Henry et al., 1996]. 2-Propanol is a common organic solvent and its removal from wastewater is an important environmental issue.

Wastewater containing 2-propanol can be purified in many manners. Distillation, aerobic biological treatment [McKinney and Jeris, 1955; Hatfield, 1957; Ludzack and Ettinger, 1960] and anaerobic biological treatment [Hovious et al., 1973; Chou et al., 1978; Terzis, 1994; Henry et al., 1996] are known methods in purifying wastewater containing 2-propanol. These methods are not without their flaws. Distillation is very energy intensive and the 2-propanol/water separation may be complicated if the 2-propanol concentration of the wastewater approaches the azeotropic value. Biological treatment of wastewater may require further disinfection via chlorination to kill harmful bacteria. Although 2-propanol has not been found in the literature to be toxic to the microorganisms in biological treatment processes [Ludzack and Ettinger, 1960; Chou et al., 1978], it can be expected that a high concentration of 2-propanol in wastewater would be potentially harmful to the organisms.

It is known that 2-propanol can dehydrate in the presence of an acid catalyst to form propylene and water. In the literature, vapor-phase catalytic dehydration reactions are often carried out in plug-flow reactor systems with little or no water in the feed. The

1

use of a vapor-phase reactor to convert 2-propanol to propylene is expensive because of the large amount of energy required to vaporize the aqueous 2-propanol/water feed. For this reason, the reaction must be conducted in the liquid-phase. The liquid-phase dehydration of 2-propanol has potential application for wastewater purification where 2-propanol is present as an impurity.

Catalytic distillation is a potential separation process for wastewaters containing 2-propanol as an impurity. Making use of a solid acid catalyst, 2-propanol would dehydrate in the liquid-phase to form propylene and water. This process is potentially attractive because the propylene/water separation is much easier than the 2-propanol/water separation. To design such a process, the liquid-phase 2-propanol dehydration kinetics must first be determined. The development of the kinetic model is the focus of this thesis.

1.1 – 2-Propanol Dehydration

It is well known that alcohols can dehydrate in the presence of solid acid catalysts to form olefinic products [Pines and Manassen, 1966]. In the case of 2-propanol, the olefin produced is propylene

$$C_3H_8O\,(l) \leftrightarrow C_3H_6\,(g) + H_2O\,(l) \qquad\qquad K_{L,298} = 0.094 \qquad\qquad (1.1.1)$$

$$\Delta H^{\circ}_{f,\,298} = 52.6\ kJ\ mole^{-1}$$

Depending on the relative strength of the solid acid, the dehydration product can also include ether, in the case of 2-propanol dehydration the product is diisopropyl ether

$$C_3H_8O\,(l) \leftrightarrow \frac{1}{2}C_6H_{14}O\,(l) + \frac{1}{2}H_2O\,(l) \qquad K_{L,298} = 2.912 \qquad\qquad (1.1.2)$$
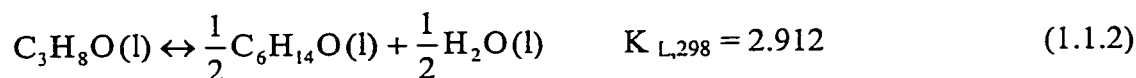
$$\Delta H^{\circ}_{f,\,298} = -0.5\ kJ\ mole^{-1}$$

If the basic sites are sufficiently strong, alcohol dehydrogenation can also occur. For the

case of 2-propanol, the dehydrogenation product is acetone

$$C_3H_8O\,(l) \leftrightarrow H_2\,(g) + C_3H_6O\,(l) \qquad K_{L,298} = 4.15 \times 10^{-5} \qquad (1.1.3)$$

$$\Delta H^{\circ}_{f,\,298} = 69.9 \text{ kJ mole}^{-1}$$

The vapor-phase dehydration of 2-propanol is widely used as a reaction to

qualitatively characterize the acidity of solid catalysts and to study the mechanism of the

catalytic dehydration of alcohols over solid acids [Jain and Pillai, 1968; Jacobs et al.,

1977; Gervasini and Auroux, 1991; Gervasini et al., 1997]. Gervasini and Auroux (1991)

concluded that the "number, the nature and the strength of the acid sites affect the

catalytic activity".

The vapor-phase dehydration of 2-propanol over a γ-alumina catalyst has been

proposed for propylene production [Fukuhara et al., 1991], although it is not a common

practice to do so.

Several solid acid catalysts have been reported to be active in the vapor phase

dehydration of 2-propanol. It is known that some metal oxide catalysts, such as alumina,

possess acidic properties, which are useful in dehydration reactions. Gamma alumina (γ-

Al_2O_3) is a solid acid known to be active in the vapor-phase dehydration of 2-propanol.

The acid-base properties of alumina and ion-exchanged alumina have been well studied

in the literature [Pines and Haag, 1960; Jain and Pillai, 1967; de Mougues et al., 1967;

Knözinger and Ratnasamy, 1978; Knözinger and Stübner, 1978; Luy and Parera, 1986;

Berteau et al., 1987; Auroux and Gervasini, 1990; Gervasini and Auroux, 1991; Mostafa

et al., 1991; de Canio et al., 1992; Saad et al., 1993; Gervasini et al., 1995; Shi and Davis,

1995; de Miguel et al., 1996; Gervasini et al., 1997; El-Hakam and El-Sharkawy, 1998].

3

There has been recent interest in the activity of alumina in reactions requiring strong acids. Solid acid catalysts, such as alumina, are known to be active in the chemical abatement of some chemical pollutants. A process has been proposed to use γ-alumina in ceramic filters for flue gas cleaning [Saracco and Montanaro, 1995; Saracco and Specchia, 1995a,b]. The use of ceramic as a porous filter allows for a high temperature to be used, as conventional polymer-based filter bags cannot withstand temperatures exceeding 200 °C. Once the filters are activated with a suitable catalyst (γ-Al_2O_3), the flue gas can be cleaned with a combined action of mechanical particulate removal and catalytic abatement of some chemical pollutants, such as nitrogen oxides and volatile organic compounds [Saracco and Montanaro, 1995].

Mixed oxides are often prepared to produce a material with properties superior to a linear combination of the constituents [Youssef et al., 1992]. Various mixed oxides have been found in the literature to be active in the vapor-phase 2-propanol dehydration. Some of these include mixed oxides of SnO_2 with P_2O_5 and V_2O_5 [Ai, 1975a,b], silica (SiO_2) with MgO and SnO_2 [Youssef et al., 1992; Salas et al., 1997], and MoO_3 with SnO_2, Fe_2O_3, P_2O_5, and TiO_2 [Ai and Suzuki, 1973; Tanabe et al., 1986; Bond et al., 1994]. A special series of mixed oxides containing alumina and silica (silica-aluminates) are known to be very active in the dehydration of 2-propanol [Youssef et al., 1990; López et al., 1992]. Their acidity and catalytic activity are related to the Al/Si ratio.

Recently, zeolites have been given attention because of their high activity in reactions involving strong acids. The vapor-phase dehydration of 2-propanol over various zeolite molecular sieves is discussed in the literature [Jacobs et al., 1977; Yue and Olaofe, 1984ab; Bezoukhanova and Kalvachev, 1994]. Other solid acids such as

4

aluminophosphates [Mishra et al., 1998; El-Sharkawy et al., 1999] and ion exchange

resins [Gottifredi et al., 1968] are also known to be active in the vapor-phase dehydration

of 2-propanol.

1.2 – Mechanism of 2-Propanol Dehydration over Solid Acid Catalysts

1.2.1   – Alumina

The mechanism of alcohol dehydration over a solid acid catalyst was first studied

using active alumina [Pines and Manassen, 1966; Jain and Pillai, 1967]. Alumina is

known to be active in reactions requiring strong acids, such as hydrocarbon cracking and

alcohol dehydration. Amphoteric oxides, such as alumina, have a balanced strength of

acid and basic sites [Gervasini et al., 1997]. There has been considerable debate upon the

nature of these acid and basic sites. The general consensus is that the active sites on

alumina consists of electron pair donors (Lewis bases) and electron pair acceptors (Lewis

acids). Using FT-IR spectroscopy of adsorbed pyridine, Berteau and co-workers (1991)

found no Brønsted-acid sites on alumina and modified aluminas. Knözinger and Kaerlein

(1971) previously concluded that alumina surfaces do not develop Brønsted acidity at

temperatures up to 300 °C which are strong enough to protonate pyridine.

The formation of Lewis acidity on the dehydrated surface of alumina was

postulated by a model suggested by Hindin and Weller (1956).
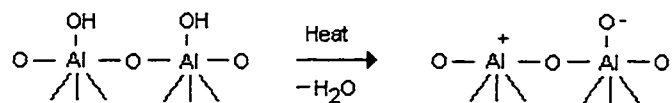
$$(1.1.4)$$

The resulting structure contains coordinately unsaturated aluminum atoms.

An E_2 type mechanism has been proposed for 2-propanol dehydration over alumina to form propylene [Krylov, 1965 ab; Fikis et al., 1978; de Miguel et al., 1996; Gervasini et al., 1996]. The acid site induces the abstraction of the hydroxyl group and the basic site induces the abstraction of the β-hydrogen. Figure 1.1 illustrates the E_2 dehydration mechanism for olefin formation, where S_1 and S_2 represent the basic and acidic sites respectively.

1.2.2 – Silica-Alumina

Silica-alumina is a mixed metal oxide catalyst commonly used in alcohol dehydration reactions. On pure alumina, the Lewis-acid site consists of an aluminum atom which is incompletely coordinated (electron pair acceptor). Unlike pure aluminas, both Brønsted and Lewis acids occur on silica-aluminas because of the isomorphous substitution of tetravalent silicon by trivalent aluminium in the silica lattice [Berteau et al., 1991]. The aluminum atom, which is normally hexacoordinated, is forced to adopt a tetracoordinated structure. The aluminum atom in the silica-alumina lattice behaves as a Lewis acid in the absence of water and as a Brønsted acid in the presence of water. It is generally accepted that silica-aluminas contain both Brønsted and Lewis acid sites [Basila et al., 1964; Fripiat et al., 1965; Luy and Parera, 1986]. Brønsted acidity is believed to be responsible for the catalytic activity of silica-alumina [Thomas, 1949], hence it has been proposed that 2-propanol dehydrates via an E_1 type mechanism [Luy and Parera, 1986]. Unlike the E_2 mechanism, which requires both acid and basic sites, the E_1 mechanism only requires acids and involves a carbenium intermediate. This carbenium cation is later transformed to an olefin by proton abstraction. This mechanism
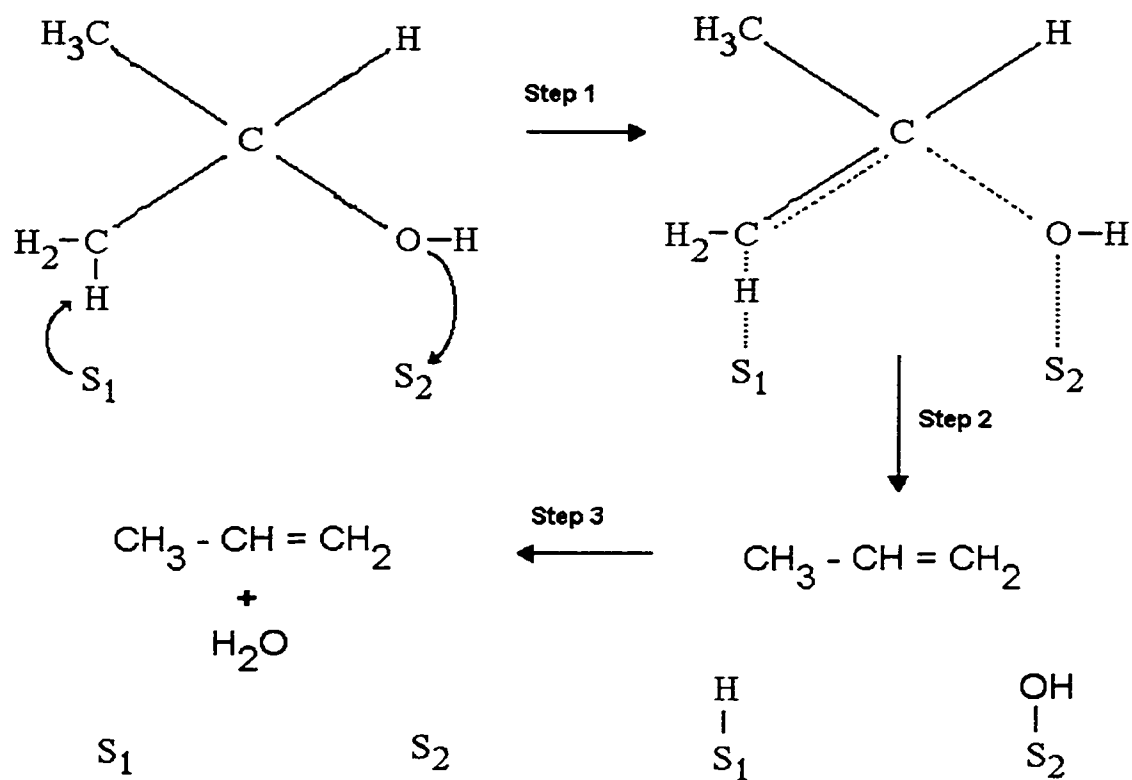
Figure 1.1 – E$_2$ Mechanism for 2-Propanol Dehydration (S$_1$ = Lewis Basic Site, S$_2$ = Lewis Acid Site): Fikis, D. V., W. J. Murphy and R. A. Ross, *Can. J. Chem.* **56**, 2530-2537 (1978)

is illustrated in Figure 1.2. A more detailed explanation of E_1 and E_2 mechanisms can be found in the literature [Lowry and Richardson, 1981].

1.2.3 – Zeolites – HZSM-5 Substitutional Series

Zeolites are a class of hydrated aluminum silicates consisting of a 3D network of –Al-O-Si- atoms in the form of linked tetrahedra [Tanabe, 1970]. They differ from silica-aluminas in terms of their crystal structure and acidity. There is evidence to suggest that zeolites, notably H-ZSM-5, act as Brønsted acids [Anderson et al., 1980; Bolis et al., 1980]. Gorte and co-workers confirmed the Brønsted acidity of ZSM-5 zeolites by the characterization of 2-propanol adsorption by temperature programmed desorption (TPD), thermogravimetric analysis (TGA) and transmission infrared spectroscopy [Grady and Gorte, 1985; Aronson et al., 1986;1987].

The structural aluminum atoms responsible for the Brønsted acidity of H-ZSM-5 zeolites are very dilute, due to the zeolite's highly siliceous nature. This dilution causes the active sites to be similar in nature [Grady and Gorte, 1985] as illustrated in the linear increase in hexane cracking with aluminum content [Olson et al., 1980]. Despite the dilute concentration of acid sites on H-ZSM-5 zeolites, the sites themselves are strong and are active in reactions requiring strong acids, such as catalytic cracking. It has been proposed that alcohols dehydrate to propylene over zeolites via an E_1 mechanism [Jacobs et al., 1977]. 2-Propanol can also dehydrate over zeolites to form diisopropyl ether, although both acid and basic sites are involved in the mechanism.

1.2.4 – Silicoaluminophosphates

Silicon and aluminum in the zeolite framework can be isomorphously substituted by elements such as gallium, cerium, beryllium, boron, iron, phosphorus, and magnesium
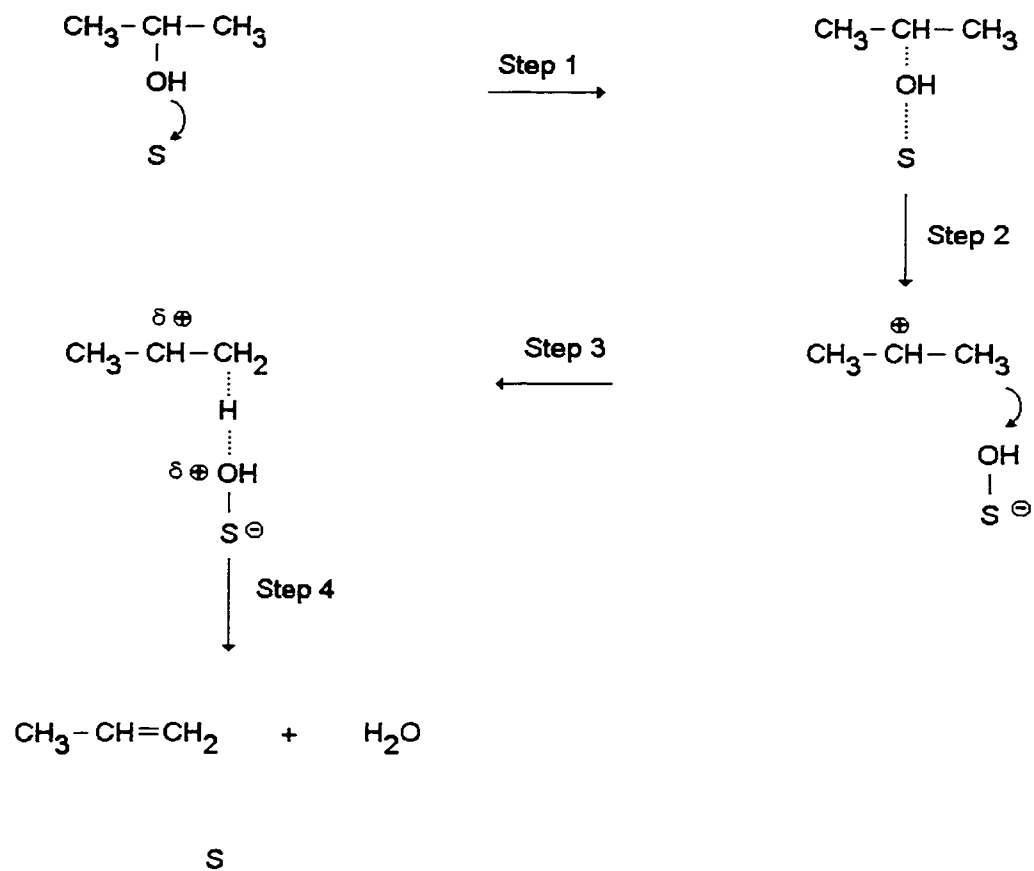
Figure 1.2 – E$_1$ Mechanism for 2-Propanol Dehydration (S = Brønsted Acid Site, H$^+$): de Miguel, S. R., A. C. Martinez, A. A. Castro, and O. A. Scelza, *J. Chem. Tech. Biotechnol.* **65**, 131-136 (1996)

[Chu and Chang, 1985]. Much attention has been drawn to the introduction of pentavalent phosphorus in the zeolite lattice [Bezoukhanova and Kalvachev, 1994]. Aluminophosphates (AlPO) and silicoaluminophosphates (SAPO) have been synthesized in this manner [Wilson et al., 1982; Lok et al., 1984]. These molecular sieves have been classified by x-ray and neutron diffraction [Flanigen et al., 1988].

Silicoaluminophosphates are produced by a replacement of the pentavalent phosphorus by tetravalent silicon [Bezoukhanova and Kalvachev, 1994]. Based on the IR spectra of cyclohexanol on SAPO-5, SAPO-11 and SAPO-31, it has been concluded that Brønsted acid sites and hydrogen-accepting sites (probably basic in character) exist in SAPO molecular sieves which is similar to what was found for H-ZSM-5 zeolites [Bezoukhanova et al., 1991]. The acidity and activity of SAPO molecular sieves are related to the (Al + P)/Si ratio. Unlike H-ZSM-5 molecular sieves, a simple relation between activity and the (Al + P)/Si ratio is not known.

1.2.5 – Ion Exchange Resins

Macroporous cation exchange resins, such as Amberlyst 15 have recently found use in the synthesis of MTBE [Subramaniam and Bhatia, 1987; Izquierdo et al., 1992; Nicolaides et al., 1993]. These resins are a polymeric three-dimensional cross-linked structure obtained by the sulphonation of a copolymer made of polystyrene and divinyl benzene. The reaction mechanism for alcohol dehydration is strongly dependent on the concentration of water as was determined from the vapor-phase dehydration of methanol, tertiary butyl alcohol and 2-propanol [Gates and Rodriguez, 1973; Thornton and Gates, 1974]. There is a transition from catalysis by bound $-SO_3H$ groups to hydrated protons

in the polymer matrix upon addition of water. The catalytic activity is proportional to the proton concentration.

The main problem with the use of polymer ion exchange resins is that they are very sensitive to temperature and lose their activity at temperatures exceeding 393 K. Current work is being performed to develop catalysts that are more thermally stable [Beasly and Jokovac, 1984; Helfferich and Hwang, 1988].

1.3 – Problem Definition

To design a process for a 2-propanol/water separation, kinetic data for 2-propanol dehydration in an aqueous media are essential. Although the vapor-phase dehydration of 2-propanol has been well studied, there exists no information in the literature on the liquid-phase dehydration of 2-propanol. Furthermore, the influence of a high concentration of water on the rate of 2-propanol dehydration is not well understood.

In this study, the performance of several well-known acid catalysts including alumina, zeolite 13X, SAPO-5 and silicalite (similar to H-ZSM-5 in structure) were evaluated with an initial 2-propanol concentration of 10 mol % at 463 K in a batch slurry reactor. The kinetic study was carried out at temperatures ranging from 434 to 463 K and initial 2-propanol concentrations of 4 – 10 mol %. The kinetic equation was derived based on a Langmuir-Hinshelwood-Hougen-Watson (LHHW) type reaction mechanism. The LHHW method of generating rate models is based on Langmuir adsorption and is often used in developing rate models for heterogeneous catalytic reactions. LHHW models have been used in developing rate equations for the catalytic vapor-phase 2-propanol dehydration [Jacobs et al., 1977; Yue and Olaofe, 1984a; Hamzaoui and Batis, 1992].

1.4 – Nomenclature

ΔH^o_f = heat of formation, kJ mole^{-1}

K = chemical equilibrium constant

Subscripts

298 = at 298 K

L = liquid

1.5 – Literature Cited

Ai, M. and S. Suzuki, "Oxidation Activity and Acidity of MoO_3-P_2O_5 Catalysts", *J. Catal.* **30**, 362-371 (1973)

Ai, M., "The Oxidation Activity and Acid-Base Properties of SnO_2-Based Binary Catalysts I. The SnO_2-V_2O_5 System", *J. Catal.* **40**, 318-326 (1975a)

Ai, M., "The Oxidation Activity and Acid-Base Properties of SnO_2-Based Binary Catalysts II. The SnO_2-MoO_3 and SnO_2-P_2O_5 Systems", *J. Catal.* **40**, 327-333 (1975b)

Anderson, J. R., T. Mole and V. Christov, "Mechanism of Some Conversions over ZSM-5 Catalyst", *J. Catal.* **61**, 477-484 (1980)

Aronson, M. T., R. J. Gorte and W. E. Farneth, "The Influence of Oxonium Ion and Carbenium Ion Stabilities on the Alcohol/H-ZSM-5 Interaction", *J. Catal.* **98**, 434-443 (1986)

Aronson, M. T., R. J. Gorte and W. E. Farneth, "An Infrared Spectroscopy Study of Simple Alcohols Adsorbed on H-ZSM-5", *J. Catal.* **105**, 455-468 (1987)

Auroux, A. and A. Gervasini, "Microcalorimetric Study of the Acidity and Basicity of Metal Oxide Surfaces", *J. Phys. Chem.* **94**, 6371-6379 (1990)

Basila, M. R., T. R. Kantner and K. H. Rhee, "The Nature of the Acidic Sites on a Silica-Alumina. Characterization by Infrared Spectroscopic Studies on Trimethylamine and Pyridine Chemisorption", *J. Phys. Chem.* **68**, 3107-3207 (1964)

Beasley, G. H. and I. J. Jakovac, "Ion Exchange Resin Catalysts Having Improved Catalytic Activity and Enhanced Thermal Stability", in *Ion Exchange Technology* (B. Naden and M. Streat eds.), Chichester, West Sussex, p. 441 (1984)

Berteau, P., B. Delmon, J-L. Dallons, and A. Van Gysel, "Acid-Base Properties of Silica-Aluminas: Use of 1-Butanol Dehydration as a Test Reaction", *Appl. Catal.* **70**, 307-323 (1991)

Berteau, P., M. Ruwet and B. Delmon, "1-Butanol Dehydration on Aluminas and Modified Aluminas. Evolution of Activity and Selectivity", *Acta Chem. Hung.* **124 (1)**, 25-33 (1987)

Bezoukhanova, C. P. and Y. A. Kalvachev, "Alcohol Reactivity on Zeolites and Molecular Sieves", *Catal. Rev. –Sci. Eng.* **36(1)**, 125-143 (1994)

Bezoukhanova, C. P., Y. A. Kalvachev and H. Lechert, "Infrared Study of Cyclohexanol Chemisorption in SAPO Molecular Sieves", *J. Chem. Soc. Faraday Trans.* **87**(19), 3315-3317 (1991)

Bolis, V., J. C. Vedrine, J. P. Van de Berg, J. P. Wolthuizen, and E. G. Debrouane, "Adsorption and Activation of Ethene by Zeolite-H-ZSM-5", *J. Chem. Soc., Faraday Trans. 1* **76**, 1606-1616 (1980)

Bond, G. C., S. A. Halawy, K. M. A. El-Salaam, E. A. Hassan, and H. M. Ragih, "MoO$_3$-Fe$_2$O$_3$ Catalysts : Characterization and Activity for Isopropyl Alcohol Decomposition", *J. Chem. Tech. Biotechnol.* **59**, 181-191 (1994)

Chou, W. L., R. E. Speece, R. H. Siddiqi, and K. McKeon, "The Effect of Petrochemical Structure on Methane Fermentation Toxicity", *Prog. Wat. Tech.* **10**, 545-558 (1978)

Chu, C. T-W. and C. D. Chang, "Isomorphous Substitution in Zeolite Frameworks. 1. Acidity of Surface Hydroxyls in [B]-, [Fe]-, [Ga]-, and [Al]-ZSM-5", *J. Phys. Chem.* **89**, 1569-1571 (1985)

de Canio, E. C., V. P. Nero and J. W. Bruno, "Identification of Alcohol Adsorption Sites on γ-Alumina", *J. Catal.* **135**, 444-457 (1992)

de Miguel, S. R., A. C. Martinez, A. A. Castro, and O. A. Scelza, "Effect of Lithium Addition upon γ-Al$_2$O$_3$ for Isopropanol Dehydration", *J. Chem. Tech. Biotechnol.* **65**, 131-136 (1996)

de Mourgues, I., F. Peyron, Y. Trambouze, and M. Prettre, "Kinetics of the Catalytic Dehydration of 2-Propanol", *J. Catal.* **7**, 117-125 (1967)

El-Hakam, S. A. and E. A. El-Sharkawy, "Structural Characterization and Catalytic Properties of Aluminum Borates-Alumina Catalysts", *Mat. Letters* **36**, 167-173 (1998)

El-Sharkawy, E. A., M. R. Mostafa and A. M. Youssef, "Changes in Surface and Catalytic Dehydration Activities of 2-Propanol on AlPO-5 Induced by Silver Impregnation", *Colloids Surf. A.* **157**, 211-218 (1999)

Fikis, D. V., W. J. Murphy and R. A. Ross, "The Formation of Propane, Propylene, and Acetone from 2-Propanol over Vanadium Pentoxide and Modified Vanadium Pentoxide Catalysts", *Can. J. Chem.* **56**, 2530-2537 (1978)

Flanigen, E. M., R. L. Patton and S. T. Wilson, "Structural, Synthetic and Physicochemical Concepts in Aluminophosphate-Based Molecular Sieves", in *Innovations in Zeolite Materials Science* (P. J. Grobet et al., eds.), Stud. Surf. Sci. Catal., Vol. 37, Elsevier, Amsterdam, p. 13. (1988)

Fripiat, J. J., A. Léonard and J. B. Uytterhoeven, "Structure and Properties of Amorphous Silicoaluminas. II. Lewis and Brønsted Acid Sites", *J. Phys. Chem.* **69**, 3274-3279 (1965)

Fukuhara, H., W. Matsanaga, M. Yasuhara, S. Araki, and T. Isaka, "Preparation of Propylene by Dehydration of Isopropanol in the Presence of a Pseudo-Bohemite Derived Gamma Alumina Catalyst", U.S. Pat. 5,227,563 (1991)

Gates, B. C. and W. Rodriguez, "General and Specific Acid Catalysts in Sulfonic Acid Resin", *J. Catal.* **31**, 27-31 (1973)

Gervasini, A. and A. Auroux, "Acidity and Basicity of Metal Oxide Surfaces. II. Determination by Catalytic Decomposition of Isopropanol", *J. Catal.* **131**, 190-198 (1991)

Gervasini, A., G. Bellussi, J. Fenyvesi, and A. Auroux, "Microcalorimetric and Catalytic Studies of the Acidic Character of Modified Metal Oxide Surfaces. 1. Doping Ions on Alumina, Magnesia, and Silica", *J. Phys. Chem.* **99**, 5117-5125 (1995)

Gervasini, A., J. Fenyvesi and A. Auroux, "Study of the Acidic Character of Modified Metal Oxide Surfaces Using the Test of Isopropanol Decomposition", *Cat. Letters* **43**, 219-228 (1997)

Gottifredi, J. C., A. A. Yeramian and R. E. Cunningham, "Vapor-Phase Reactions Catalyzed by Ion Exchange Resins I. Isopropanol Dehydration", *J. Catal.* **12**, 245-256 (1968)

Grady, M. C. and R. J. Gorte, "Adsorption of 2-Propanol and Propene on H-ZSM-5: Evidence for Stable Carbenium Ion Formation", *J. Phys. Chem.* **89**, 1305-1308 (1985)

Hamzaoui, H. and H. Batis, "Propriétés Physico-Chimiques des Phosphates de Zirconium. II. Cinétique de Déshydratation de L'Isopropanol en Propène", *J. Chim. Phys.* **89**, 111-122 (1992)

Hatfield, R., "Biological Oxidation of Some Organic Compounds", *Ind. Eng. Chem.* **49**, 192-196 (1957)

Helfferich, F. G. and Y-L. Hwang, "Ion Exchangers as Catalysts", in *Ion Exchange for Industry* (M. Streat ed.), Chichester, New York, p. 585 (1988)

Henry, M. P., B. A. Donlon, P. N. Lens, and E. M. Colleran, "Use of Anaerobic Hybrid Reactors for Treatment of Synthetic Pharmaceutical Wastewaters Containing Organic Solvents", *J. Chem .Tech. Biotechnol.* **66**, 251-264 (1996)

Hindin, S. G. and S. W. Weller, *J. Phys. Chem* **60**, 1501 (1956)

Hovious, J. C., R. A. Conway and C. W. Ganze, "Anaerobic Lagoon Pretreatment of Petrochemical Wastes", *J. Wat. Pollut. Control Fed.* **45**, 71-84 (1973)

Izqulerdo, J. F., F. Cunill, M. Vila, J. Tejero, and M. Iborra, "Equilibrium Constants for Methyl *tert*-Butyl Ether Liquid-Phase Synthesis", *J. Chem. Eng. Data* **37**, 339-343 (1992)

Jacobs, P. A., M. Tielen and J. B. Uytterhoeven, "Active Sites in Zeolites. Part 6. Alcohol Dehydration over Alkali Cation-Exchanged X and Y Zeolites", *J. Catal.* **50**, 98-108 (1977)

Jain, J. R. and C. N. Pillai, "Catalytic Dehydration of Alcohols over Alumina. Mechanism of Ether Formation", *J. Catal.* **9**, 322-330 (1967)

Knözinger, H. and B. Stübner, "Adsorption of Alcohols on Alumina 1. Gravimetric and Infrared Spectroscopic Investigation", *J. Phys. Chem.* **82**, 1526-1532 (1978)

Knözinger, H. and C-P. Kaerlein, "A Test for the Development of Protonic Acidity in Alumina at Elevated Temperatures", *J. Catal.* **24**, 436-438 (1971)

Knözinger, H. and P. Ratnasamy, "Catalytic Aluminas : Surface Models and Characterization of Surface Sites", *Catal. Rev. –Sci. Eng.* **17(1)**, 31-70 (1978)

Krylov, O. V., "Mechanism of the Dehydration of Alcohols", *Russ. J. Phys. Chem.* **39**, 1422 (1965a)

Krylov, O. V., "Mechanism of the Dehydrogenation of Alcohols", *Russ. J. Phys. Chem.* **39**, 1554 (1965b)

Lok, B. M., C. A. Messina, R. L. Patton, R. T. Gajek, T. R. Cannan, and E. M. Flanigen, "Silicoaluminophosphate Molecular Sieves: Another New Class of Microporous Crystalline Inorganic Solids", *J. Am. Chem. Soc.* **106**, 6092-6093 (1984)

López, T., M. Asomoza and R. Gómez, "Catalytic Properties of Silico-Aluminates Prepared by the Sol-Gel Method : Isopropanol Dehydration", *J. Non-Cryst. Solids* **147-148**, 769-772 (1992)

Lowry, T. H. and K. S. Richardson, "Mechanism and Theory in Organic Chemistry", 2nd. Ed.. p. 531-542. Harper & Row, New York (1981)

Ludzack, F. J. and M. B. Ettinger, "Chemical Structures Resistant to Aerobic Biochemical Stabilization", *J. Wat. Pollut. Control Fed.* **32**, 1173-1200 (1960)

Luy, J. C. and J. M. Parera, "Acidity Control in Alcohol Dehydration", *Appl. Catal.* **26**, 295-304 (1986)

McKinney, R. E. and J. S. Jeris, "Metabolism of Low Molecular Weight Alcohols by Activated Sludge", *Sewage and Ind. Wastes*, **27**, 728-735 (1955)

Mishra, T., K. M. Parida and S. B. Rao, "Transition Metal Promoted $AlPO_4$ Catalyst 2. The Catalytic Activity of $M_{0.05}Al_{0.95}PO_4$ for Alcohol Conversion and Cumene Cracking/Dehydrogenation Reactions", *Appl. Catal. A.* **166**, 115-122 (1998)

Mostafa, M. R., A. M. Youssef and S. M. Hassan, "Conversion of Ethanol and Isopropanol on Alumina, Titania and Alumina-Titania Catalysts", *Mat. Letters* **12**, 207-213 (1991)

Nicolaides, C. P., C. J. Stotijn, E. R. A. van der Veen, and M. S. Visser, "Conversion of Methanol and Isobutanol to MTBE", *Appl. Catal.* **103**, 223-232 (1993)

Olson, D. H., W. O Haag and R. M. Lago, "Chemical and Physical Properties of the ZSM-5 Substitutional Series", *J. Catal.* **61**, 390-396 (1980)

Pines, H. and J. Manassen, "The Mechanism of Dehydration of Alcohols over Alumina Catalysts", *Advan. Catal.* **16**, 49-93 (1966)

Pines, H. and W. O. Haag, "Alumina : Catalyst and Support. IX. The Alumina Catalyzed Dehydration of Alcohols", *J. Am. Chem. Soc.* **83**, 2847-2852 (1961)

Saad, A. B. M., V. A. Ivanov, J. C. Lavalley, P. Nortier, and F. Luck, "Comparative Study of the Effects of Sodium Impurity and Amorphisation on the Lewis Acidity of γ-Alumina", *Appl. Catal. A.* **94**, 71-83 (1993)

Salas, P., J. G. Hernández, J. A. Montoya, J. Navarrete, J. Salmones, I. Schifter, and J. Morales, "Effect of Tin Content on Silica Mixed Oxides : Sulfated and Unsulfated Catalysts", *J. Mol. Catal. A.* **123**, 149-154 (1997)

Saracco, G. and L. Montanaro, "Catalytic Ceramic Filters for Flue Gas Cleaning. 1. Preparation and Characterization", *Ind. Eng. Chem. Res.* **34**, 1471-1479 (1995)

Saracco, G. and V. Specchia, "Catalytic Ceramic Filters for Flue Gas Cleaning. 2. Performance and Modeling Thereof", *Ind. Eng. Chem. Res.* **34**, 1480-1487 (1995a)

Saracco, G. and V. Specchia, "Studies on Sol-Gel Derived Catalytic Filters", *Chem. Eng. Sci.* **50**, 3385-3394 (1995b)

Shi, B. and B. H. Davis, "Alcohol Dehydration : Mechanism of Ether Formation using an Alumina Catalyst", *J. Catal.* **157**, 359-367 (1995)

Subramainam, C. and S. Bhatia, "Liquid Phase Synthesis of Methyl *tert*-Butyl Ether Catalyzed by Ion Exchange Resin", *Can. J. Chem. Eng.* **65**, 613-620 (1987)

Tanabe, K., "Solid Acids and Bases", Chap. 4. Kodansha, Tokyo and Academic Press, New York (1970)

Tanabe, K., H. Hattori, T. Yamaguchi, T. Iizuka, H. Matsuhashi, A. Kimura, and Y. Nagase, "Function of Metal Oxide and Complex Oxide Catalysts for Hydrocracking of Coal", *Fluid Proc. Technol.* **14**, 247-260 (1986)

Terzis, E., "Anaerobic Treatment of Industrial Wastewater Containing Organic Solvents", *Wat. Sci. Tech.* **29**, 321-329 (1994)

Thomas, C. L., "Chemistry of Cracking Catalysts", *Ind. Eng. Chem.* **41**, 2564-2572 (1949)

Thornton, R. and B. C. Gates, "Catalysis by Matrix-Bound Sulfonic Acid Groups: Olefin and Paraffin Formation from Butyl Alcohols", *J. Catal.* **34**, 275-287 (1974)

Wilson, S. T., B. M. Lok, C. A. Messina, T. R. Cannan, and E. M. Flanigen, "Aluminophosphate Molecular Sieves: A New Class of Microporous Crystalline Inorganic Solids", *J. Am. Chem. Soc.* **104**, 1146-1147 (1982)

Youssef, A. M., A. I. Ahmed and S. E. Samra, "Surface and Acidic Properties of Some Mixed Oxide Catalysts in Relation to Their Catalytic Activities", *Mat. Letters* **10**, 175-180 (1990)

Youssef, A. M., I. B. Khalil and B. S. Girgis, "Decomposition of Isopropanol on Magnesium Oxide/Silica in Relation to Texture, Acidity and Chemical Composition", *Appl. Catal. A*, **81**, 1-13 (1992)

Yue, P. L. and O. Olaofe, "Kinetic Analysis of the Catalytic Dehydration of Alcohols over Zeolites", *Chem. Eng. Res. Des*. **62**, 81-91 (1984a)

Yue, P. L. and O. Olaofe, "Molecular Sieving Effects of Zeolites in the Dehydration of Alcohols", *Chem. Eng. Res. Des*. **62**, 167-172 (1984b)

Chapter 2

Experimental

2.1 – Experimental Apparatus

All experimental runs were conducted in a batch slurry reactor system (Figure 2.1). The reactor was a high pressure Parr reactor (Model 4841, Parr Instruments Inc. USA) made of SS-316 stainless steel. The vessel had a volume of 320 mL and was equipped with an impeller. A thermocouple (J-type) was used to measure the reactor temperature and provide feedback to the heater/controller. The heating device/controller was used to maintain a constant reactor temperature within ± 1 K. The liquid sampling line consisted of a 1/8-inch o.d. stainless steel tube connected to a stainless steel sampling valve. A pressure transducer (Foxboro electronic transmitter, Model 841 GM-D) measured the reactor pressure at an accuracy of ± 6.89 kPa.

2.2 – Analysis Techniques and Experimental Procedure

The liquid samples were analyzed using a Hewlett Packard 5890 Series II Gas Chromatograph with a TCD detector. A 0.914 m long column with Poropak R packing (mesh 50-80) was used to separate 2-propanol, water, diisopropyl ether, and acetone. Despite the formation of propylene as a dehydration product, propylene was not analyzed in the liquid-phase by gas chromatography due to its low solubility in 2-propanol. The column temperature was kept constant at 423 K.

During the kinetic runs, a known amount of 2-propanol (analytical grade, BDH), deionized water and dried catalyst were fed to the reactor. The 2-propanol/water mixture corresponds to a 2-propanol concentration between 4 – 10 mol %. This concentration range was chosen to represent the concentrations one might expect to find in a typical
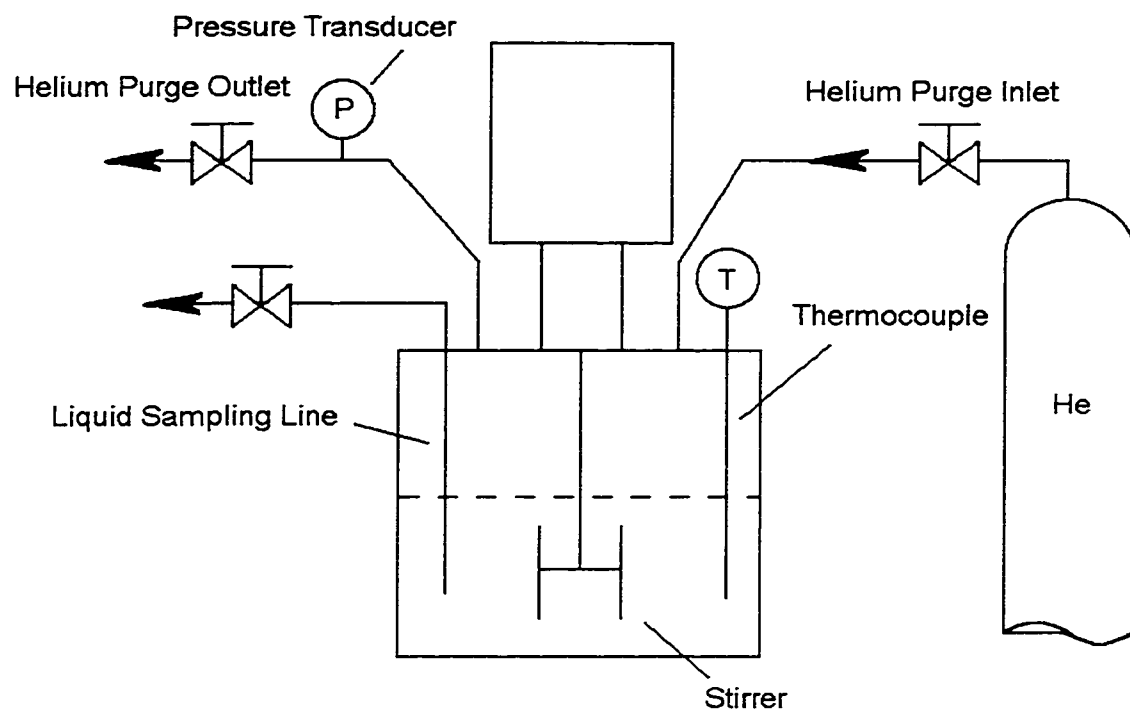
Figure 2.1 – Experimental Setup

wastewater stream, where 2-propanol will be present in low concentrations. Typically, 150 mL of the 2-propanol/water mixture was added to the reactor so that approximately one half of the vessel was initially filled with the liquid. The liquid expands at high temperatures, hence room must be allocated in the vessel for this expansion.

The reactor was then purged with helium to remove air that might be present initially in the reactor. Despite the fact that the catalytic reaction only occurs in the liquid phase, we wish to minimize any possible reactions of the olefin product with air at high-temperatures. For this reason, helium was used to provide an inert atmosphere.

The inlet and outlet of the reactor were then closed. The amount of helium initially present in the reactor prior to heating can be determined based on the initial reactor temperature, pressure and vapor volume. The amount (moles) of helium initially present in the reactor is necessary in performing the material balance on the reactor in determining the reaction rate (see Chapter 3).

The reactor contents were then heated to the desired reaction temperature, between 434 and 463 K. It will be later shown (Chapter 4, section 4.2) that there is a negligible amount of reaction product produced during the heating time. This temperature range was chosen for three reasons. First, 434 K appears to be the minimum temperature at which there is a noticeable amount of propylene produced in a reasonable time period (1.5 hours). Second, because accurate pressure measurements are essential in the determination of the reaction rate (Chapter 3), we are limited to reactor pressures less than 4238 kPa, the range of accuracy of the pressure transducer. For this reason, a maximum temperature of 463 K was chosen so that this maximum pressure was not exceeded. Finally, the liquid-phase catalytic reaction may not be industrially feasible at

temperatures exceeding 463 K due to the high pressure required to liquefy most of the reactants.

The reactor contents were stirred at 1080 rpm for 1.5 to 2.5 hours. The stirrer speed was chosen to minimize the influence of external mass transfer, which will be later discussed (Chapter 4, section 4.3). During the catalyst screening tests, a small sample of liquid (~ 1 mL) was taken every half-hour and analyzed by gas chromatography.

Chapter 3

Kinetic Modeling

3.1 – Determination of the Rate of Formation of Propylene

The rate of propylene formation per gram of catalyst in a batch slurry reactor can be written in the following manner:

$$r = \frac{1}{m_C}\frac{d\alpha}{dt} = f(C_A, C_W, T) \tag{3.1.1}$$

where α is the cumulative amount of propylene produced, m_C is the mass of catalyst, C_A is the liquid-phase 2-propanol concentration and C_W is the liquid-phase water concentration.

The batch slurry reactor consists of a liquid phase, where 2-propanol reacts over the suspended solid catalyst to form dehydration products and a vapor phase, where the reactants, products and inerts will be present. Since the dehydration occurs only in the liquid phase, 2-propanol, water and product propylene can be assumed to be at their vapor-liquid equilibrium at any given reaction time, t.

If the vapor and liquid phases are in equilibrium, the liquid and vapor phase fugacity of component, i, are equal:

$$\hat{f_i^V} = \hat{f_i^L} \tag{3.1.2}$$

Theoretically, the above equation can be solved by the use of an equation of state. However, the use of a single equation of state to calculate the vapor-liquid equilibria is reserved for highly ideal systems containing nonpolar compounds. For non-ideal systems such as alcohol/water systems, a "dual method" is often used to compute the phase equilibria. An equation of state is used to model the vapor phase where non-idealities are

not severe and an excess Gibbs free energy model along with vapor-pressure data is used to compute the liquid phase fugacity. The liquid and vapor phase fugacities in equation 3.1.2 can be rewritten in terms of total pressure, P, and the fugacity coefficient, ϕ as

$$\hat{f}_i^V = f_i^{0V} y_i \tag{3.1.3}$$

and

$$\hat{f}_i^L = f_i^{0L} \gamma_i x_i \tag{3.1.4}$$

where

$$\phi_i^0 = \frac{f_i^0}{P} \tag{3.1.5}$$

Equation 3.1.3 – 3.1.5 can be substituted into equation 3.1.2 to yield the following relationship for the vapor-liquid equilibrium for a component i:

$$P\phi_i^V y_i = P\phi_i^{0L} \gamma_i x_i \tag{3.1.6}$$

As the total pressure approaches zero, the vapor-phase fugacity coefficient ϕ_i^V approaches 1 and the value of $P\phi_i^{0L}$ approaches the saturation vapor pressure P_i^{SAT}. At low pressures, equation 3.1.6 simplifies to:

$$P y_i = P_i^{SAT} \gamma_i x_i \tag{3.1.7}$$

A modified Peng-Robinson equation of state (PRSV), developed by Stryjek and Vera (1986) is able to reproduce vapor pressures of nonpolar, polar or associating compounds by calculating the product $P\phi_i^{0L}$. The authors report a reproducibility of vapor pressures down to 1.5 kPa, which is comparable to what can be calculated from Antoine equations. For this reason, the PRSV equation of state was used in calculating the liquid-phase fugacity coefficient for a pure component ϕ_i^{0L}. In general, most cubic

equations of state are considered to be able to reasonably describe the vapor-phase. For this reason the PRSV equation of state was used to calculate the vapor-phase fugacity coefficient for a component in a gas mixture ϕ_i^V.

The Peng-Robinson equation of state [Peng and Robinson, 1976] is of the form:

$$P = \frac{RT}{v-b} - \frac{a}{v^2 + 2bv - b^2} \tag{3.1.8}$$

with

$$a = \left(0.457235R^2 T_C^2 / P_C\right)\alpha \tag{3.1.9}$$

and

$$b = 0.077796R\, T_C / P_C \tag{3.1.10}$$

The form proposed by Soave (1972) was used in determining α.

$$\alpha = \left[1 + \kappa\left(1 - T_R^{0.5}\right)\right]^2 \tag{3.1.11}$$

In the PRSV equation of state, the model parameter κ is considered to be a function of the accentric factor ω and temperature:

$$\kappa = \kappa_0 + \kappa_1\left(1 + T_R^{0.5}\right)\!\left(0.7 - T_R\right) \tag{3.1.12}$$

with

$$\kappa_0 = 0.378893 + 1.4897153\omega - 0.17131848\omega^2 + 0.0196554\omega^3 \tag{3.1.13}$$

Table 3.1 gives the values of T_C, P_C, ω and κ_1 for water, 2-propanol, propylene and helium.

For computational convenience, equation 3.1.8 can be rewritten in terms of the compressibility factor Z [Kyle, 1992]:

$$Z^3 + (B-1)Z^2 + (A - 3B^2 - 2B)Z + (B^3 + B^2 - AB) = 0 \qquad (3.1.14)$$

with

$$A = Pa/(RT)^2 \qquad (3.1.15)$$

and

$$B = Pb/RT \qquad (3.1.16)$$

For a gas-mixture, the following conventional mixing rules were used [Stryjek and Vera, 1986]:

$$b = \sum y_i b_i \qquad (3.1.17)$$

and

$$a = \sum y_i y_j a_{ij} \qquad (3.1.18)$$

with

$$a_{ij} = (a_i a_j)^{0.5}(1 - k_{ij}) \qquad (3.1.19)$$

The binary interaction parameter k_{ij} is set to zero because the non-idealities associated with polar compounds and their mixtures are not as pronounced in the vapor-phase as in the liquid-phase. When the temperature and pressure are fixed, equation 3.1.8 can be solved for the molar volume υ. Below the critical temperature, equation 3.1.8 has three real roots. The smallest and largest roots correspond to the liquid and vapor saturated molar volumes, respectively. When using a cubic equation of state to represent the P-υ isotherm for $T < T_C$, the region between υ_L and υ_G is unstable. A cubic equation of state is too simple to be able to accurately represent the P-υ isotherm for the liquid-vapor region and for this reason the calculated value of υ between υ_L and υ_G has no physical significance. When using equation 3.1.14 to solve for the compressibility factor, Z, the

smallest and largest roots correspond to the liquid and vapor phase respectively. These roots are used in calculating the fugacity coefficient ϕ.

For a pressure-explicit equation of state, the fugacity coefficient for a component in a gas mixture is written mathematically as [Kyle, 1992]:

$$\ln\phi_i^V = \frac{1}{RT}\int_v^\infty\left[\left(\frac{\delta P}{\delta n_i}\right)_{T,V,n_j} - \frac{RT}{v}\right]dv - \ln Z^G \tag{3.1.20}$$

When evaluated with the PRSV equation of state, this equation yields:

$$\ln\phi_i^V = \frac{A}{2\sqrt{2}\,B}\left[\frac{B_i}{B} - \frac{2\sum\limits_{j=1}^c y_i A_{ij}}{A}\right]\ln\left[\frac{Z^G + \left(1 + \sqrt{2}\right)B}{Z^G + \left(1 - \sqrt{2}\right)B}\right] + \frac{B_i}{B}\left(Z^G - 1\right) - \ln\left(Z^G - B\right) \tag{3.1.21}$$

The liquid-phase fugacity coefficient for a pure component is written mathematically for a pressure-explicit equation of state as [Kyle, 1992]

$$\ln\phi_i^{0L} = Z_i^L - 1 - \ln Z_i^L + \frac{1}{RT}\int_{v_i}^\infty\left[P - \frac{RT}{v_i}\right]dv_i \ , \tag{3.1.22}$$

which, when combined with the PRSV equation of state, yields

$$\ln\phi_i^{0L} = Z_i^L - 1 - \ln\left(Z_i^L - B_i\right) - \frac{A_i}{2\sqrt{2}\,B_i}\ln\left[\frac{Z_i^L + \left(1 + \sqrt{2}\right)B_i}{Z_i^L + \left(1 - \sqrt{2}\right)B_i}\right] \tag{3.1.23}$$

As mentioned previously, an equation of state is not sufficient to describe the vapor-liquid equilibria for systems containing a mixture of polar compounds. The activity coefficient, γ_i, which is dependent on the liquid-phase composition and temperature must be determined experimentally. The compositional dependency of the activity coefficient is often modeled by making use of an excess Gibbs free energy model.

There are several excess Gibbs free energy models with varying degrees of sophistication. Of the more notable models, the van Laar, Margules [Wohl, 1946], Wilson [Wilson, 1963], NRTL [Renon and Prausnitz, 1968] and the UNIQUAC [Abrams and Prausnitz, 1975] models are often used in modeling the activity coefficients of binary and/or multicomponent mixtures. These models are semi-empirical and require experimental data to fit the model parameters. Unfortunately, vapor-liquid-equilibria data for 2-propanol/water mixtures at elevated temperatures are not readily available, hence experiments were performed to determine these empirical constants.

The van Laar model was used due to its simplicity and accuracy in modeling 2-propanol/water vapor-liquid equilibria [Bergmann and Eckert, 1991]. The van Laar excess Gibbs free energy model is written as:

$$\ln \gamma_i = \frac{C_{ij}}{\left[1 + \frac{C_{ij} x_i}{C_{ji} x_j} \right]^2}$$

(3.1.24)

The binary interaction parameters C_{12} and C_{21} (1 = 2-propanol, 2 = water) were determined at different temperatures by fitting pressure-liquid composition diagrams. The following function was minimized over the range of 2-propanol concentration at a constant temperature using non-linear least squares regression:

$$\varepsilon = P_{EXP} \left(1 - y_H \right) - P_{EXP} \frac{\phi_A^{OL} \gamma_A}{\phi_A^V} x_A - P_{EXP} \frac{\phi_W^{OL} \gamma_W}{\phi_W^V} \left(1 - x_A \right)$$

(3.1.25)

The temperature dependency of the van Laar binary parameters can be thermodynamically derived by taking the limits of equation 3.1.24 as component x_i approaches zero:

$$\left(\ln \gamma_i \right)_{x_i = 0} = C_{ij}$$

(3.1.26)

The activity coefficient of component, i, approaches a definite limit as x_i becomes smaller and smaller. This limit is often called the limiting activity coefficient at infinite dilution. The governing thermodynamic relationship for the limiting activity coefficient at infinite dilution is:

$$\left[\frac{\delta \ln \gamma_i^{\infty}}{\delta(1/T)}\right]_{P,x} = \frac{h_i^{E\infty}}{R} \tag{3.1.27}$$

Over a small temperature range, the excess enthalpy at infinite dilution is considered to be relatively constant. A plot of C_{ij} versus $1/T$ should yield a straight line. Despite the validity of equation 3.1.27, it is not a common practice to determine the excess enthalpy or the limiting activity coefficient at infinite dilution with the above method, i.e. fitting pressure-composition data with an excess Gibbs free energy model. An accurate determination of these limiting parameters is outside the scope of this thesis and is detailed elsewhere [Bergmann and Eckert, 1991; Slocum and Dodge, 1964; Trampe and Eckert, 1990; 1991]. With the binary parameters of the van Laar equation known, the vapor-liquid equilibrium can be completely described.

The amount of diisopropyl ether and acetone formed during the dehydration reaction was assumed to be negligible compared to the amount of propylene produced and will be present in the wastewater in small amounts. The solubility of propylene at elevated temperatures is small enough to be negligible. From the previous statements, the following equation can be written to describe the liquid-phase composition:

$$x_W = 1 - x_A \tag{3.1.28}$$

The cumulative moles of propylene (α) formed at reaction time t can thus be obtained from the reaction stoichiometry and the overall material balance:

32

$$V = M_{T0} + \alpha - L \qquad (3.1.29)$$

From the component balance of helium and propylene and from equation 3.1.29, the vapor phase mole fractions of helium and propylene are:

$$y_P = \frac{\alpha}{M_{T0} + \alpha - L} \qquad (3.1.30)$$

$$y_H = \frac{M_H}{M_{T0} + \alpha - L} \qquad (3.1.31)$$

The relationship between the liquid-composition (2-propanol and water) with their vapor counterparts is illustrated in equations 3.1.6, 3.1.21, 3.1.23 and 3.1.24. The reaction temperature T and the reactor pressure P are easily measured and are known to high accuracy at any time t. To be able to completely describe the reactor contents, we need to know, in addition, x_A, y_A, y_W, L, α, and Z^G. The following outlines the set of non-linear equations, which must be solved for each data point.

Compressibility Factor Z

Equation 3.1.10 must be solved for the largest root, which yields Z^G. PRSV parameters A and B are functions of the vapor-composition as well, making the equation highly non-linear.

Water Component Balance

Either the component balance for 2-propanol or the component balance for water needs to be included to describe the system. From the overall material balance and the reaction stoichiometry, the component balance for water is:

$$L(1 - x_A) + (M_{T0} + \alpha - L)y_W = M_{W0} + \alpha \qquad (3.1.32)$$

Vapor-Liquid Equilibrium for 2-Propanol and Water

Making use of the PRSV equation of state and the experimentally determined van Laar parameters, the relationship between the liquid-phase components and their vapor-phase counterparts are written as:

$$y_A \phi_A^V = x_A \gamma_A \phi_A^{OL} \tag{3.1.33}$$

$$y_W \phi_W^V = (1 - x_A) \gamma_A \phi_W^{OL} \tag{3.1.34}$$

Vapor-Phase Component Balance

From equations 3.1.30, 3.1.31 and the overall vapor-phase balance, the following equation can be obtained:

$$y_A + y_W + \frac{\alpha + M_H}{M_{T0} + \alpha - L} = 1 \tag{3.1.35}$$

Equation of State for a Closed System

The final equation is derived from the physical limits imposed by the batch reactor itself. A relationship between the reactor pressure, the vapor volume (hence the liquid volume) and the moles of vapor in the vessel can be evaluated using the following equation of state:

$$P \cdot 10^3 \left[319 \cdot 10^{-6} - L \left(\frac{x_A Mw_A}{\rho_A \cdot 10^6} + \frac{(1 - x_A) Mw_W}{\rho_W \cdot 10^6} \right) \right] = ZRT(M_{T0} + \alpha - L) \tag{3.1.36}$$

The saturated liquid densities ρ_A and ρ_W can be calculated using the COSTALD correlation [Hankinson and Thomson, 1979]. The COSTALD correlation is summarized below

$$\frac{V_S}{V^0} = V_R^{(0)} \left[1 - \omega_{SRK} V_R^{(\delta)} \right] \tag{3.1.37}$$

with

$$V_R^{(0)} = 1 + a(1-T_R)^{1/3} + b(1-T_R)^{2/3} + c(1-T_R) + d(1-T_R)^{4/3} \qquad (3.1.38)$$

and

$$V_R^{(\delta)} = \frac{e + f \cdot T_R + g \cdot T_R^2 + h \cdot T_R^3}{T_R - 1.00001} \qquad (3.1.39)$$

Characteristic volumes V^0 and accentric factors from the Soave equation of state ω_{SRK} are given in Table 3.1. The empirical parameters for equations 3.1.38 and 3.1.39 (a - h) are given in Table 3.2. The above set of non-linear equations can be solved numerically using a commercial package (Maple V). The Maple V worksheet used to solve these equations is found in Appendix A1.

From the above analysis, the rate of reaction can thus be described using only pressure and temperature data. As many data points can be taken as required without influencing the reactor condition. The only requirement of using such a method is to have adequate vapor-liquid equilibrium (VLE) data at our disposal. Since VLE data for 2-propanol/water at elevated temperatures greater than 413 K are not readily available, experiments were performed to acquire the required information.

3.2 – Determination of the Rate Equation

The Langmuir-Hinshelwood-Hougen-Watson (LHHW) method of generating rate models based on Langmuir adsorption is often used in developing rate models for heterogeneous catalytic reactions. This model assumes that the adsorbed species are attached to the catalyst surface at definite sites and each active site can only accommodate one adsorbed species. The energy of all the adsorbed species is the same and is independent of the presence or absence of adsorbed species on adjacent sites.

Several LHHW models were developed for catalytic dehydration of 2-propanol in the liquid phase. The adsorption/desorption of 2-propanol and/or water was assumed to either occur via a single-site mode, where acid sites are involved or a dual-site mode, where both acid and basic sites are involved. As well, the rate of propylene formation was considered to be either inhibited or unaffected by the presence of water. For all models derived, the reaction was considered to be irreversible. The validity of this assumption will be further discussed in Chapter 4. In all models, A, W, P, and S represent 2-propanol, water, propylene and the active surface site respectively. The LHHW rate models are derived below.

3.2.1 – Single-Site Mode Adsorption with the Water Term Excluded (SSM-1)

The SSM-1 model involves the chemisorption of 2-propanol on an active site and a surface reaction to form 2-propanol and adsorbed water. In this model, fast desorption of water was assumed, hence water will occupy no active sites during the reaction. Only the forward reaction to form propylene and water will be considered. This model is represented by the following mechanism:

$$A + S \leftrightarrow A \cdot S \qquad \text{(Step 1, chemisorption of 2-propanol)}$$

$$A \cdot S \leftrightarrow W \cdot S + P(g) \qquad \text{(Step 2, surface reaction)}$$

$$W \cdot S \leftrightarrow W + S \qquad \text{(Step 3, desorption of water)}$$
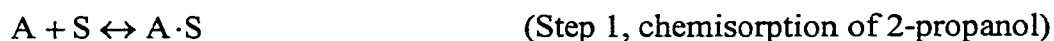
It can be seen that propylene is not an adsorbed entity, which is consistent with other mechanisms previously developed for 2-propanol dehydration in the vapor phase over solid acid catalysts [Youssef et al., 1992]. Let the surface reaction, Step 2, be the rate-determining step, the overall rate of propylene formation can be expressed in terms of the fraction of sites occupied by adsorbed 2-propanol θ_A :

$$\left(-r_A\right) = r_S = k_S \theta_A \tag{3.2.1}$$

The rate of adsorption of 2-propanol is given by the Langmuir model as:

$$r_{ads(A)} = k_{a(A)} C_A \theta_V - k_{d(A)} \theta_A \tag{3.2.2}$$

where the fraction of active sites which are vacant, θ_V, can be expressed as:

$$\theta_V = 1 - \theta_A \tag{3.2.3}$$

In the LHHW method of developing kinetic equations, one step is considered to be rate-determining, all other steps are considered to be at equilibrium. In this model, the rate of 2-propanol adsorption is considered to be at equilibrium. Setting equation 3.2.2 equal to zero yields:

$$\theta_A = K_A C_A \theta_V, \tag{3.2.4}$$

where the equilibrium adsorption constant for 2-propanol K_A is defined as:

$$K_A = \frac{k_{a(A)}}{k_{d(A)}} \tag{3.2.5}$$

From equation 3.2.3, the fraction of active sites occupied by 2-propanol can be written as:

$$\theta_A = \frac{K_A C_A}{1 + K_A C_A} \tag{3.2.6}$$

Substituting equation 3.2.6 into equation 3.2.1 yields the SSM-1 kinetic model:

$$r_S = \frac{k_S K_A C_A}{1 + K_A C_A} \tag{3.2.7}$$

3.2.2 – Single-Site Mode Adsorption with the Water Term Included (SSM-2)

The catalytic dehydration mechanism is similar to what was proposed for the SSM-1 model previously derived. The only exception is that the desorption of water is

not instantaneous, hence adsorbed water occupies active sites which are necessary for 2-propanol dehydration which inhibits the reaction. The adsorption/desorption of both 2-propanol and water are considered to be at equilibrium. The fraction of active sites occupied by water can be written as:

$$\theta_W = K_W C_W \theta_V \qquad (3.2.8)$$

The fraction of active sites occupied by 2-propanol is the same as in equation 3.2.4. The fraction of vacant active sites is written as:

$$\theta_V = 1 - \theta_A - \theta_W \qquad (3.2.9)$$

Making use of equations 3.2.4, 3.2.8 and 3.2.9, the fraction of vacant active sites can be written as:

$$\theta_V = \frac{1}{1 + K_A C_A + K_W C_W} \qquad (3.2.10)$$

Substituting equation 3.2.10 into 3.2.4 and 3.2.1 yields the SSM-2 model:

$$r_S = \frac{k_S K_A C_A}{1 + K_A C_A + K_W C_W} \qquad (3.2.11)$$

3.2.3 – Dual-Site Mode Adsorption with the Water Term Excluded (DSM-1)

It has been proposed in the literature that the catalytic dehydration over a solid acid catalyst, notably metal oxides, require both acidic and basic sites [Youssef et al., 1992]. 2-Propanol dissociatively adsorbs on an acidic site and a neighboring basic site. Figure 1.1 illustrates this proposed mechanism for olefin formation.

The previous two models assumed that 2-propanol adsorbs only on one type of surface site, i.e. acid site. The following dual-site models attempts to incorporate the above mechanism where both acid and basic sites are involved.

The so-called "dual-site" model, developed by Hougen and Watson (1947), is summarized by the following steps:

$A + S \leftrightarrow A \cdot S$ (Step 1,chemisorption of 2-propanol)

$A \cdot S + S \leftrightarrow W \cdot S + P \cdot S$ (Step 2, surface reaction)

$P \cdot S \leftrightarrow P + S$ (Step 3, desorption of propylene)

$W \cdot S \leftrightarrow W + S$ (Step 4, desorption of water)

In the DSM-1 model, adsorbed 2-propanol reacts with an adjacent vacant site to produced adsorbed water and propylene. Although the above steps do not strictly adhere to the E_2 mechanism proposed in the literature, it has found use in the literature to model 2-propanol dehydration in the vapor phase [Yue and Oloafe, 1984]. In the proposed "dual site" mechanism, two adsorption sites are required for propylene formation although the sites themselves do not differ from one another. This assumption is quite different from the E_2 mechanism where acid and basic sites differ substantially from one another.

Since propylene is assumed to be a vapor-phase product, fast desorption of propylene will be assumed for the derived dual site models. In the DSM-1 model, fast desorption is assumed for water, hence water will not occupy any active sites during the reaction. The rate of propylene formation is written in the following manner:

$$(-r_A) = r_s = k_s \theta_A \theta_v \tag{3.2.12}$$

The rate of adsorption of 2-propanol on the acid catalyst surface is written in the same manner as in equation 3.2.2. The fraction of sites that contain adsorbed 2-propanol and the fraction of vacant sites are derived in the same manner as in the SSM-1 model and are written as:

$$\theta_V = \frac{1}{1 + K_A C_A} \tag{3.2.13}$$

$$\theta_A = \frac{K_A C_A}{1 + K_A C_A} \tag{3.2.14}$$

Making use of equations 3.2.12 – 3.2.14, the DSM-1 rate model was derived as:

$$r_s = \frac{k_s K_A C_A}{\left(1 + K_A C_A\right)^2} \tag{3.2.15}$$

3.2.4 – Dual-Site Mode Adsorption with the Water Term Included (DSM-2)

In this model, 2-propanol dissociatively adsorbs on to an acid and basic site and

reacts to form propylene and water. The adsorption/desorption of water on the active

sites inhibits the rate of propylene formation by occupying active sites necessary for

propylene formation. The model is derived in a similar manner as in the DSM-1 model,

except the fraction of sites occupied by water θ_W is included in the mechanism. Making

use of equations 3.2.4, 3.2.10 and 3.2.12, the DSM-2 model was derived as:

$$r_s = \frac{k_s K_A C_A}{\left(1 + K_A C_A + K_W C_W\right)^2} \tag{3.2.16}$$

Models SSM-1, SSM-2, DSM-1 and DSM-2, expressed mathematically in

equations 3.2.7, 3.2.11, 3.2.15 and 3.2.16 respectively, will be used in the model

screening procedure. Mathematically, the single-site and dual-site models differ by the

exponent in the denominator. For models SSM-2 and DSM-2, the rate of propylene

formation is inhibited by the adsorption/desorption of water on the active sites. The rate

constant for the surface reaction should follow an Arrhenius type temperature

dependency. The temperature dependence of the adsorption/desorption equilibrium

constant K_i can be expressed in terms of the van't Hoff equation. The temperature dependence of the kinetic and adsorption parameters can be expressed mathematically as:

$$k_S = k_S^0 \exp\left(\frac{-E_A}{RT}\right)$$
(3.2.17)

$$K_i = K_i^0 \exp\left(\frac{-\Delta H_{A,i}}{RT}\right)$$
(3.2.18)

The above parameters were determined by fitting the LHHW models with experimental rate data. The rate equation is integrated numerically with the trapezoidal rule and the model parameters were determined from least-squares non-linear regression. The error to be minimized is written as:

$$\varepsilon = \frac{\alpha_t - \alpha_0}{m_C} - \int_0^t f(t)\,dt,$$
(3.2.19)

where f(t) are the models expressed in equations 3.2.7, 3.2.11, 3.2.15, and 3.2.16. For each data point, the absolute value of the error function, ε, is determined. The summation of these absolute errors over the set of data points was minimized using the Solver option in Microsoft Excel 2000. The solver method chosen for the minimization procedure was the "Standard GRG Non-linear" method. The search direction method was chosen through an estimation method, because using the pure form of Newton's method is far too expensive. A quasi-Newton (or BFGS) method, which maintains an approximation to the Hessian matrix, was used instead. The derivatives were determined using a forward difference approximation. Estimations for the forward difference approximation method were determined using the "tangent" method, which uses linear extrapolation from the line tangent to the reduced objective function. For these models, the liquid phase concentration C_i is expressed as:

$$C_i = \frac{x_i}{\sum \dfrac{x_i Mw_i}{\rho_i \cdot 10^3}}$$

(3.2.20)

3.3 – Nomenclature

a, b = equation of state parameters for the PRSV equation of state

A, B = dimensionless terms, $A = Pa/(RT)^2$; $B = Pb/RT$

a – h = parameters for the COSTALD correlation

C = binary constant for the van Laar equation

  = liquid phase concentration of component, mole L^{-1}

E_A = activation energy, kJ mole^{-1}

f = fugacity of component, kPa

ΔH_A = heat of adsorption, kJ mole^{-1}

h_i^{∞} = partial molar excess enthalpy of component i at infinite dilution, kJ mole^{-1}

k = binary interaction parameter for the PRSV equation of state

  = rate constant for 2-propanol dehydration, moles g^{-1} min^{-1}

K = adsorption/desorption equilibrium constant, L mole^{-1}

k^0 = pre-exponential factor for the rate constant, mole g^{-1} min^{-1}

K^0 = adsorption/desorption pre-exponential factor, L mole^{-1}

L = moles of liquid, mole

m = mass, g

M = moles of component prior to reaction, mole

Mw = molecular weight of component, g / mole

n = number of moles, mole

P = pressure, kPa

42

r = rate of formation, mole g^{-1} min^{-1}

R = gas constant, 8.31451 J $mole^{-1}$ K^{-1}

t = time, min

T = temperature, K

V = moles of vapor, mole

$V_R^{(0)}$ = corresponding states function for normal fluids (COSTALD)

$V_R^{(\delta)}$ = deviation function for COSTALD correlation

V_S = saturated liquid volume, L $mole^{-1}$

V^0 = characteristic volume, L $mole^{-1}$

x = liquid mole fraction

y = vapor mole fraction

Z = compressibility factor

Greek Letters

α = cumulative amount of propylene produced at time t, mole

= function of reduced temperature and accentric factor (Soave)

ε = error in regression fit, mole; kPa

ϕ = fugacity coefficient

γ = activity coefficient

κ = function of reduced temperature and accentric factor (PRSV)

κ_0 = function of accentric factor

κ_1 = pure compound parameter

θ_i = fraction of active sites occupied by component i

43

θ_V = fraction of vacant sites

ρ = saturated liquid density, $g\ mL^{-1}$

Σ = summation

v = molar volume, $m^3\ mole^{-1}$

ω = accentric factor

ω_{SRK} = accentric factor from the Soave equation of state

Subscripts

0 = initial, $t = 0$

a = adsorption

A = 2-propanol

C = at critical conditions

= catalyst

d = desorption

EXP = experimental

H = helium

i, j = component

P = propylene

R = reduced

S = at catalyst surface

SAT = at saturated conditions

T = total

W = water

Superscripts

0   = pure phase

∞ = infinite dilution

G   = gas phase

L   = liquid phase

V   = vapor phase

Table 3.1 – Critical Constants of Reactants, Products and Inerts

Component	Tc (K)	Pc (kPa)	$\kappa 1$	ω	ω_{SRK}	V^0 (L mole^{-1})
2-Propanol	508.4	4764.25	0.23264	0.66372	0.6637	0.2313
Water	647.286	22089.75	-0.06635	0.3438	-0.65445	0.043567
Propylene	365.57	4664.55	0.044	0.1408	0.1455	0.1829
Helium	5.3	228.99	-	-0.365	-0.4766	0.05457

Table 3.2 – COSTALD Correlation Parameters

a	-1.52816
b	1.43907
c	-0.81446
d	0.190454
e	-0.29612
f	0.386914
g	-0.04273
h	-0.04806

3.4 – Literature Cited

Abrams, D. S. and J. M. Prausnitz, "Statistical Thermodynamics of Liquid Mixtures : A New Expression for the Excess Gibbs Energy of Partly or Completely Miscible Systems", *AIChE J.* **21**, 116-128 (1975)

Bergmann, D. L. and C. A. Eckert, "Measurement of Limiting Activity Coefficients for Aqueous Systems by Differential Ebulliometry", *Fluid Phase Equilibria* **63**, 141-150 (1991)

Hankinson, R. W. and G. H. Thomson, "A New Correlation for Saturated Densities of Liquids and Their Mixtures", *AIChE J.* **25**, 653-663 (1979)

Hougen, O. A. and K. M. Watson, "Chemical Process Principles", Part 3, John Wiley and Sons, New York (1947)

Kyle, B. G., "Chemical and Process Thermodynamics", 2nd Ed., Prentice Hall, Englewood Cliffs (1992)

Peng, D. Y. and D. B. Robinson, "A New Two-constant Equation of State", *Ind. Eng. Chem. Fund.* **15**, 59-64 (1976)

Renon, H. and J. M. Prausnitz, "Local Composition in Thermodynamic Excess Functions for Liquid Mixtures", *AIChE J.* **14**, 135-144 (1968)

Slocum, E. W. and B. F. Dodge, "Activity Coefficients at Infinite Dilution : 2-Propanol – Water System", *AIChE J.* **10**, 364-368 (1964)

Soave, G., "Equilibrium Constants from a Modified Redlich-Kwong Equation of State", *Chem. Eng. Sci.* **27**, 1197-1203 (1972)

Stryjek, R. and J. H. Vera, "PRSV: An Improved Peng-Robinson Equation of State for Pure Compounds and Mixtures", *Can. J. Chem. Eng.* **64**, 323-333 (1986)

Trampe, D. M. and C. A. Eckert, "Calorimetric Measurement of Partial Molar Excess Enthalpies at Infinite Dilution", *J. Chem. Eng. Data* **36**, 112-118 (1991)

Trampe, D. M. and C. A. Eckert, "Limiting Activity Coefficients from an Improved Differential Boiling Point Technique", *J. Chem. Eng. Data* **35**, 156-162 (1990)

Wilson, G. M., "Vapor-Liquid Equilibrium. XI. A New Expression for the Excess Free Energy of Mixing", *J. Am. Chem. Soc.* **86**, 127-130 (1964)

Wohl, K., "Thermodynamic Evaluation of Binary and Ternary Liquid Systems", *Trans. AI ChE* **42**, 215-249 (1946)

Youssef, A. M., I. B. Khalil and B. S. Girgis, "Decomposition of Isopropanol on Magnesium Oxide/Silica in Relation to Texture, Acidity and Chemical Composition", *Appl. Catal. A* **81**, 1-13 (1992)

Yue, P. L. and O. Oloafe, "Kinetic Analysis of the Catalytic Dehydration of Alcohols over Zeolites", *Chem. Eng. Res. Des.* **62**, 81-91 (1984)

Chapter 4

Experimental Results and Discussion

4.1 – Determination of the Vapor-Liquid Equilibria for 2-Propanol/Water System

Total pressure-liquid composition data were collected over a temperature range of

433 to 463 K with a 2-propanol concentration range of 2 – 10 mol % using a procedure

similar to that described in Chapter 2, but without added catalyst. Making use of

appropriate material balances, the binary parameters for the van Laar equation can be

determined from the total pressure at a particular temperature and the initial amounts of

2-propanol, water and helium added to the reactor. The following details the methods

used to accomplish this. The liquid phase will contain only water and 2-propanol, since

no reaction will occur when the catalyst is absent.

$$x_W = 1 - x_A \tag{4.1.1}$$

The liquid-phase 2-propanol mole fraction can be written in terms of the vapor-phase

mole fraction y_A and the total moles of liquid, L, at equilibrium by making use of the

total material balance for the system and the component balance for 2-propanol:

$$x_A = \frac{M_{A0} - (M_{T0} - L)y_A}{L} \tag{4.1.2}$$

The vapor-phase water mole fraction can also be written in terms of the vapor-phase 2-

propanol mole fraction y_A and the total moles of liquid, L, at equilibrium by making use

of the helium component balance, the overall material balance and the vapor-phase

material balance:

$$y_W = 1 - y_A - \frac{M_H}{M_{T0} - L} \tag{4.1.3}$$

If the binary parameters of the van Laar equation C_{12} and C_{21} are known (see equation 3.1.24), the equilibrium value of y_A and L can be determined by making use of the vapor liquid equilibrium of 2-propanol/water and an appropriate equation of state for a closed system. These two minimization equations will be referred to as f_1 and f_2

Vapor-Liquid Equilibria for 2-Propanol

$$f_1 = y_A - \left(\frac{\phi_A^{OL}}{\phi_A^V}\right) \exp\left[\frac{C_{12}}{\left(1 + \frac{C_{12}x_A}{C_{21}(1 - x_A)}\right)^2}\right] x_A \qquad (4.1.4)$$

Equation of State for a Closed System

$$f_2 = P \cdot 10^3 \left[319 \cdot 10^{-6} - L\left(\frac{x_A Mw_A}{\rho_A \cdot 10^6} + \frac{(1 - x_A)Mw_w}{\rho_w \cdot 10^6}\right)\right] - Z^G R T(M_T - L) \qquad (4.1.5)$$

The determination of the fugacity coefficients, saturated liquid densities and the compressibility factor are outlined in Chapter 3, section 3.1.

The binary constants for the van Laar equation have to be determined experimentally. An additional function must be developed and minimized for each data point in addition to the functions derived above. Making use of the vapor-liquid equilibria for water, the following minimization function, f_3, was developed:

$$f_3 = 1 - y_A - \frac{M_H}{M_{T0} - L} - \left(\frac{\phi_w^{OL}}{\phi_w^V}\right) \exp\left[\frac{C_{21}}{\left(1 + \frac{C_{21}(1 - x_A)}{C_{12}x_A}\right)^2}\right](1 - x_A) \qquad (4.1.6)$$

Function f_3 was minimized by non-linear least-squares regression by varying the binary parameters of the van Laar equation. The minimization procedure is outlined in Chapter 3, section 3.2. The vapor-phase mole fraction of 2-propanol and the equilibrium amount

50

of liquid in the vessel were calculated by minimizing functions f_1 and f_2. The results of these minimization procedures are shown in Figures 4.1 – 4.3. Figure 4.1 compares the calculated value of y_A with what is expected from the van Laar equation (f_1). Figure 4.2 compares the experimental pressure value P with the pressure calculated using an equation of state for a closed system (f_2). The calculated value of the vapor-phase mole fraction of water, y_W determined from material balances is compared to the mole-fraction determined from the van Laar equation in Figure 4.3 (f_3).

The ability of the van Laar model to fit the experimental pressure-liquid composition data is illustrated in Figure 4.4. A very good fit is found for 2-propanol concentrations greater than 6 mol % over the range of temperatures tested. The temperature dependence of the binary parameters, as expressed mathematically in Chapter 3, equation 3.1.23, is shown in Figure 4.5. It should be noted that these parameters were determined under a relatively small range of 2-propanol concentrations. Caution should be exercised in extrapolating these parameters to other concentration ranges. An accurate description of the vapor-liquid equilibria for the entire range of concentration $0 < x_A < 1$ is outside the scope of this thesis. The temperature dependence of the van Laar binary constants are determined to be:

$$C_{12} = \frac{2299.1}{T} - 3.624, \qquad r^2 = 0.995 \qquad (4.1.7)$$

$$C_{21} = -\frac{2228.6}{T} + 5.953, \qquad r^2 = 0.893 \qquad (4.1.8)$$

The contents of the reactor vessel can now be completely described using only pressure-temperature data.
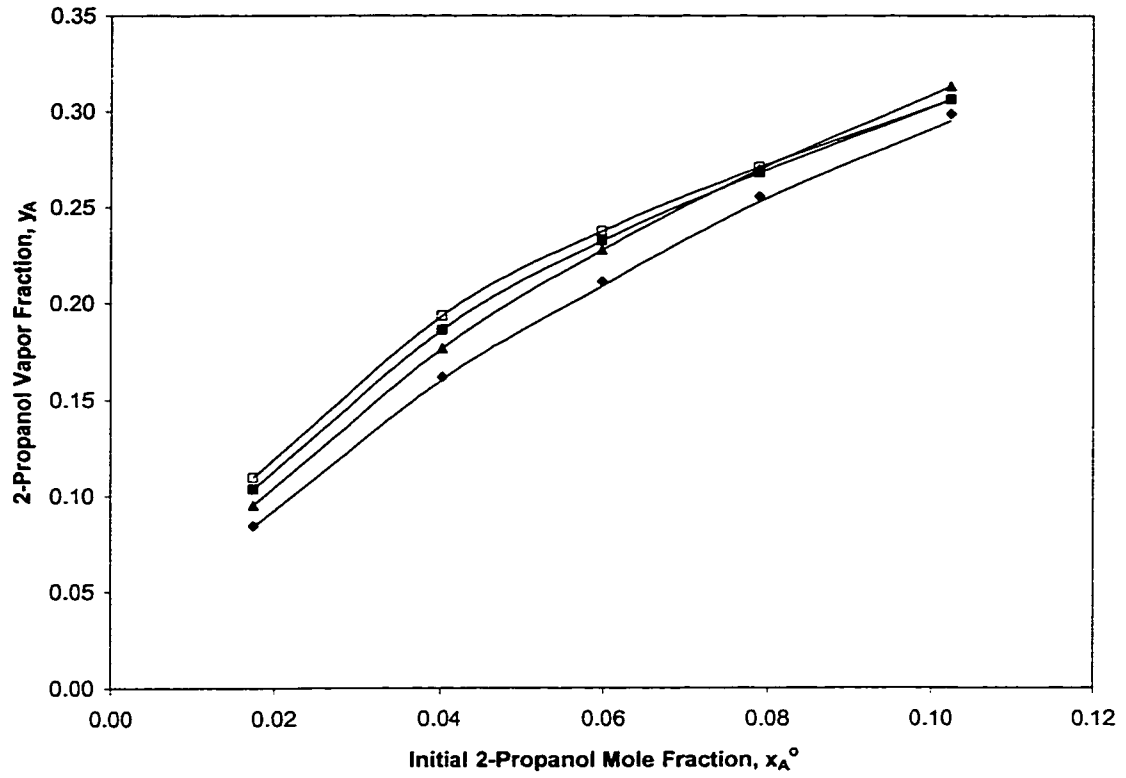
Figure 4.1 – Minimization of Function f_1 for the Determination of the van Laar Binary

Parameters: (□) 433 K, (■) 443 K, (▲) 453 K, (◆) 463 K, (—) van Laar model fit
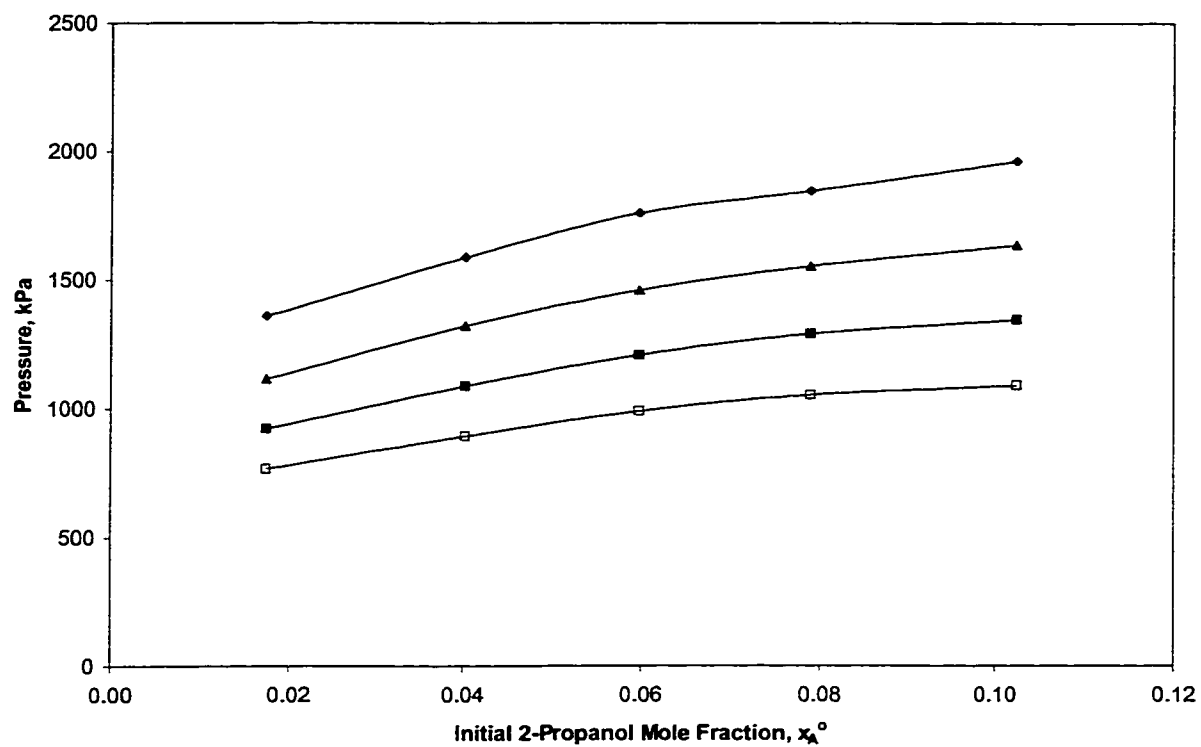
Figure 4.2 - Minimization of Function f_2 for the Determination of the van Laar Binary

Parameters: (□) 433 K, (■) 443 K, (▲) 453 K, (◆) 463 K, (—) van Laar model fit
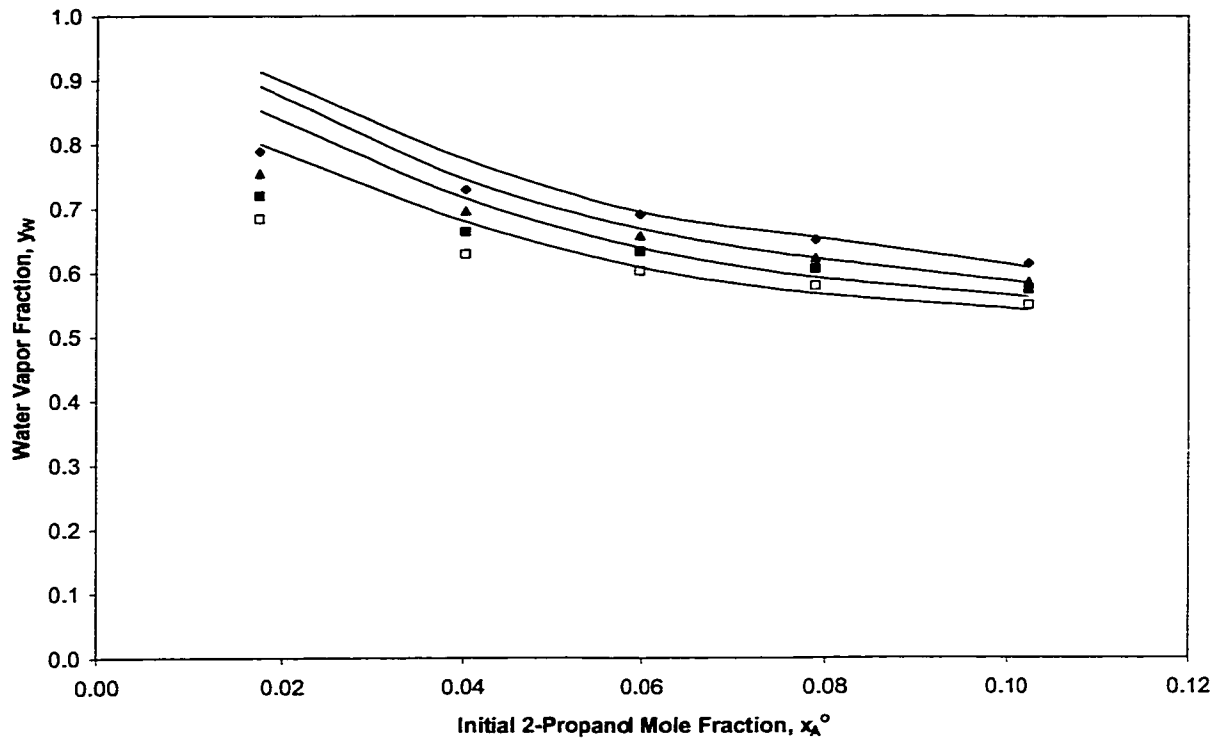
Figure 4.3 - Minimization of Function f_3 for the Determination of the van Laar Binary

Parameters: ($\square$) 433 K, ($\blacksquare$) 443 K, ($\blacktriangle$) 453 K, ($\blacklozenge$) 463 K, (——) van Laar model fit
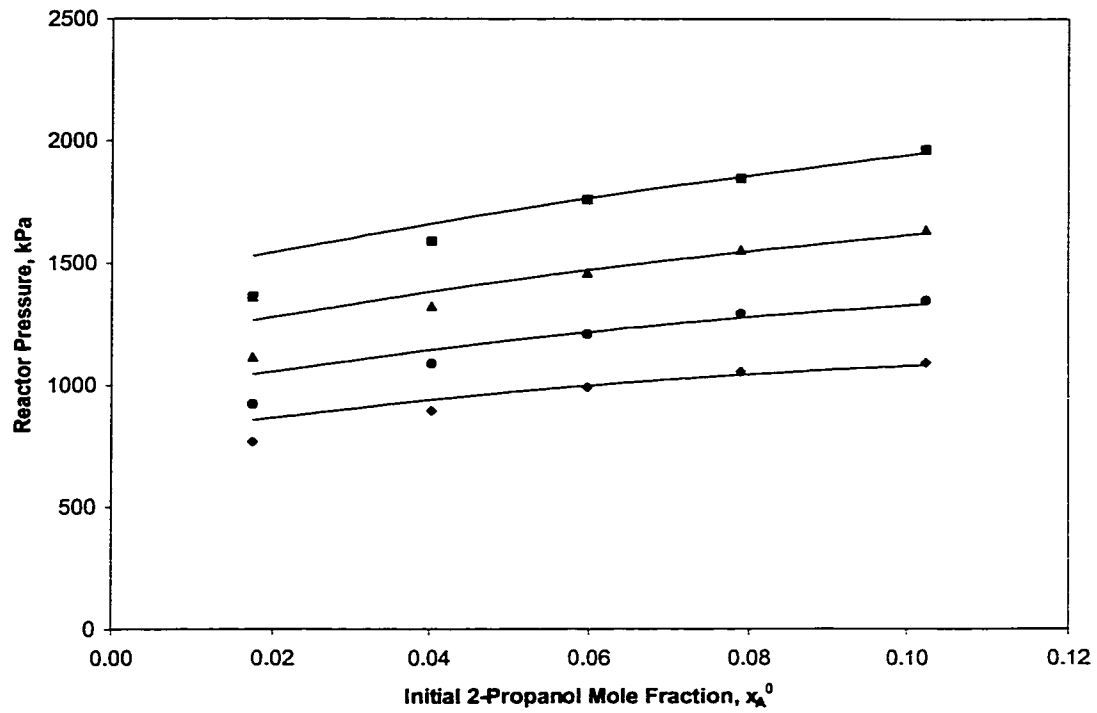
Figure 4.4 - The Equilibrium Pressure versus Liquid Composition : PRSV Equation of

State with the van Laar Excess Gibbs Free Energy Model: (◆) 433 K, (●) 443 K, (▲)

453 K, (■) 463 K, (——) van Laar model fit
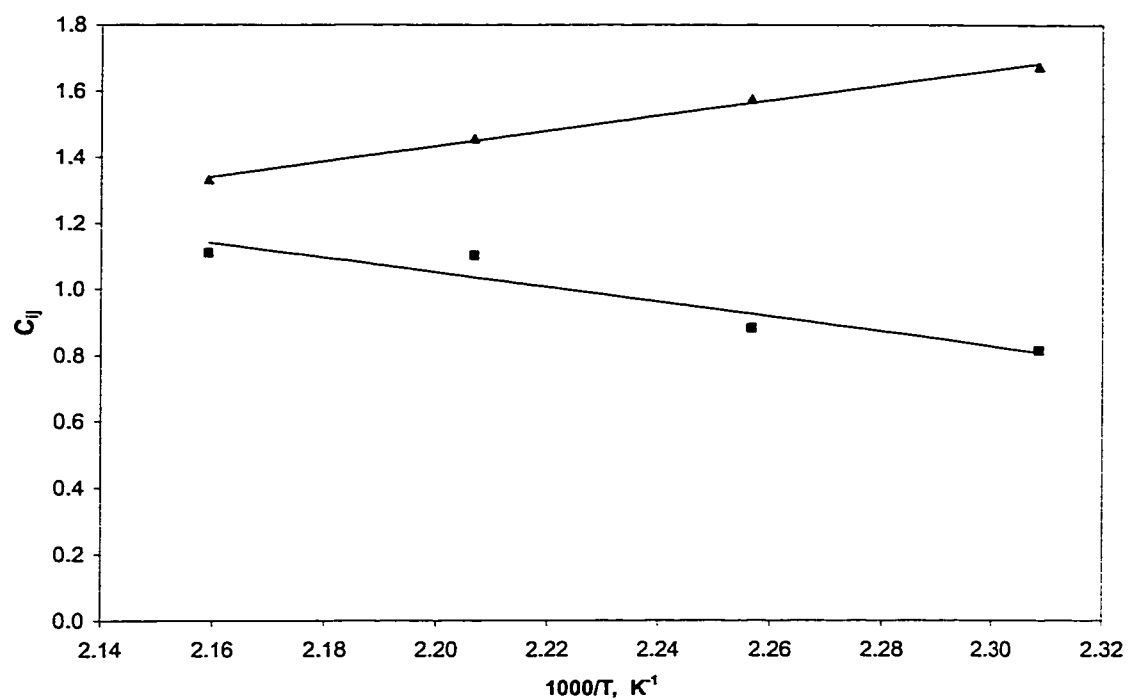
Figure 4.5 - Temperature Dependence of the Binary Parameters for the van Laar Excess Gibbs Free Energy Model (1 = 2-propanol, 2 = water): ($\blacktriangle$) C_{12}, ($\blacksquare$) C_{21}

4.2 – Catalyst Screening

4.2.1 – Preliminary Screening

Various metal oxide and molecular sieve solid acid catalysts with varying acidities and hydrophobicities were screened for 2-propanol dehydration activity. These include samples of active alumina, zeolite 13X (Aldrich; 20,3864-7), SAPO-5 (MHZN2-34, Laval University, PQ, Canada), silicalite with a silica binder (S-115 SiO_2 ExT., UOP, LOT 15228-32), and silicalite with an alumina binder (S-115 Al_2O_3 ExT., UOP, LOT 09296-29C). The BET surface areas for the screened catalysts and their x-ray diffraction patterns are found in Table 4.1 and Figure 4.6 respectively. Alumina and zeolite 13X were selected for screening due to the fact that they are known to be active in the vapor-phase dehydration of 2-propanol.

HZSM-5 catalysts are known to be active in the vapor-phase catalytic dehydration of ethanol in the presence of water [Phillips and Datta, 1997; Schulz and Bandermann, 1994; Le van Moa et al., 1990; Oudejans et al., 1982]. The dehydration mechanism of ethanol and 2-propanol are considered to be very similar. For this reason, HZSM-5 type zeolites were considered for screening. The silicalite catalysts were chosen because they are very hydrophobic [Flanigen et al., 1978], which is an attractive property for wastewater applications and they are considered to be structurally similar to HZSM-5 catalysts [Olson et al., 1980; Rees, 1982].

Silicoaluminophosphates, such as SAPO-5, are known to be active in reactions requiring strong acids [Hedge at al., 1988]. The results of the catalyst screening are shown in Figure 4.7. The 2-propanol conversion is defined as the mole percent of 2-propanol that is converted to propylene.
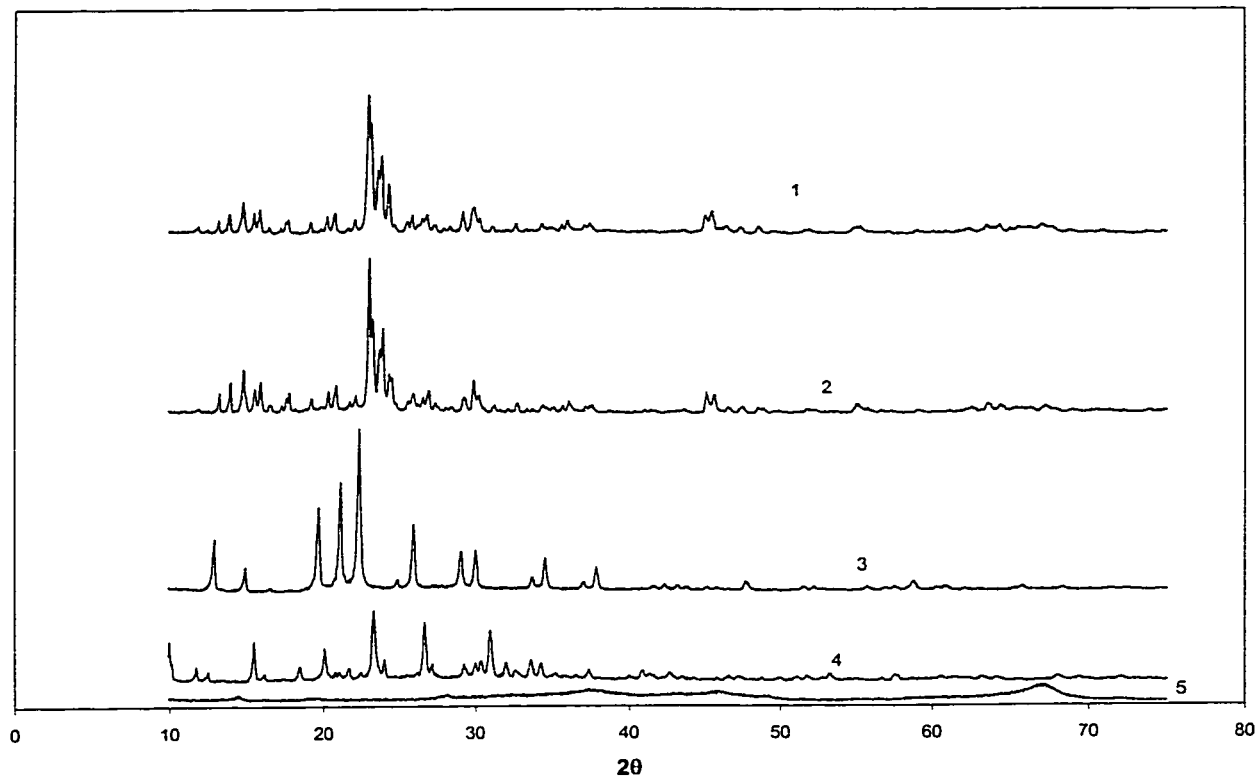
Figure 4.6 – X-Ray Diffraction Pattern for the Screened Catalysts: 1 = S-115 Al₂O₃

ExT., 2 = S-115 SiO₂ ExT., 3 = SAPO-5, 4 = Zeolite 13X, 5 = Alumina
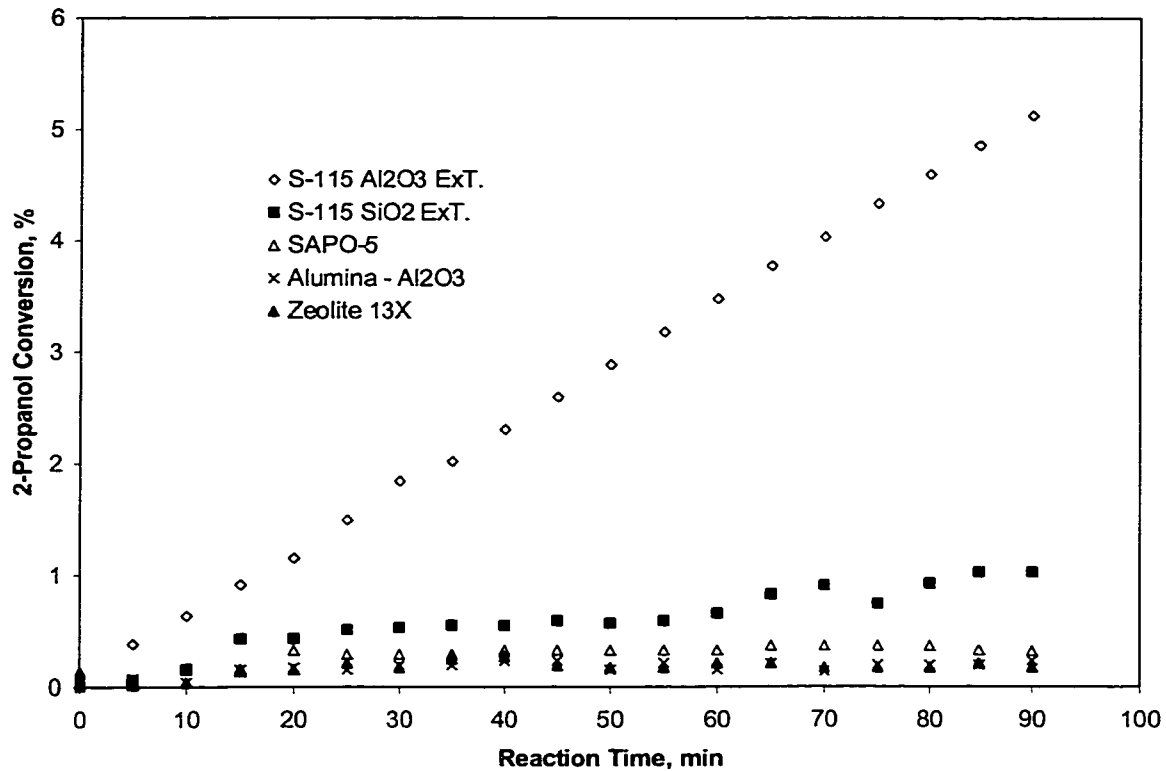
Figure 4.7 - Catalyst screening – Reaction Temperature = 463 K, Stirrer Speed = 1004

rpm, 400 - 595 μm Particle Size (Except Powder SAPO-5), 1.6 wt % Catalyst Loading,

10 mol % 2-Propanol/Water Feed

For all catalysts tested, propylene is the major reaction product. Only trace amounts of di isopropyl ether and acetone were found. These results justify the assumption of a negligible amount of other components in the liquid phase except water and 2-propanol. Further analysis of the liquid samples indeed confirmed that negligible amounts of propylene are present in the liquid phase.

S-115 Al_2O_3 ExT was found to be the most active catalyst among the screened samples, followed by S-115 SiO_2 ExT. In an aqueous media, the rate of propylene formation may depend on the number and strength of acid sites and also on the hydrophobicity of the catalyst. It has been found previously that silicalite is both more hydrophobic and more acidic than SAPO-5 [Hedge et al., 1988]. This may explain the higher activity of the silicalite catalysts compared to the SAPO-5 catalyst. It should be noted that the acidity and hydrophobicity of zeolites, such as silicalite, are dependent on the silica/alumina ratio [Olson et al., 1980]. However, more tests are needed with respect to catalyst acidity and hydrophobicity in order to make definite conclusions with regards to the influence of these parameters on the catalytic activity in the aqueous phase. For all kinetic runs, silicalite S-115 Al_2O_3 ExT is the catalyst used to determine the kinetic parameters.

4.2.2 – Validation of Irreversible Reaction

From the preliminary catalyst screening, the assumption that 2-propanol dehydrates to propylene irreversibly can be validated by calculating the equilibrium conversion in the batch slurry reactor and comparing this conversion with what was found experimentally. A theoretical equilibrium conversion which far exceeds the

conversion attained in the transient mode would indicate that the reaction is not approaching its equilibrium conversion, hence a reverse reaction would not be significant.

The equilibrium conversion calculations were performed by making use of the reactor equations developed in Chapter 3, section 3.1. For the equilibrium conversion calculations the final reactor pressure is not known, hence an additional equation is required to describe the equilibrium product composition. The previous assumptions made with regards to the liquid phase composition and the reaction products are assumed to apply for these calculations as well. In terms of the component activities, the equilibrium constant is given as

$$K = \prod a_i^{v_i} = \frac{a_P \cdot a_W}{a_A} \tag{4.2.1}$$

where

$$a_P = \frac{f_P^V}{f_P^{0,V}} = \frac{P \phi_P^V y_P}{101.3} \tag{4.2.2}$$

and

$$a_W = \frac{f_W^L}{f_W^{0,L}} = \frac{P \phi_W^{0L} \gamma_W x_W}{P_W^{SAT}} \tag{4.2.3}$$

and

$$a_A = \frac{f_A^L}{f_A^{0,L}} = \frac{P \phi_A^{0L} \gamma_A x_A}{P_A^{SAT}} \tag{4.2.4}$$

Substituting equations 4.2.2 – 4.2.4 into 4.2.1 yields

$$K = \frac{P}{101.3} \frac{\phi_P^V \phi_W^{0L}}{\phi_A^{0L}} \frac{P_A^{SAT}}{P_W^{SAT}} \frac{\gamma_W}{\gamma_A} \frac{(1 - x_A)}{x_A} y_P \tag{4.2.5}$$

To calculate the equilibrium composition from the above equation, the equilibrium constant must be determined at the required temperature. The temperature dependence of K is known thermodynamically to be [Kyle, 1992]:

$$\frac{d \ln K}{dT} = \frac{\Delta H^0}{RT^2} \qquad (4.2.6)$$

where the standard enthalpy change for the reaction ΔH^0 is written as:

$$\Delta H^0 = \Delta H_f^0 + \int_{298}^{T} \left(\sum v_i C_{P_i}^0 \right) dT \qquad (4.2.7)$$

where the heat capacity for the reactants and products have the following temperature dependence:

$$C_{P_i}^0 = a_i + b_i T + c_i T^2 + d_i T^3 \qquad (4.2.8)$$

Empirical constants a, b, c, and d for gaseous propylene and liquid water and 2-propanol are given in Table 4.2.

Making use of the temperature dependence of the standard enthalpy change of the reaction and equation 4.2.6, the equilibrium constant can be expressed as

$$\ln K = -\frac{\Delta H_0}{RT} + \left(\frac{\sum v_i a_i}{R} \right) \ln T + \left(\frac{\sum v_i b_i}{2R} \right) T + \left(\frac{\sum v_i c_i}{6R} \right) T^2$$
$$+ \left(\frac{\sum v_i d_i}{12R} \right) T^3 + I \qquad (4.2.9)$$

The standard enthalpy change ΔH^0 and the integration factor I were determined to be 67.3 kJ mole^{-1} and 165.3 respectively. The equilibrium constants at a temperature range of 433 to 463 K are shown in Figure 4.8. The liquid-phase dehydration of 2-propanol to form propylene is an endothermic reaction, therefore the equilibrium constant and the equilibrium 2-propanol conversion increases with increasing temperature.
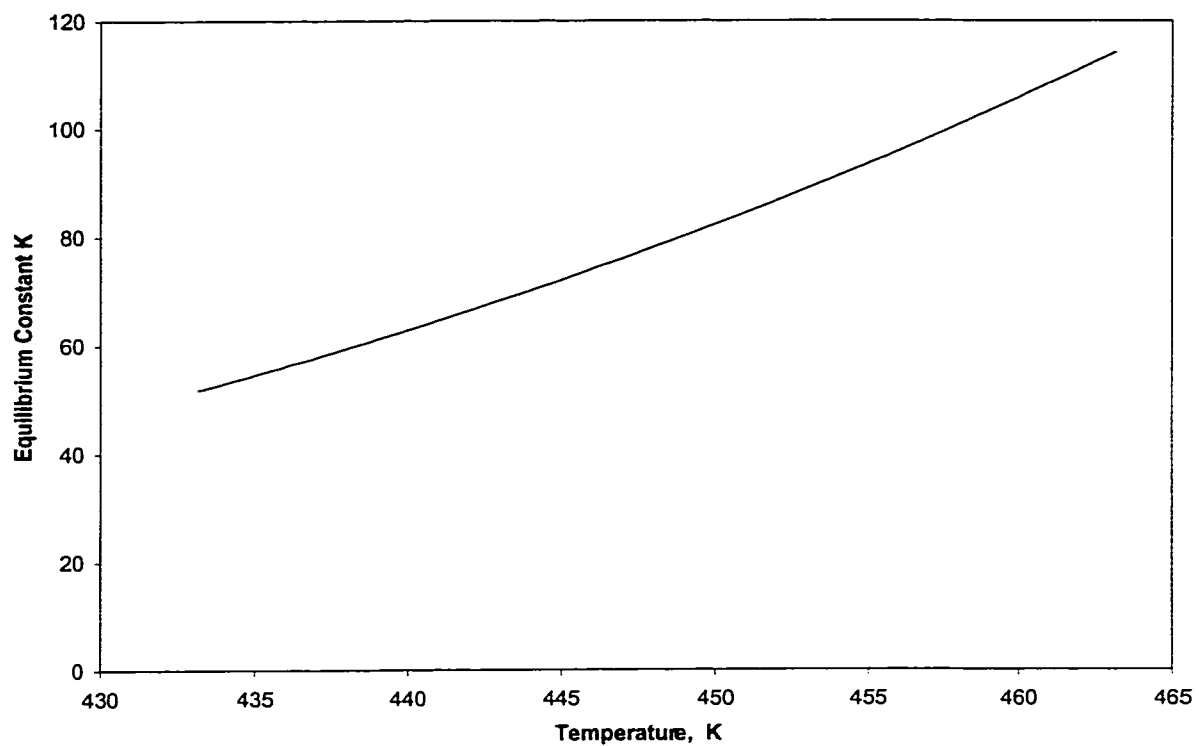
Figure 4.8 – Chemical Equilibrium Constant for the Liquid-Phase Dehydration of 2-Propanol to Propylene at Various Reaction Temperatures

Chemical equilibrium is attained when equation 4.2.5 and the exponential of equation 4.2.9 are equal. Making use of the equations developed in Chapter 3, section 3.1 and this additional equation, the equilibrium conversion of liquid 2-propanol to propylene was calculated at a temperature range of 433 to 463 K at 2-propanol concentrations of 4 – 10 mol %. The results of these calculations are given in Figure 4.9. As is expected from Figure 4.4, the equilibrium conversion increases with increasing temperature. As well, the presence of water in the reactor feed is expected to inhibit the equilibrium conversion to propylene, as can be seen in equation 4.2.5.

It should be noted that these equilibrium conversions were calculated for the experimental batch slurry reactor used to determine the rate data. They do not necessarily reflect the highest conversion one would expect in an industrial setting. As the reactor is operating in a batch mode, the reactor pressure is allowed to increase as volatile propylene is being produced. As can be seen in equation 4.2.5, a high pressure lowers the equilibrium conversion to propylene. If propylene were to be continuously removed (for example, in a catalytic distillation column) very high conversions would be expected.

When comparing Figure 4.7 to 4.9, it is very evident that, even with the relatively active silicalite S-115 Al_2O_3 catalyst, the reaction is far from its equilibrium conversion, even after 1.5 hours. At 463 K with an initial 2-propanol concentration of 10 mol %, the conversion of 2-propanol over silicalite S-115 Al_2O_3 was 5.1 % after 90 minutes. The equilibrium conversion at these conditions was calculated to be 35.3 %, almost seven times higher than the conversions attained during the kinetic runs. These results indicate
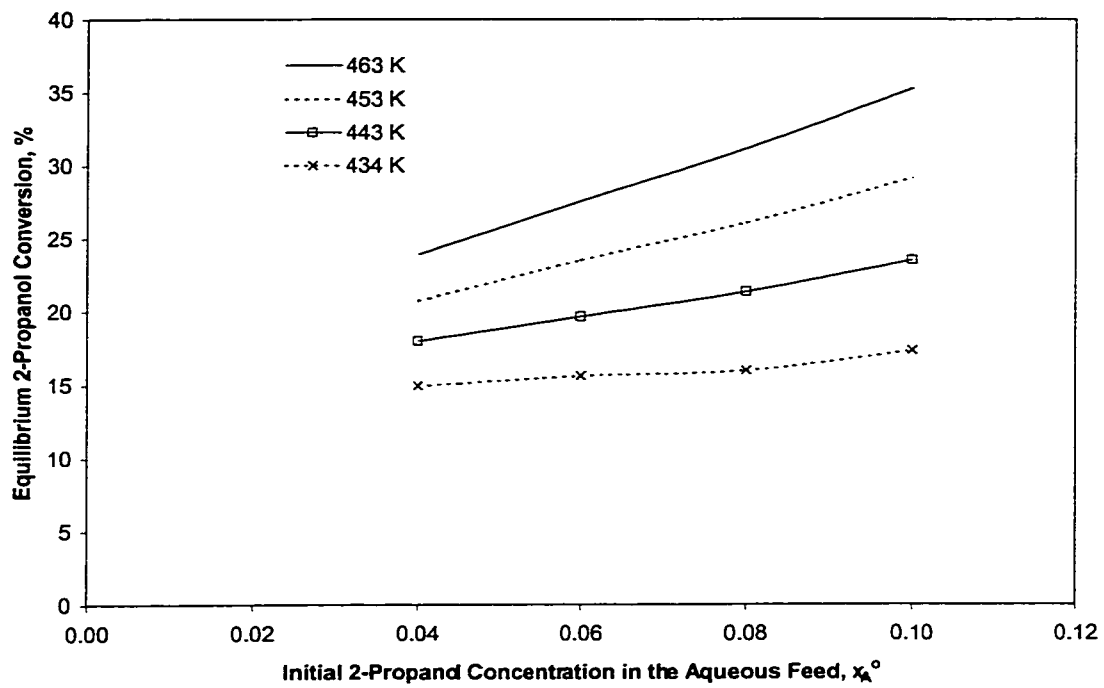
Figure 4.9 – Influence of Reactor Temperature and Initial 2-Propanol Concentration on

the Equilibrium Conversion of 2-Propanol to Propylene in a Batch Slurry Reactor

that the assumption of an irreversible reaction in the development of the kinetic model in Chapter 3 (section 3.2) appears to be reasonable.

4.3 – Mass Transfer Limitations

Heterogeneous catalytic reactions can be said to occur through the following steps

Step 1 – Transport of reactant material to the catalyst surface

Step 2 – Diffusion of the reactant through the porous structure to the active catalyst surface

Step 3 – Chemisorption of the reactant on to the active site(s)

Step 4 – Catalytic surface reaction to form reaction product(s)

Step 5 – Desorption of reactants from the active site(s)

Step 6 – Diffusion of reaction products through the porous structure to the bulk phase

Step 7 – Transport of the reactant material through boundary layer to the bulk media

The external mass transfer is described in steps 1 and 7. Internal mass transfer through the porous catalyst via molecular and pore diffusion is described in steps 2 and 6. The surface reaction, which consists of the adsorption/desorption of the reactants/products and the surface reaction are detailed in steps 3-5. The observed rate of reaction depends on all of the above steps. True surface reaction rates can only be directly determined from rate data if the experiments are performed under conditions where the observed rate is not limited by diffusional processes, otherwise the mass transfer processes must be modeled.

The region where the external mass transfer is no longer rate limiting was determined by varying the stirrer speed. Tests with silicalite S-115 Al_2O_3 ExT. at 463 K with a catalyst loading of 1.57 weight %, an initial 2-propanol concentration of 10 mol % and a catalyst particle size of 90 - 150 μm indicates that external mass transfer is no longer rate limiting at stirrer speeds greater than 1080 rpm (Figure 4.10). It can be expected that when an initial concentration less than 10 mol % is used, the kinetic experiments will still be performed in a region where the external mass transfer is not rate limiting.

The transport of reactant molecules from the surface of the catalyst to the bulk fluid through the boundary layer can be expressed as [Levenspiel, 1972]

$$\frac{1}{-S_{ex}} = \frac{dN_A}{dt} = k_L^{'} \left(C_{Ab} - C_{As} \right) \qquad (4.3.1)$$

where C_{Ab} and C_{As} are the liquid phase concentrations of 2-propanol in the bulk and at the surface respectively. The liquid phase mass transfer coefficient $k_L^{'}$ can be expressed using the following correlation for highly turbulent mixers [Geankoplis, 1993]

$$k_L^{'} N_{sc}^{2/3} = 0.13 \left(\frac{[P/V]\mu_c^2}{\rho_c^2} \right)^{1/4} \qquad (4.3.2)$$

where the Schmidt number, N_{sc}, is defined as

$$N_{sc} = \frac{\mu_c}{\rho_c D_{AW}} \qquad (4.3.3)$$

The above correlation is valid when the agitation power is increased beyond that needed for the suspension of solid particles and the turbulent forces become larger than the gravitational forces. The ratio $[P/V]$ is the power input per unit volume. Power consumption is related to the fluid viscosity of the continuous phase μ_c, the fluid density
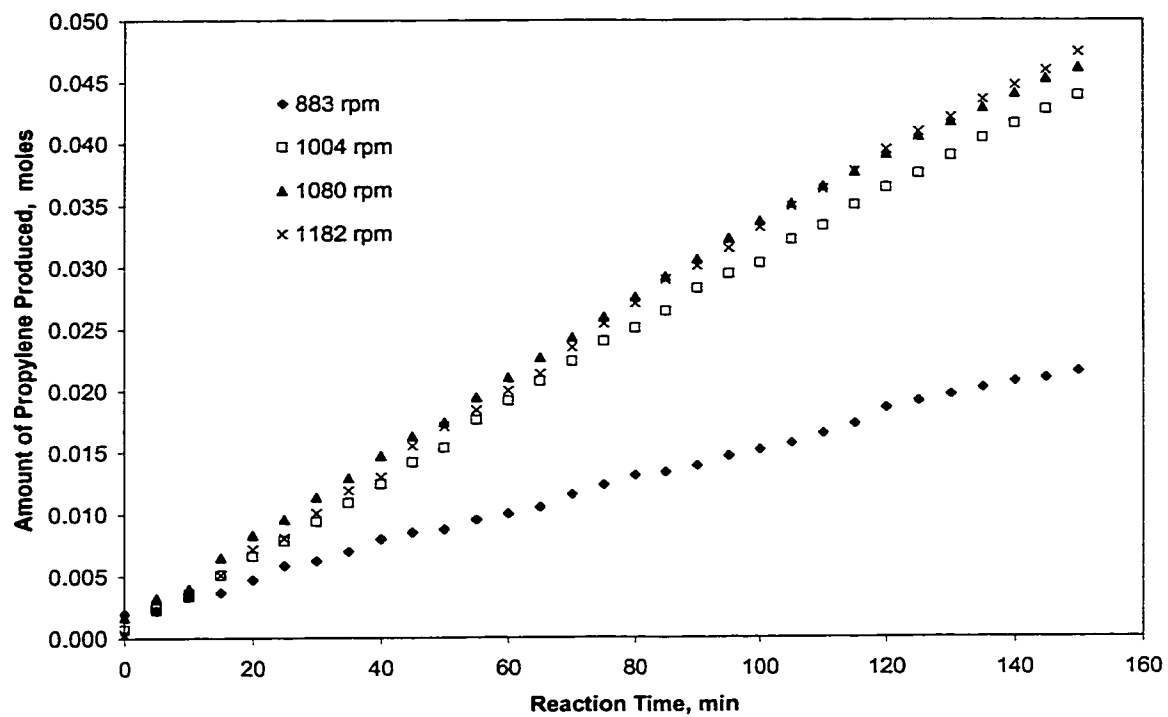
Figure 4.10 – Effect of Stirrer Speed on the Observed Rate of Propylene Formation over

Silicalite S-115 Al$_2$O$_3$: 10 mol % 2-propanol/water feed, 90 - 150 μm particle size, 463

K Reaction Temperature

of the continuous phase ρ_C, the impeller rotation speed N, and the impeller diameter D_a.

The power consumption, P, can be related to the above physical conditions through

experimental curves for various impeller types [Geankoplis, 1993] using the following

dimensionless parameters

$$N_{Re} = \frac{D_a^2 N \rho_C}{\mu_C}$$ (4.3.4)

and

$$N_P = \frac{P}{\rho_C N^3 D_a^5}$$ (4.3.5)

From equations 4.3.3 - 4.3.5, it can be seen that the Schmidt number and the power

consumption will remain nearly constant for initial 2-propanol concentrations less than

10 mol % because of the weak concentration dependency of the bulk fluid properties. It

can then be concluded that the external mass transfer coefficient k_L' will remain nearly

constant at a constant impeller stirrer speed. For this reason, the stirrer speed which

minimizes the influence of external mass transfer on the observed rate of propylene

formation for a 10 mol % 2-propanol feed will also minimize the influence of external

mass transfer on initial 2-propanol concentrations slightly lower than 10 mol %.

The region where the internal mass transfer is no longer rate limiting was

determined by varying the catalyst particle size and observing its influence on the

observed rate of propylene formation. Tests at 463 K at a catalyst loading of 1.57 weight

%, an initial 2-propanol concentration of 10 mol % and a stirrer speed of 1080 rpm

indicate that internal mass transfer is not rate limiting at particle size ranges of 595 - 850

μm, 400 - 595 μm and 90 - 150 μm (Figure 4.11).
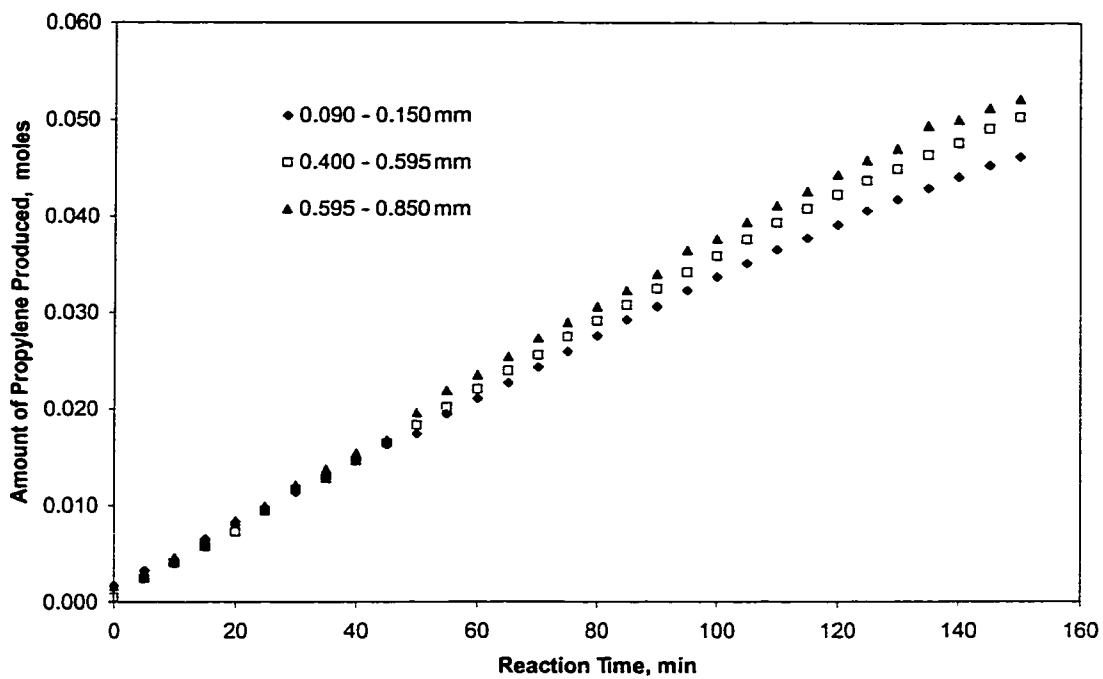
Figure 4.11 - Effect of Particle Size on the Observed Rate of Propylene Formation over

Silicalite S-115 Al$_2$O$_3$: 10 mol % 2-propanol/water feed, 1080 rpm Stirrer Speed, 463 K

Reaction Temperature

4.4 – Kinetic Study

All kinetic experiments were conducted at a stirrer speed of 1080 rpm with 400 -

595 μm particle sizes. A 10 mol % 2-propanol/water mixture was fed to the reactor along

with 1.57 weight % silicalite S-115 Al_2O_3 ExT. catalyst. Reaction rates were determined

at 434, 444, 453, and 463 K. The experimental data were fitted with several Langmuir-

Hinshelwood-Hougen-Watson (LHHW) type rate equations derived in Chapter 3

(equations 3.2.7, 3.2.11, 3.2.15, and 3.2.16). Model parameters, such as activation

energies and the heats of adsorption, calculated from the above fitted models are given in

Table 4.3.

A good kinetic model should not only be able to fit the experimental data, but it

should be able to predict the reaction rates under different conditions. To this end,

additional kinetic runs were carried out at 463 K for 2-propanol feed concentrations of 4,

6, and 8 mol %. This concentration range was chosen because it is in a dilute region,

which would correspond to typical wastewater concentrations. A concentration of 2 mol

% 2-propanol was not performed because the van Laar equation did not fit this dilute

region well (Figure 4.4). The kinetic parameters established using the 10 mol % initial 2-

propanol concentration kinetic runs were in turn used to predict the rate of propylene

formation at other initial 2-propanol concentrations.

It can be seen in Table 4.3 that the SSM-2 model, which has single-site adsorption

of both 2-propanol and water in the rate model is best able to predict the rate of propylene

formation for 2-propanol concentrations ranging from 4 – 10 mol %. This is consistent

with the E_1 type mechanism, involving only acid sites, which was proposed for 2-

propanol dehydration to propylene over zeolite catalysts (Chapter 1). Both models that

71

include the water adsorption/desorption parameter were better able to predict the rate of propylene formation than the models that did not include this term in the equation. This indicates that water does in fact inhibit the rate of propylene formation, despite the relative high hydrophobicity of silicalite. This partly explains the poor dehydration activity of some of the hydrophilic catalysts such as zeolite 13X and SAPO-5 found during the catalyst screening (Figure 4.7).

Figure 4.12 illustrates the amount of propylene produced with varying time at several reaction temperatures with the fitted SSM-2 model. The model gives a good fit of the experimental data for temperatures between 434 and 463 K. The temperature dependency of the rate constant, as seen in Chapter 3 (equation 3.2.17) is shown in Figure 4.13. As can be seen from Figures 4.12 and 4.13, the rate of propylene formation is strongly dependent on temperature. This high activation energy indicates that the kinetic data were obtained in a region where the diffusional effects are not rate limiting. The temperature variation of the adsorption constants for the SSM-2 rate model is shown in Figure 4.14. The adsorption plots have positive slopes, which indicates that the heat of adsorption is exothermic. It should be noted that these calculated heats of adsorptions are model parameters only and do not necessarily reflect any real physical phenomena. It has been found in the literature that calculated heats of adsorption are strongly dependent on the type of model used, i.e. single versus dual-site [Yue and Oloafe, 1984]. The calculated heats of adsorption for the SSM-2 model are much lower than one would expect to find for chemisorption.

The ability of the SSM-2 model to predict the rates of propylene formation at lower 2-propanol concentrations is demonstrated in Figure 4.15. It can be seen that the
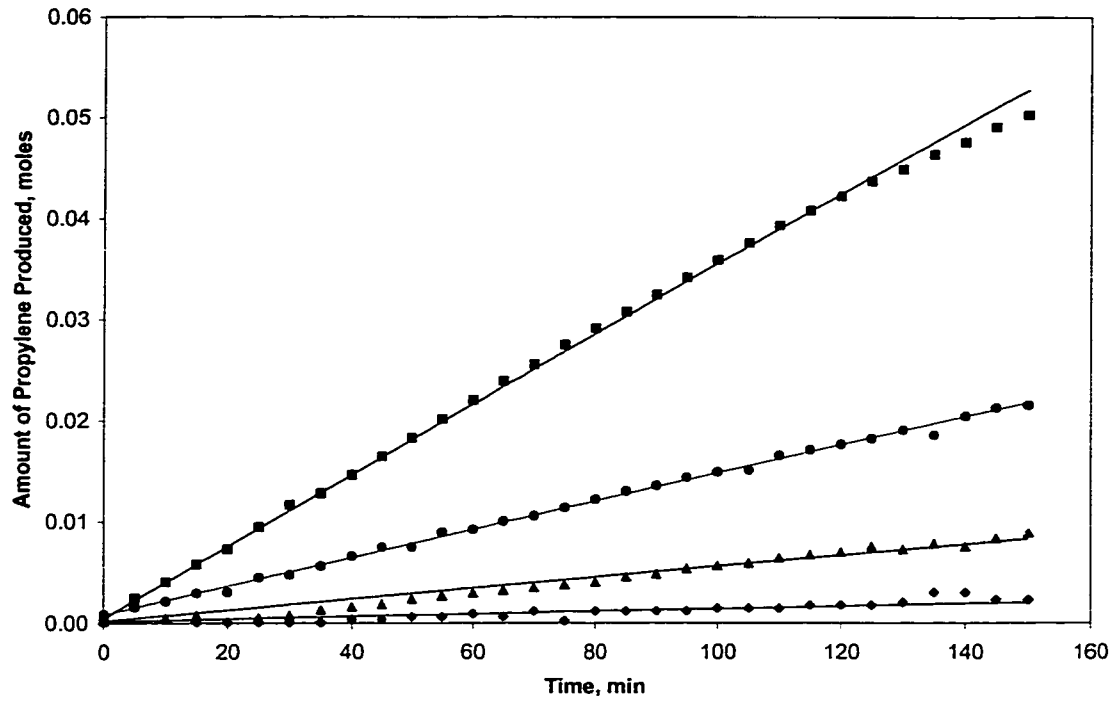
Figure 4.12 - Comparison of Experimental Rate Data with the Fitted SSM-2

Model at a Temperature Range of 434 – 463 K: (◆) 434 K, (▲) 444 K, (●) 453 K, (

■) 463 K, (—) SSM-2 Model Fit
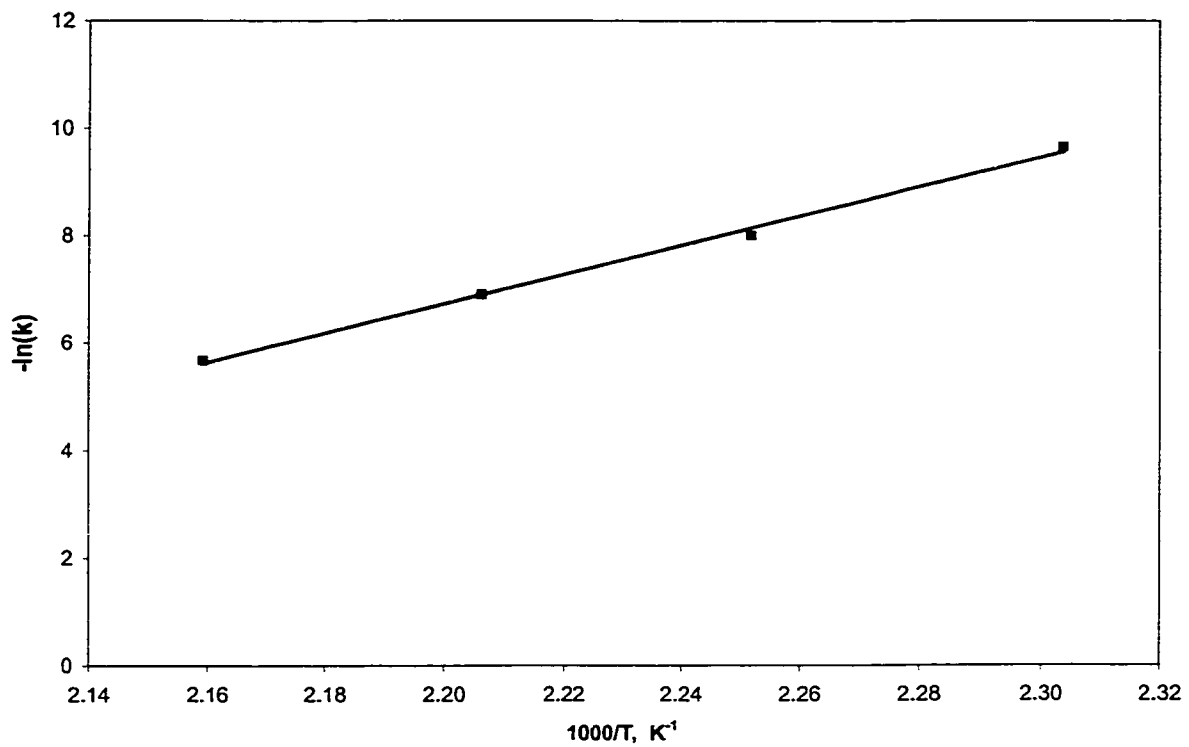
Figure 4.13 - Temperature Dependence of the Kinetic Parameters k, Determined from

the Fitted SSM-2 LHHW Model
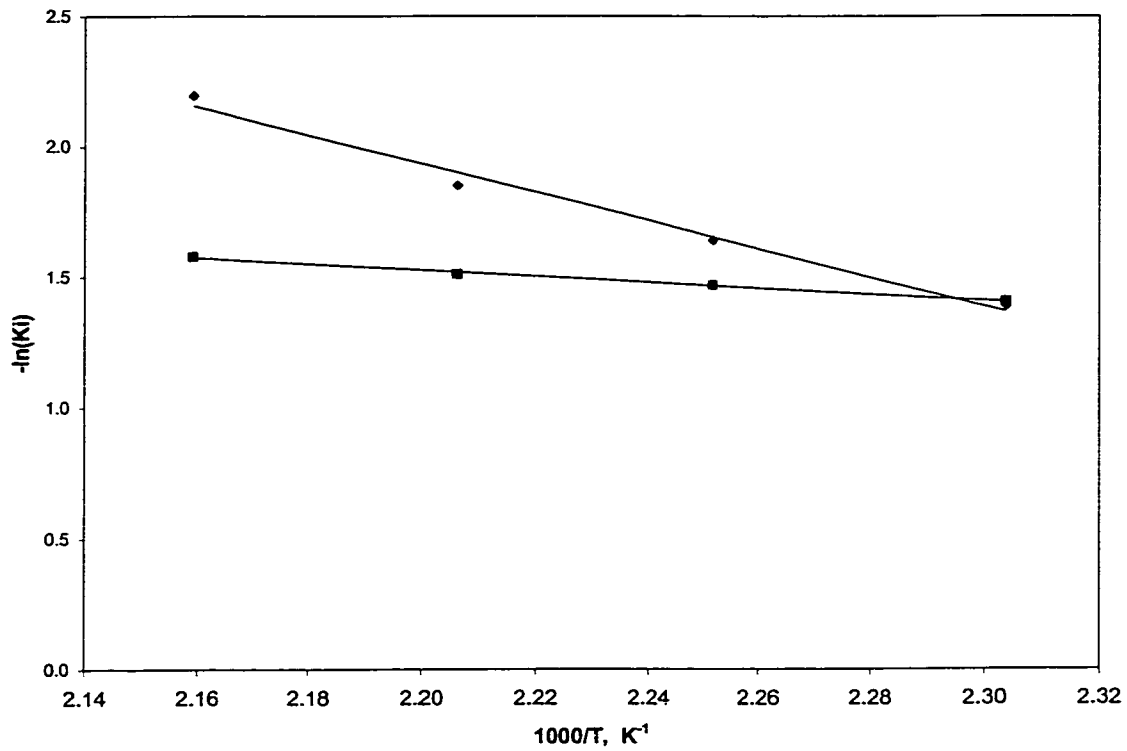
Figure 4.14 - Temperature Dependence of the Adsorption/Desorption Equilibrium

Constants Determined from the Fitted SSM-2 LHHW Model: (◆) 2-Propanol, (■)

Water
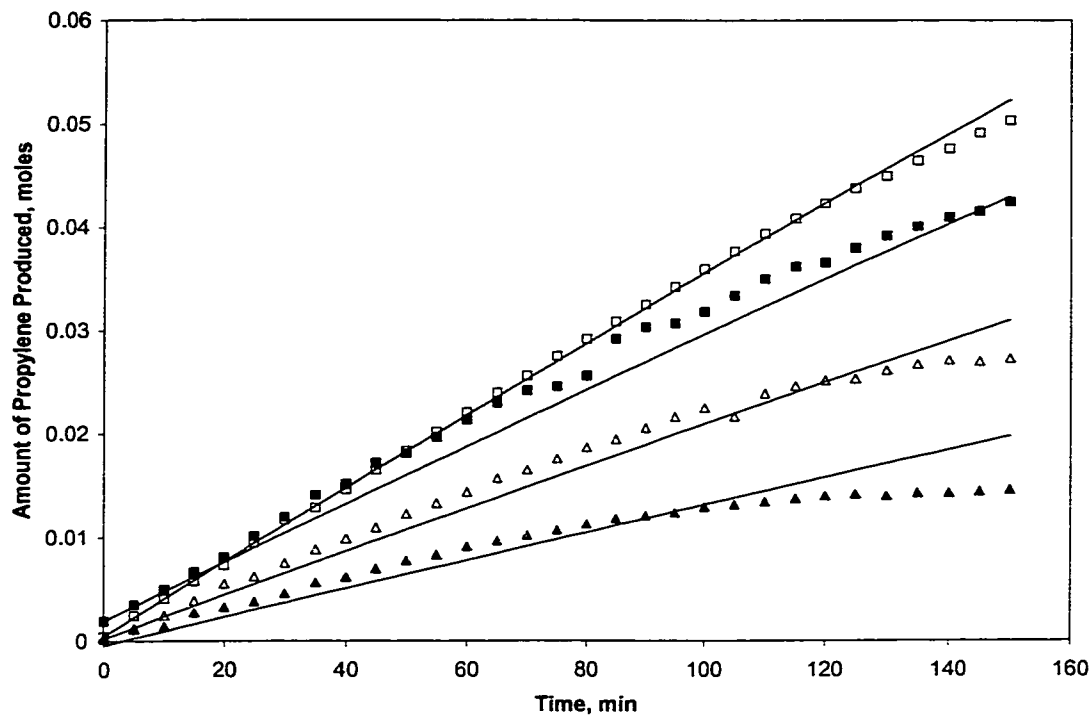
Figure 4.15 - Comparison of SSM-2 Model Prediction with the Rate of Propylene

Produced under Different Initial 2-Propanol Mole Fraction: (▲) 4 mol % 2-Propanol

Feed, (△) 6 mol % 2-Propanol Feed, (■) 8 mol % 2-Propanol Feed, (□) 10 mol % 2-

Propanol Feed, (——) SSM-2 Model

SSM-2 model is able to adequately predict the rates of propylene formation, but the fit is not perfect. Upon inspection of Figure 4.15, one would assume that a reverse reaction is occurring during the reaction. However, as was illustrated in section 4.2.2 of this Chapter, a reversible reaction was not significant during the kinetic runs. Another possible explanation for the apparent drop in propylene formation would be due to catalyst deactivation. Fresh and used samples of silicalite S-115 Al_2O_3 ExT. were examined using x-ray diffraction and BET. The used sample indicates a catalyst that was used for a typical kinetic run at a reaction temperature of 463 K for a duration of 2 hours. An observable change in the catalyst structure before and after the kinetic run would indicate that deactivation does occur during the run. The x-ray diffraction pattern for the fresh and 'used' catalyst is illustrated in Figure 4.16. From the x-ray diffraction pattern, there does not appear to be any noticeable difference in the catalyst structure before and after the dehydration run. The BET surface area for the fresh and used catalyst was determined to be 320.9 and 342.0 m^2 g^{-1} respectively; this difference in surface area is not significant. Based on the above measurements, the structure of the silicalite catalyst does not appear to undergo any significant structural change during the course of the kinetic run. Kinetic experiments on silicalite were performed using a fresh catalyst and a used catalyst that was reacted at 463 K with an initial 2-propanol concentration of 10 mol % for 2.5 hours. As can be seen in Figure 4.17, there does not appear to be any significant deactivation of the catalyst after the kinetic run. The apparent drop in propylene formation illustrated in Figure 4.15 cannot be attributed to the reversible reaction or catalytic deactivation. This indicates that a simple LHHW type rate equation is not sufficient to completely describe the observed phenomena, especially at high water
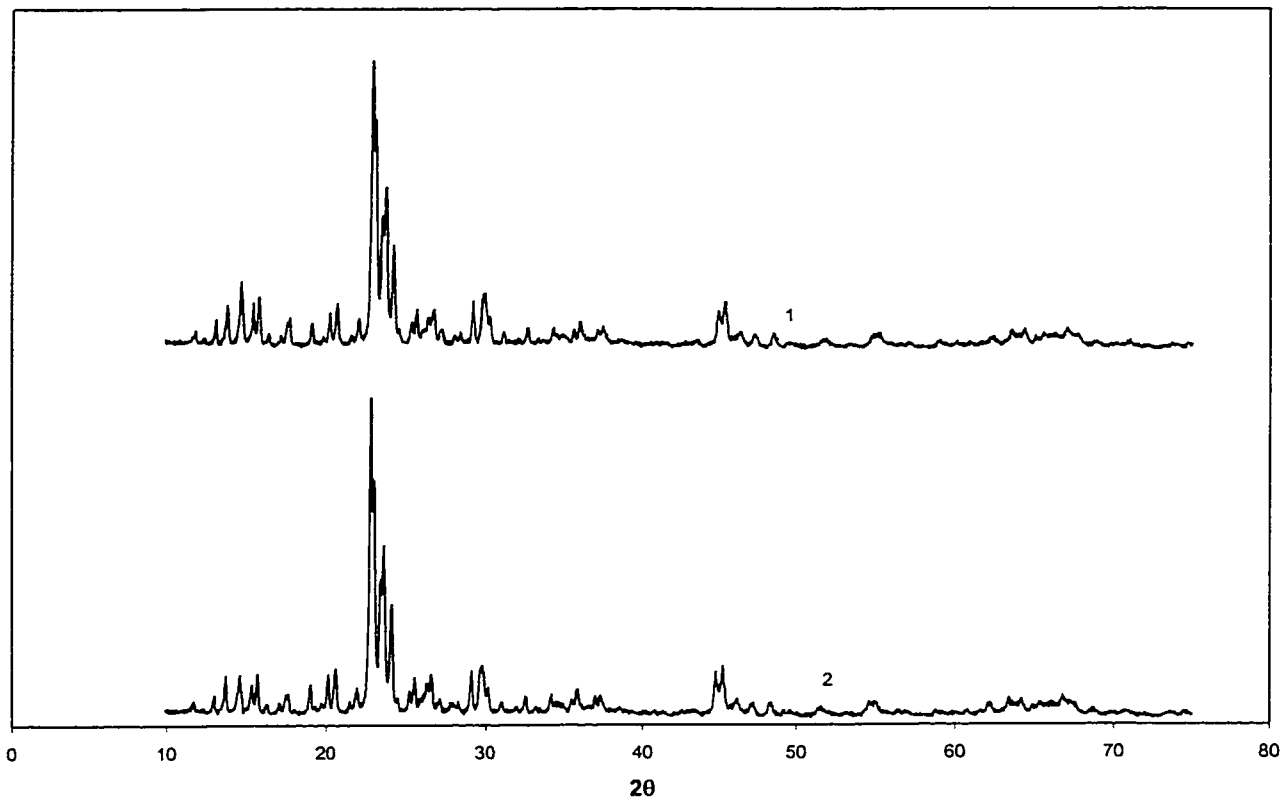
Figure 4.16 – Comparison of X-Ray Diffraction Pattern of Fresh Silicalite (S-115 Al$_2$O$_3$

ExT.) with Reacted Silicalite: 1 = Fresh, 2 = Reacted
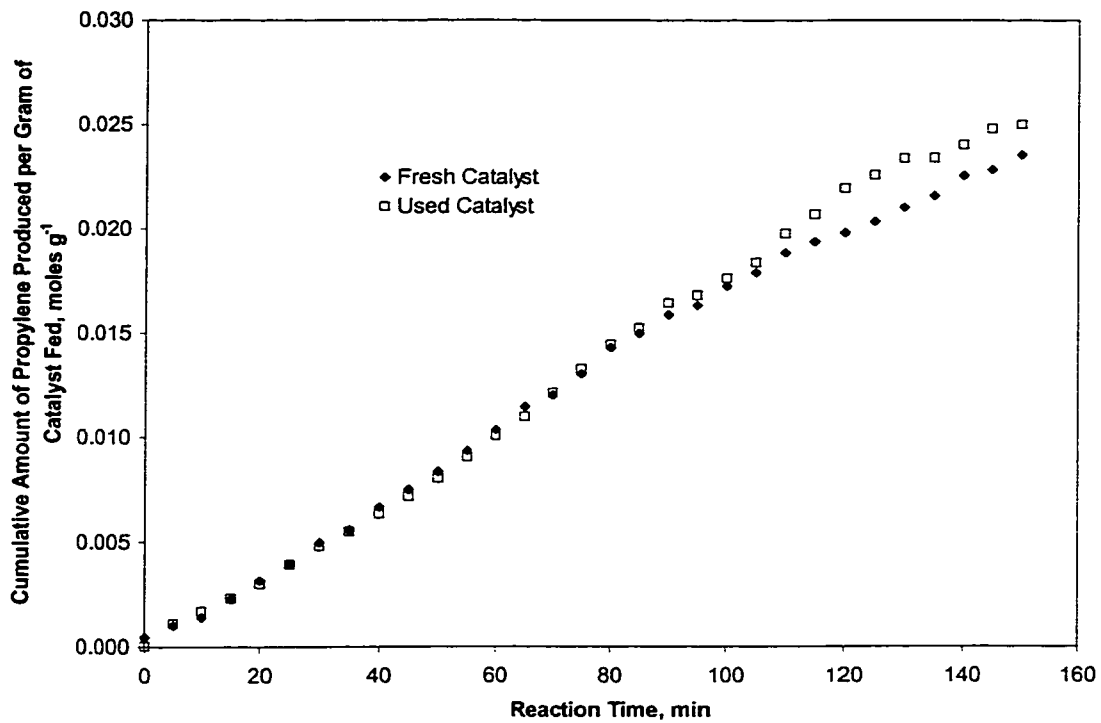
Figure 4.17 – Silicalite S-115 Al_2O_3 ExT. Catalyst Reusability: Initial 2-propanol

Concentration of 10 mol %, 30-40 Mesh Particle Size, 1080 rpm Stirrer Speed, Reaction

Temperature of 463 K: Used Catalyst Reacted for 2.5 Hours

concentrations. It is possible that a change in the reaction mechanism at very high water concentration may occur. Despite the deviations, the SSM-2 model does provide a very reasonable prediction of propylene formation. This kinetic model can be used in a suitable simulation package to design an appropriate wastewater purification process at an accuracy of ± 8.8 %.

4.5 – Catalyst Loading

The effect of the catalyst loading on the rate of propylene formation was determined by performing kinetic runs at catalyst loadings of 0.762 wt %, 1.106 wt % and 1.556 wt %. The experiments were performed at 463 K at an initial 2-propanol concentration of 10 mol %. The results of these experiments and the fitted SSM-2 model are given in Figure 4.18. The calculated kinetic parameters should not be affected by the catalyst loading, otherwise the assumption of a uniformly mixed vessel is invalid. As can be seen in Figure 4.19, the calculated kinetic parameters appear to be independent of the catalyst loading.

The established LHHW rate equation is:

$$r = \frac{1}{m_C} \frac{d\alpha}{dt} = \frac{k_s K_A C_A}{1 + K_A C_A + K_w C_w} \tag{4.4.1}$$

$$k_s = 1.406 \cdot 10^{23} \exp\left(-\frac{25148}{T}\right) \tag{4.4.2}$$

$$K_A = 8.32 \cdot 10^{-7} \exp\left(\frac{5472}{T}\right) \tag{4.4.3}$$

$$K_w = 1.66 \cdot 10^{-2} \exp\left(\frac{1154}{T}\right) \tag{4.4.4}$$
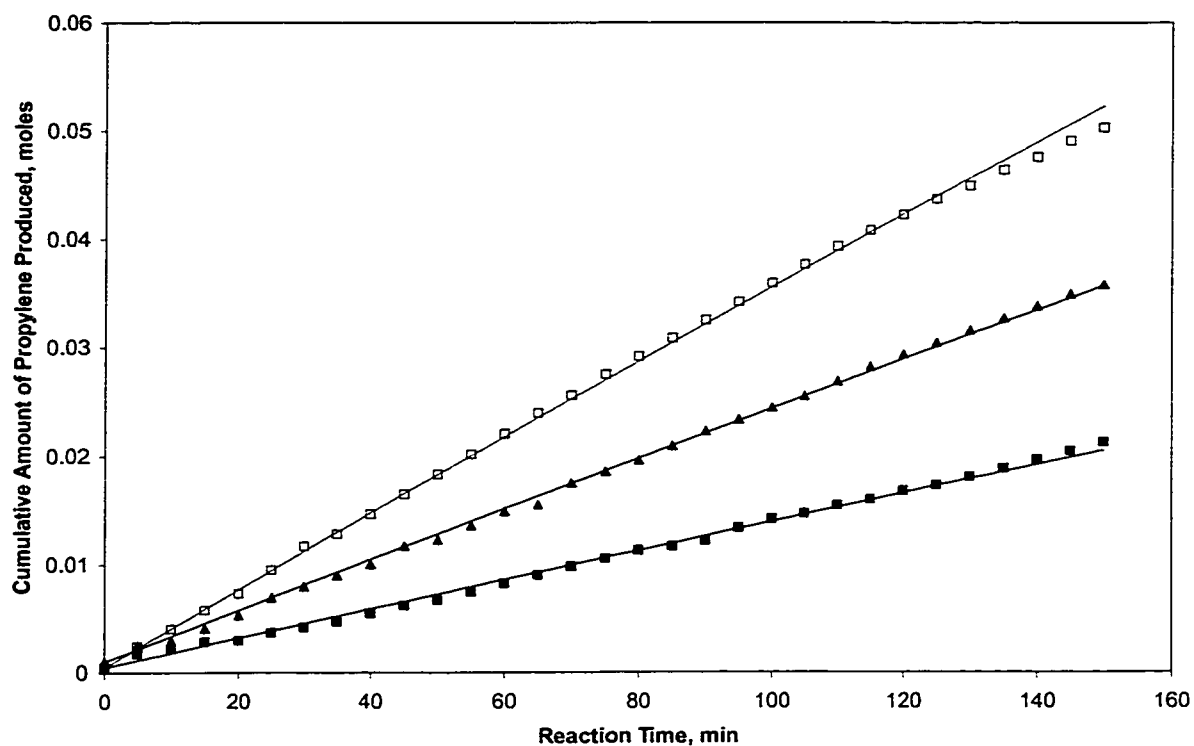
Figure 4.18 – Effect of Silicalite S-115 Al_2O_3 ExT. Loading on the Rate of Propylene

Formation: 10 mol % 2-Propanol Feed at a Reaction Temperature of 463 K: (□) 1.556

wt %, (▲) 1.106 wt %, (■) 0.762 wt %, (—) SSM-2 Model Fit
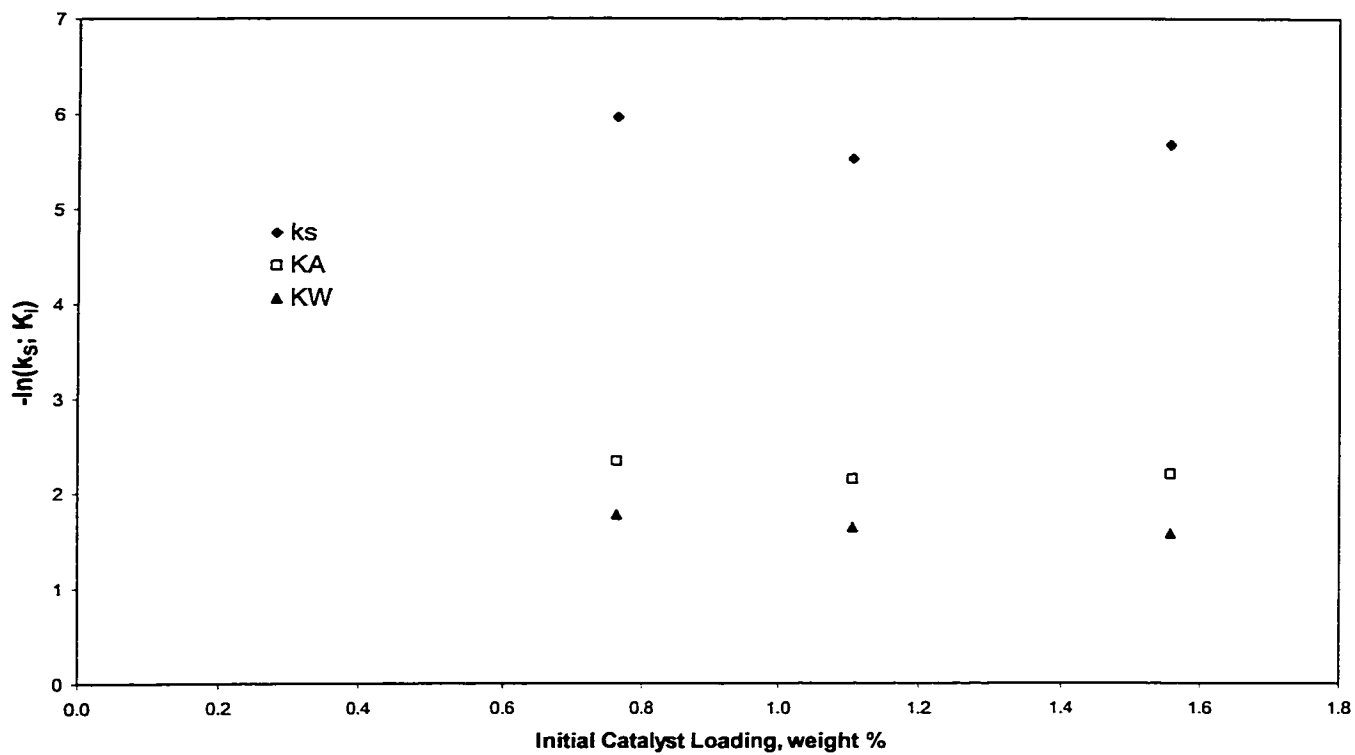
Figure 4.19 – Effect of Silicalite S-115 Al_2O_3 ExT. Loading on the Kinetic Parameters:

10 mol % 2-Propanol Feed at a Reaction Temperature of 463 K

4.6 – First Order Model

The previous chapters outlined a method which can be used to fit experimental rate data for the liquid-phase dehydration of 2-propanol. LHHW rate models were derived and fitted with experimental data because of their wide acceptance in vapor phase alcohol dehydration reactions. With this in mind, it should be noted that the experimental data was fitted over a fairly narrow range of 2-propanol concentrations and that a six-parameter model is perhaps too complex for such a small range. A simple firstconcentrations. Figure 4.20 illustrates the first order model fit at 463 K over a 2-propanol concentration range of 4 – 10 mol %. The temperature dependence of the rate of propylene formation at reaction temperatures ranging from 434 to 463 K is illustrated in Figure 4.21. The Arrhenius temperature dependence of the rate constant (equation 3.2.17) is illustrated in Figure 4.22. As was previously concluded, the high activation energy (195.8 kJ mole^{-1}) indicates that the kinetic experiments were performed in a region where the influence of internal and external mass transfer is not significant. The first order rate model is expressed mathematically as:

$$r = \frac{1}{m_c}\frac{d\alpha}{dt} = k_s\, C_A \tag{4.6.1}$$

$$k_s = 6.488 \cdot 10^{17}\, \exp\left(\frac{23548}{T}\right) \tag{4.6.2}$$

It is recommended that for the purposes of simulating a wastewater purification process, where 2-propanol will be present in dilute concentrations, that the first order model be used due to it's mathematical simplicity and accuracy. This model should not be used to extrapolate rates of propylene formation beyond the experimental concentration range. If
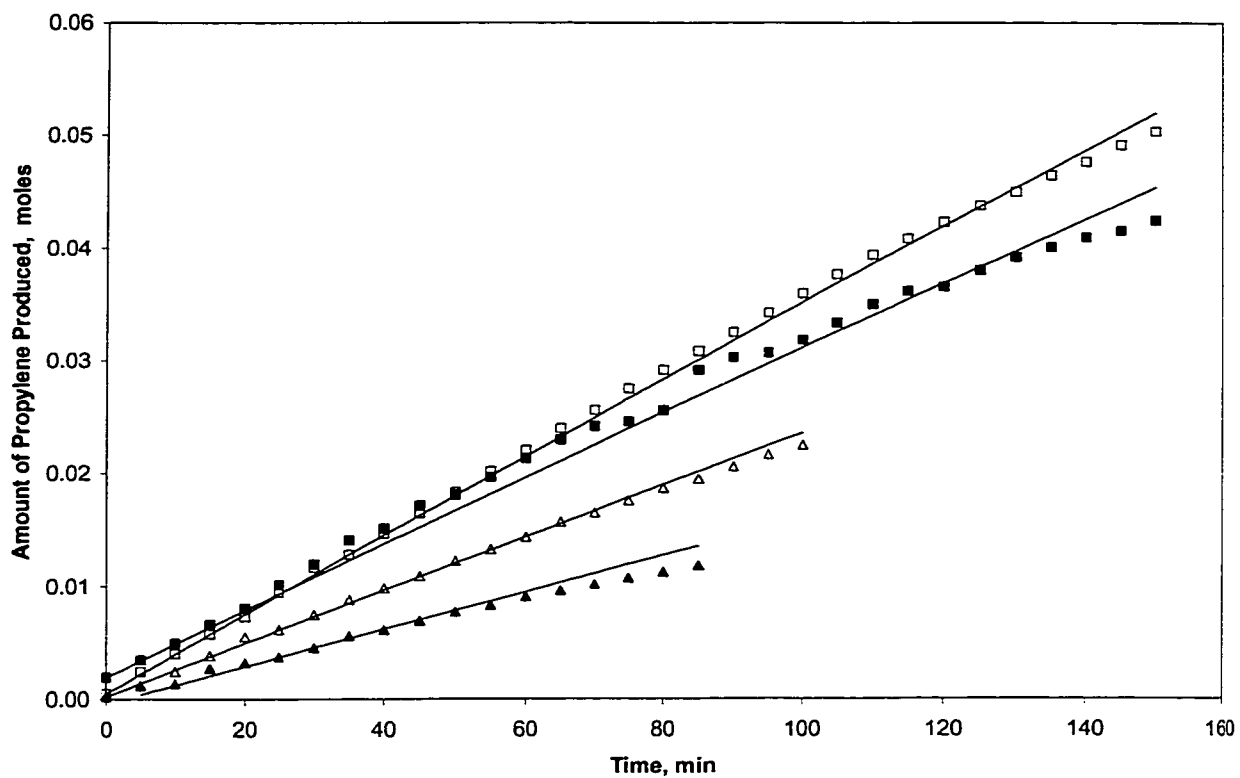
Figure 4.20 – Concentration Dependence of 2-Propanol on the Rate of Propylene

Formation at 463 K:(▲) 4 mol % 2-Propanol Feed, (△) 6 mol % 2-Propanol Feed, (■)

8 mol % 2-Propanol Feed, (□) 10 mol % 2-Propanol Feed, (—) 1st Order Model Fit
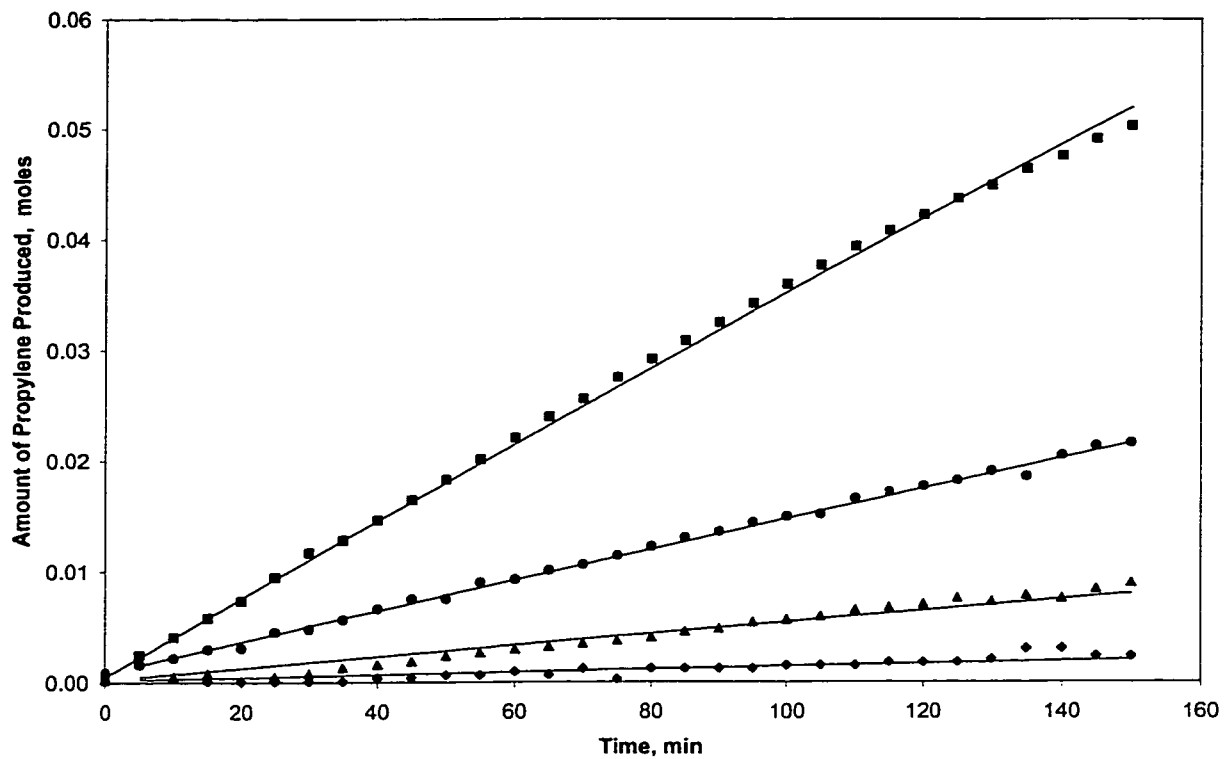
Figure 4.21 - Comparison of Experimental Rate Data with the Fitted 1st Order Model at a

Temperature Range of 434 – 463 K: (◆) 434 K, (▲) 444 K, (●) 453 K, (■) 463 K,

(—) 1st Order Model Fit
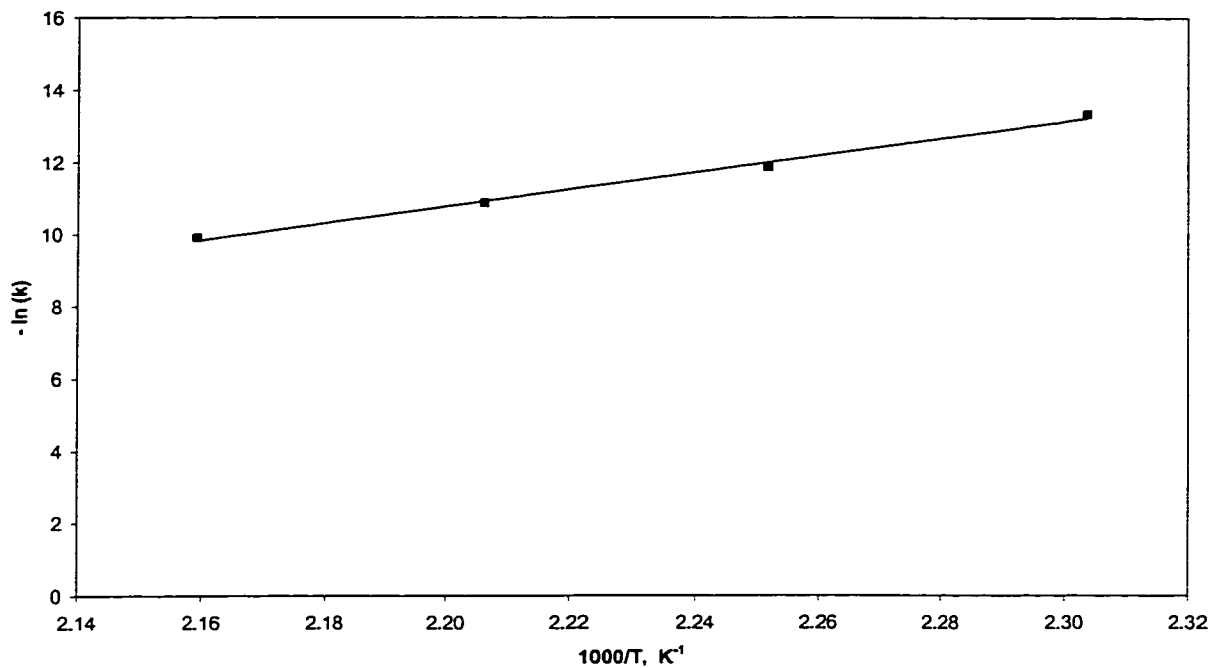
**Figure 4.22** - Temperature Dependence of the Kinetic Parameters k, Determined from the

Fitted 1st Order Model

rate data is acquired over a large range of 2-propanol concentrations, it is recommended that the LHHW models previously derived be used to fit the experimental data because of their wide acceptance in vapor-phase dehydration kinetics.

4.7 – Nomenclature

a $\quad$ = activity

C $\quad$ = binary constant for the van Laar equation

$\quad$ = liquid phase concentration of component, mole L^{-1}

C_P^0 $\quad$ = constant pressure heat capacity, J mole^{-1} K^{-1}

D $\quad$ = diameter, m

$\quad$ = diffusivity, m^2 /s

E_A $\quad$ = acitvation energy, kJ mole^{-1}

f $\quad$ = fugacity, kPa

ΔH_A $\quad$ = heat of adsorption, kJ mole^{-1}

ΔH^0 $\quad$ = standard enthalpy change for the reaction, kJ mole^{-1}

K $\quad$ = adsorption/desorption equilibrium constant, L mole^{-1}

$\quad$ = chemical equilibrium constant

k $\quad$ = rate constant for 2-propanol dehydration, mole g^{-1} min^{-1}

k_L' $\quad$ = liquid mass transfer coefficient, m/s

L $\quad$ = moles of liquid, mole

m $\quad$ = mass, g

M $\quad$ = moles of component prior to reaction, mole

Mw $\quad$ = molecular weight of component, g / mole

N $\quad$ = moles of compound, mole

N	= impeller rotation speed, rev/s
N_P	= number of data points
	= power consumption number
N_{sc}	= Schmidt number
P	= pressure, kPa
	= agitator power consumption, kJ
R	= gas constant, 8.31451 J mole^{-1} K^{-1}
r	= rate of formation, mole g^{-1} min^{-1}
S_{ex}	= external catalyst surface area, m^2
T	= temperature, K
t	= time, min; sec
V	= moles of vapor, mole
	= volume, m^3
x	= liquid mole fraction
y	= vapor mole fraction
Z	= compressibility factor

Greek Letters

α	= cumulative amount of propylene produced at time t, mole
ϕ	= fugacity coefficient
γ	= activity coefficient
μ	= liquid-phase viscosity, kg/m s
ρ	= saturated liquid density, g/cc; kg/m^3
Σ	= summation

υ = stoichiometric coefficient

Subscripts

0 = standard state, 298 K, 1 atm

a = impeller/agitator

A = 2-propanol

b = bulk phase

C = catalyst

  = continuous phase

f = formation

H = helium

i = component

P = propylene

S = surface

T = total

W = water

Superscripts

0 = pure phase

G = gas phase

L = liquid phase

SAT = saturated

V = vapor phase

Table 4.1 – BET Surface Area for the Screened Catalysts

Catalyst	BET Surface Area (m²/g)
S-115 Al_2O_3 ExT.	320.89
S-115 SiO_2 ExT.	348.33
SAPO-5	327.05
Zeolite 13X	239.52
Alumina	323.21

Table 4.2 – Enthalpy and Gibbs Free Energy of Formation and the Temperature

Dependence of the Heat Capacity for Reactant and Products

Compound	$\Delta H^{\circ}f$ (J/mol)	$\Delta G^{\circ}f$ (J/mol K)	a (J/mol K)	b (J/mol K^2)	c (J/mol K^3)	d (J/mol K^4)
2-Propanol	-318200	-180500	331.2	-2.7507	0.010227	-1E-05
Water	-286000	-237400	65.656	0.12677	-0.00051	6.66E-07
Propylene	20400	62760	3.14754	0.237884	-0.00012	2.46E-08
Σvi	52600	5860	-262.396	3.115354	-0.01086	1.06E-05

Table 4.3 – Parameters and Predictions of the Developed LHHW Kinetic Models

Model	E_A (kJ mol^{-1})	r^2	$\Delta H_{A,A}$ (kJ mol^{-1})	r^2	$\Delta H_{A,W}$ (kJ mol^{-1})	r^2	model fit * (%)
SSM-1	209.1	0.994	-26.9	0.991	-	-	18.2
DSM-1	199.7	0.996	-36.4	0.842	-	-	26.7
SSM-2	226.8	0.996	-45.5	0.987	-9.6	0.994	8.8
DSM-2	166.6	0.981	-30.3	0.870	-30.5	0.835	11.8

$$* \ \% \ \text{Model Fit} = \frac{100}{N_P} \sum_{i=1}^{N} \left| \frac{\alpha_{EXP} - \alpha_{PRED}}{\alpha_{EXP}} \right|$$

4.8 – Literature Cited

Flanigen, E. M., J. M. Bennett, R. W. Grose, J. P. Cohen, R. L. Patton, R. M. Kirchner, and J. V. Smith, "Silicalite, a New Hydrophobic Crystalline Silica Molecular Sieve", *Nature* **271**, 512-516 (1978)

Geankoplis, C. J., "Transport Processes and Unit Operations", 3rd. Ed., Prentice-Hall, Englewood Cliffs (1993)

Hedge, S. G., P. Ratnasamy, L. M. Kustov, and V. B. Kazansky, "Acidity and Catalytic Activity of SAPO-5 and AlPO-5 Molecular Sieves", *Zeolites* **8**, 137-141 (1988)

Kyle, B. G., "Chemical and Process Thermodynamics", 2nd. Ed. Prentice Hall, Englewood Cliffs (1992)

Le van Mao, R., T. M. Nguyen and J. Yao, "Conversion of Ethanol in Aqueous Solution over ZSM-5 Zeolites. Influence of Reaction Parameters and Catalyst Acidic Properties as Studied by Ammonia TPD Technique", *Appl. Catal.* **61**, 161-173 (1990)

Levenspiel, O., "Chemical Reaction Engineering", 2nd. Ed., John Wiley and Sons, New York (1972)

Olson, D. H., W. O. Haag and R. M. Lago, "Chemical and Physical Properties of the ZSM-5 Substitutional Series", *J. Catal.* **61**, 390-396 (1980)

Oudejans, J. C., P. F. van den Oosterkamp and H. van Bekkum, "Conversion of Ethanol over Zeolite H-ZSM-5 in the Presence of Water", *Appl. Catal.* **3**, 109-115 (1982)

Phillips, C. B., and R. Datta, "Production of Ethylene from Hydrous Ethanol on H-ZSM-5 Under Mild Conditions", *Ind. Eng. Chem. Res.* **36**, 4466-4475 (1997)

Rees, L. V. C., "When is a Zeolite not a Zeolite?", *Nature* **296**, 491-492 (1982)

Schulz, J., and F. Bandermann, "Conversion of Ethanol over Zeolite H-ZSM-5", *Chem. Eng. Tech.* **17**, 179-186 (1994)

Yue, P. L. and O. Olaofe, "Kinetic Analysis of the Catalytic Dehydration of Alcohols over Zeolties", *Chem. Eng. Res. Des.* **62**, 81-91 (1984)

Chapter 5

Conclusions and Recommendations

5.1 – Conclusions

2-Propanol dehydrates over solid acid catalyst in an aqueous medium to form propylene and trace amounts of diisopropyl ether and acetone. Alumina, zeolite 13X, silicoaluminophosphate, silicalite with a silica binder (S-115 SiO_2 ExT.) and silicalite with an alumina binder (S-115 Al_2O_3 ExT.) were active for the catalytic dehydration of 2-propanol at 463 K. Of these catalysts, silicalite with an alumina binder (S-115 Al_2O_3 ExT.) was the most active in the dehydration of 2-propanol in the aqueous medium. The use of alumina as a binder greatly influences the 2-propanol dehydration activity of silicalite.

The kinetics of the catalytic dehydration in an aqueous medium was determined for 2-propanol concentrations between 4 - 10 mol % and temperatures ranging between 434 and 463 K in a batch slurry reactor system. The influence of stirrer speed, catalyst particle size, catalyst loading, reaction temperature, and 2-propanol concentration on the rate of propylene formation was investigated. The influence of external mass transfer on the rate of propylene formation was insignificant at stirrer speeds greater than 1000 rpm. The influence of internal mass transfer on the rate of propylene formation was insignificant at particle diameters ranging from 90 - 850 μm.

Several Langmuir-Hinshelwood-Hougen-Watson (LHHW) mechanisms were proposed and screened. The equilibrium conversion of 2-propanol to propylene is much higher than what was attained during the kinetic runs, hence all LHHW models assumed a negligible reversible reaction. The models which include the adsorption/desorption of

water on the active sites were better able to predict the rate of propylene formation than models in which fast desorption of water was assumed. A single site LHHW type mechanism was found to describe the kinetic data well. This model is consistent with the E_1 type mechanism involving only acid sites proposed in the literature for the 2-propanol dehydration to propylene over zeolite catalysts.

The developed rate equation is:

$$r = kK_AC_A /(1 + K_AC_A + K_WC_W)$$

The influence of reactor temperature on the rate of propylene formation is significant. The activation energy was determined to be 226.8 kJ/mol while the heat of adsorption for 2-propanol and water was -45.5 and -9.6 kJ/mol, respectively. These heats of adsorptions are model parameters only and do not necessarily reflect any real physical phenomena. The high activation energy indicates that the kinetic data were obtained in a region where the diffusional effects were not rate limiting.

A simplified first order model was also found to fit the experimental data well. The activation energy was determined to be 195.8 kJ/mol. For the purpose of designing an appropriate separation process for wastewater purification it is recommended that the simple first order model be used, due to its simplicity and accuracy at low 2-propanol concentrations. Due to the small range of 2-propanol concentrations studied in this thesis, a six-parameter model may be too complex. Rate data over a wider range of 2-propanol concentrations need to be determined in order to make the LHHW models more feasible.

5.2 – Recommendations for Future Work

5.2.1 – Simulation of Wastewater Purification Process

In order to determine whether a separation process, such as catalytic distillation, is more economically feasible than a conventional separation process, such as distillation, a computation simulation must be performed using the developed kinetic model. A commercial software package such as Aspen plus could be used for the simulation. The influence of operating parameters on the number of stages would be performed for both the catalytic distillation and the conventional distillation process. The catalytic distillation process may be more economical than conventional distillation.

5.2.2 – Hydration of Propylene over Solid Acid Catalysts

Recent work on the hydration of propylene over H-ZSM-5 catalysts have been found in the literature [Sonnermans, 1993ab]. Catalytic hydration of alkenes to give alcohols and ethers is an established commercial technology of significant commercial interest [Waddams, 1978]. However, like the dehydration of 2-propanol, propylene hydration has only been studied in the vapor-phase. In studying the kinetics of the liquid-phase catalytic hydration of propylene the reverse reaction (dehydration of 2-propanol) must be known. The techniques developed in this thesis for the dehydration of 2-propanol can be used for this end.

The reaction temperatures used to determine the dehydration kinetics in this thesis ranged from 434-463 K. At these temperatures, the forward reaction is dominant. The liquid-phase hydration of propylene is more thermodynamically favorable at a lower reaction temperature, hence it would occur at more moderate reaction temperatures

ranging between 363 – 393 K. The dehydration of 2-propanol over silicalite requires

reaction temperatures higher than 434 K for any significant conversion. It is unlikely that

any significant conversion would occur at the low reaction temperatures required for

propylene hydration. It was recently determined that Amberlyst 38, a commercial ion-

exchange resin, is active at reaction temperatures as low at 373 K. The 2-propanol

dehydration kinetics should be determined for Amberlyst 38 at reaction temperature

ranging from 363 K to 423 K. The 2-propanol dehydration kinetics would be used with

the propylene hydration kinetics (determined separately) for the complete reaction model.

5.2.3 – Effect of Silica/Alumina Ratio on the Rate of Propylene Formation

As was recently concluded by Olson and co-workers (1980), the acidity and

hydrophilicity of H-ZSM-5 catalysts are directly proportional to the alumina content. As

was seen in section 4.2.2, the type of binder used in silicalite had a great effect on the rate

of propylene formation in the aqueous phase. The alumina present in the binder appeared

to influence the rate of propylene formation greatly.

The influence of the silica/alumina ratio of H-ZSM-5 type zeolites on the rate of

propylene formation should be determined. It is hypothesized that an ideal Si/Al ratio

could be determined because a high alumina content would contain a high amount of acid

sites necessary for 2-propanol dehydration, but would also be more hydrophilic which is

detrimental to propylene formation.

5.2.4 – Effect of Metal Ion Concentration in Wastewater on the Rate of Propylene Formation

The experiments used to determine the reaction kinetics of silicalite were

performed using deionized water. It can be assumed that wastewater containing 2-

propanol may contain metal ions in a significant concentration which may be detrimental to the life of the catalyst and the rate of propylene formation. It has been determined that cation exchanged alumina is less active in 2-propanol dehydration than alumina which has not been exchanged [Saad et al., 1993; Gervasini et al., 1995; 1997].

Kinetic experiments performed using tap water instead of deionized water indicate that cations present in tap water has a detrimental effect on the rate of propylene formation. Figure 5.1 illustrates that the resulting catalyst, which was reacted with a mixture of 2-propanol and tap water at 463 K, is less active in propylene formation. It is concluded that silicalite can undergo an ion exchange with the cations present in water and that the resulting catalyst is more basic in nature.

A more scientific and systematic method in studying this phenomena should be performed in future experiments. The influence of the loading of various ions present in industrial wastewater on the rate of propylene formation and on the catalyst deactivation should be studied.
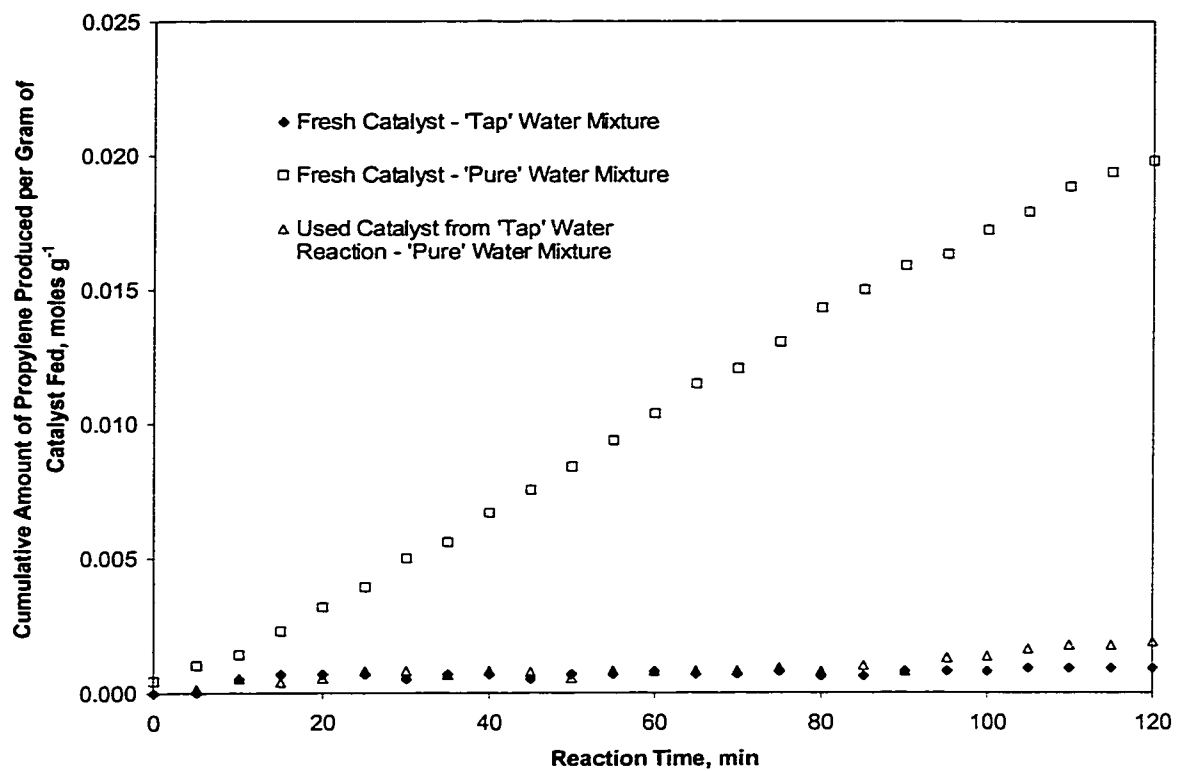
Figure 5.1 – Effect of Metal Ions Present in Tap Water on the Rate of Propylene

Formation and Catalyst Deactivation: 10 mol % 2-Propanol Feed, Reaction Temperature

of 463 K (Used Catalyst from Tap Water Reaction used in Kinetic Run with Deionized

Water in the Feed)

5.3 – Literature Cited

Gervasini, A., G. Bellussi, J. Fenyvesi, and A. Auroux, "Microcalorimetric and Catalytic Studies of the Acidic Character of Modified Metal Oxide Surfaces. 1. Doping Ions on Alumina, Magnesia, and Silica", *J. Phys. Chem.* **99**, 5117-5125 (1995)

Gervasini, A., J. Fenyvesi and A. Auroux, "Study of the Acidic Character of Modified Metal Oxide Surfaces Using the Test of Isopropanol Dehydration", *Cat. Letters.* **43**, 219-228 (1997)

Olson, D. H., W. O. Haag and R. M. Lago, "Chemical and Physical Properties of the ZSM-5 Substitutional Series", *J. Catal.* **61**, 390-396 (1980)

Saad, A. B. M., V. A. Ivanov, J. C. Lavalley, P. Nortier, and F. Luck, "Comparitive Study on the Effects of Sodium Impurity and Amorphisation on the Lewis Acidity of γ-Alumina", *Appl. Catal. A.* **94**, 71-83 (1993)

Sonnemans, M. H. W., "Hydration and Etherification of Propene over H-ZSM-5. 2. Deposition of Carbonaceous Compounds on the Catalysts", *Ind. Eng. Chem. Res.* **32**, 2512-2515 (1993a)

Sonnemans, M. W. H., "Hydration of Propene over Acidic Zeolites", *Appl. Catal. A.* **94**, 215-229 (1993b)

Waddams, A. L., "Chemicals from Petroleum : An Introductory Survey", 4th Ed., Murray, London (1978)

Appendix A1

Maple V Worksheet for the Determination of the Amount of Propylene Produced

Note : 'Pgauge' is the gauge pressure measured by the pressure transducer in psig
'T' is the reaction temperature in degrees Celsius
'massA' and 'massW' are the grams of isopropanol and water added to the reactor, respectively
'Tnaught' is the reactor temperature prior to heating in degrees Celsius
'Pnaught' is the gauge pressure prior to heating (after helium purge) in psig
Units of the calculated parameters are found at the end of Chapter 3
Determination of the Amount of Propylene Produced at T and P   Physical Conditions
- Initial and Final T and P, Initial Moles of Inert and Reactant > Pgauge:=451:
> P:=(Pgauge+14.7+4)*101.325/14.7:
> T:=190:
> massA:=38.109:
> massW:=100.173:
> Tnaught:=24:
> Pnaught:=-1.5:
> Ma:=massA/60.096:
> Mw:=massW/18.015:
> Mh:=(Pnaught+14.7+4)*101325*(319-massA/0.75-massW)*1e-6/(8.31451*(Tnaught+273.15)*14.7);

$$Mh := .008062382275$$

> Mt:=Ma+Mw+Mh;

$$Mt := 6.202730655$$

> R:=8.31451:
      Determination of the Liquid Phase Fugacity of Pure Components 2-Propanol (1) and Water (2)
      Modified Peng-Robinson Equation of State (PRSV)
> Tc1:=508.40:Pc1:=4764.25:omega1:=0.66372:kappa11:=0.23264:
> Tc2:=647.286:Pc2:=22089.75:omega2:=0.34380:kappa12:=-0.06635:
> Tr1:=(T+273.15)/Tc1:Tr2:=(T+273.15)/Tc2:
> kappa1:=(0.378893+1.4897153*omega1-0.17131848*(omega1)^2+0.0196554*(omega1)^3)+kappa11*(1+sqrt(Tr1))*(0.7-Tr1):
> kappa2:=(0.378893+1.4897153*omega2-0.17131848*(omega2)^2+0.0196554*(omega2)^3)+kappa12*(1+sqrt(Tr2))*(0.7-Tr2):
> a11:=(0.457235*R^2*Tc1^2/Pc1)*(1+kappa1*(1-sqrt(Tr1)))^2:
> a22:=(0.457235*R^2*Tc2^2/Pc2)*(1+kappa2*(1-sqrt(Tr2)))^2:
> b1:=0.077796*R*Tc1/Pc1:
> b2:=0.077796*R*Tc2/Pc2:
> A1L:=a11*P/(R*(T+273.15))^2:
> A2L:=a22*P/(R*(T+273.15))^2:

```
> B1L:=b1*P/(R*(T+273.15)):
> B2L:=b2*P/(R*(T+273.15)):
> q:=Z1L^3+(B1L-1)*(Z1L)^2+(A1L-3*(B1L)^2-2*B1L)*Z1L+((B1L)^3+(B1L)^2-
A1L*B1L)=0:
> w:=solve(q,Z1L):
> e:=w[1]:
> r:=Z2L^3+(B2L-1)*(Z2L)^2+(A2L-3*(B2L)^2-2*B2L)*Z2L+((B2L)^3+(B2L)^2-
A2L*B2L)=0:
> t:=solve(r,Z2L):
> y:=t[1]:
> phi1L:=exp(e-1-ln(e-B1L)-A1L/(2*sqrt(2)*B1L)*ln((e+(1+sqrt(2))*B1L)/(e+(1-
sqrt(2))*B1L))):
> phiAL:=simplify(phi1L):
> phi2L:=exp(y-1-ln(y-B2L)-A2L/(2*sqrt(2)*B2L)*ln((y+(1+sqrt(2))*B2L)/(y+(1-
sqrt(2))*B2L))):
> phiWL:=simplify(phi2L):
> fugAL:=phiAL*P;
```

$$fugAL := 1691.188114$$

```
> fugWL:=phiWL*P;
```

$$fugWL := 1195.745861$$

Determination of the Saturated Liquid Molar Volume of Pure Components 2-
Propanol(1) and Water (2)
        COSTALD (1979) Correlation
```
> Vo1:=0.2313:omega1SRK:=0.6637:
> Vo2:=0.0435669:omega2SRK:=-0.65445:
> ax:=-1.52816:bx:=1.43907:cx:=-0.81446:dx:=0.190454:ex:=-0.296123:fx:=0.386914:
> gx:=-0.0427258:hx:=-0.0480645:
> Vro1:=1+ax*(1-Tr1)^(1/3)+bx*(1-Tr1)^(2/3)+cx*(1-Tr1)+dx*(1-Tr1)^(4/3):
> Vro2:=1+ax*(1-Tr2)^(1/3)+bx*(1-Tr2)^(2/3)+cx*(1-Tr2)+dx*(1-Tr2)^(4/3):
> Vrd1:=(ex+fx*(Tr1)+gx*(Tr1)^2+hx*(Tr1)^3)/(Tr1-1.00001):
> Vrd2:=(ex+fx*(Tr2)+gx*(Tr2)^2+hx*(Tr2)^3)/(Tr2-1.00001):
> Vsat1:=Vo1*Vro1*(1-omega1SRK*Vrd1):
> Vsat2:=Vo2*Vro2*(1-omega2SRK*Vrd2):
> rhoA:=1/(Vsat1*1000/60.096);
```

$$rhoA := .5441071276$$

```
> rhoW:=1/(Vsat2*1000/18.015);
```

$$rhoW := .8644972067$$

Temperature Dependent Binary Constants for the van Laar Excess Gibbs Free
Energy Equation
```
> C21:=-2228.6/(T+273.15)+5.953:
> C12:=2299.1/(T+273.15)-3.624:
```

Critical/Reduced Variables and Other Constants for 'Volatile' Components
Propylene (3) and Helium (4)

Used to Determine Compressibility of a Gas Mixture with PRSV

> Tc3:=365.57:Pc3:=4664.55:omega3:=0.14080:

> Tc4:=5.3:Pc4:=2.26*101.325:omega4:=-0.365:

> kappa3:=0.378893+1.4897153*omega3-
0.17131848*(omega3)^2+0.0196554*(omega3)^3:

> kappa4:=0.378893+1.4897153*omega4-
0.17131848*(omega4)^2+0.0196554*(omega4)^3:

> Tr3:=(T+273.15)/Tc3:

> Tr4:=(T+273.15)/Tc4:

> a33:=(0.457235*R^2*Tc3^2/Pc3)*(1+kappa3*(1-sqrt(Tr3)))^2:

> a44:=(0.457235*R^2*Tc4^2/Pc4)*(1+kappa4*(1-sqrt(Tr4)))^2:

> b3:=0.077796*R*Tc3/Pc3:

> b4:=0.077796*R*Tc4/Pc4:

> a12:=sqrt(a11*a22):

> a21:=a12:

> a13:=sqrt(a11*a33):

> a31:=a13:

> a14:=sqrt(a11*a44):

> a41:=a14:

> a23:=sqrt(a22*a33):

> a32:=a23:

> a24:=sqrt(a22*a44):

> a42:=a24:

> a34:=sqrt(a33*a44):

> a43:=a34:

Define Mole Fractions

> xw:=1-xa:

> V:=Mt+alpha-L:

> yh:=Mh/V:

> yp:=alpha/V:

Activity Coefficients - van Laar Gibbs Free Energy Equation

> gammaa:=exp(C12/(1+C12*xa/(C21*xw))^2):

> gammaw:=exp(C21/(1+C21*xw/(C12*xa))^2):

Modified Peng-Robinson Equation of State Parameters - Determination of the
Compressibility Factor for a Gas Mixture, Z and Vapor Phase Fugacity
Coefficients

>
a:=(ya)^2*a11+2*ya*yw*a12+2*ya*yp*a13+2*ya*yh*a14+(yw)^2*a22+2*yw*yp*a23
+2*yw*yh*a24+(yp)^2*a33+2*yp*yh*a34+(yh)^2*a44:

> b:=ya*b1+yw*b2+yp*b3+yh*b4:

> A:=a*P/(R*(T+273.15))^2:

> B:=b*P/(R*(T+273.15)):

```
> phiAV:=exp(b1/b*(Z-1)-ln(Z-B)-
A/(2*sqrt(2)*B)*(2*(ya*a11+yw*a12+yp*a13+yh*a14)/a-
b1/b)*ln((Z+(1+sqrt(2))*B)/(Z+(1-sqrt(2))*B))):
> phiWV:=exp(b2/b*(Z-1)-ln(Z-B)-
A/(2*sqrt(2)*B)*(2*(ya*a21+yw*a22+yp*a23+yh*a24)/a-
b2/b)*ln((Z+(1+sqrt(2))*B)/(Z+(1-sqrt(2))*B))):
```
  Set of Equations to be Solved to Determine xa, ya, yw, L, alpha and Z

  Z : Modified Peng-Robinson Equation of State for a Gas Mixture
```
> qq:=Z^3+(B-1)*Z^2+(A-3*B^2-2*B)*Z+(B^3+B^2-A*B)=0:
```
xa: Water Component Balance - Reaction Stoichiometry
```
> ww:=L*xw+V*yw=Mw+alpha:
```
  ya: Liquid 2-Propanol Fugacity = Vapor 2-Propanol Fugacity, VLE
```
> ee:=ya*P*phiAV=xa*gammaa*fugAL:
```
  yw: Liquid Water Fugacity = Vapor Water Fugacity, VLE
```
> rr:=yw*P*phiWV=xw*gammaw*fugWL:
```
  L : Summation of Vapor Phase Mole Fractions = 1
```
> tt:=ya+yw+yp+yh=1:
```
  alpha: 'Force Balance', i.e. PV=nZRT - assume negligible change of volume on mixing
```
> yy:=P*1000*(319e-6-
L*(xa*60.096/(rhoA*1e6)+xw*18.015/(rhoW*1e6)))=V*R*Z*(T+273.15):
>
fsolve({qq,ww,ee,rr,tt,yy},{Z,xa,ya,yw,L,alpha},{Z=0.5..1,xa=0..1,ya=0..1,yw=0..1,L=0.
.9,alpha=-1..1});
```

  {alpha = .05032457627, Z = .8267580817, L = 6.108746232,

    ya = .1950923325, xa = .09096092816, yw = .4003108739}
```
> clear;
```

                          clear
```
> reset;
```

                          reset
```

# Appendix A2
# Raw Data for the Kinetic Runs

Table A2.1 – Catalyst Screening Raw Data : Alumina

| T avg | 190°C | Ma,° | 38.274g | cat | 2.185g |
|-------|-------|------|---------|-----|--------|
|       | 463.15K | Mw,° | 100.078g | Mh,° | 0.0063moles |

| time (min) | T (°C) | P (psig) | $x_A$ | $x_W$ | α (moles) | Conv (%) |
|------|-------|--------|---------|---------|---------|-------|
| 0    | 190   | 259    | 0.10033 | 0.89967 | 0.00002 | 0.003 |
| 5    | 191   | 266    | 0.10022 | 0.89978 | 0.00050 | 0.078 |
| 10   | 190   | 260    | 0.10028 | 0.89972 | 0.00026 | 0.041 |
| 15   | 188   | 253    | 0.10020 | 0.89980 | 0.00097 | 0.153 |
| 20   | 188.5 | 256    | 0.10017 | 0.89983 | 0.00111 | 0.174 |
| 25   | 190   | 263    | 0.10015 | 0.89985 | 0.00100 | 0.157 |
| 30   | 191   | 269    | 0.10009 | 0.89991 | 0.00123 | 0.193 |
| 35   | 190   | 264    | 0.10011 | 0.89989 | 0.00124 | 0.195 |
| 40   | 190   | 265    | 0.10007 | 0.89993 | 0.00149 | 0.233 |
| 45   | 189   | 260    | 0.10009 | 0.89991 | 0.00149 | 0.233 |
| 50   | 191   | 268    | 0.10014 | 0.89986 | 0.00099 | 0.155 |
| 55   | 189.5 | 262    | 0.10010 | 0.89990 | 0.00137 | 0.214 |
| 60   | 190   | 263    | 0.10015 | 0.89985 | 0.00100 | 0.157 |
| 65   | 191.5 | 272    | 0.10006 | 0.89994 | 0.00134 | 0.210 |
| 70   | 190.5 | 265    | 0.10012 | 0.89988 | 0.00087 | 0.137 |
| 75   | 190   | 264    | 0.10011 | 0.89989 | 0.00124 | 0.195 |
| 80   | 190   | 264    | 0.10011 | 0.89989 | 0.00124 | 0.195 |
| 85   | 190   | 264    | 0.10011 | 0.89989 | 0.00124 | 0.195 |
| 90   | 190   | 265    | 0.10007 | 0.89993 | 0.00149 | 0.233 |

## Table A2.2 — Catalyst Screening Raw Data: Zeolite 13X

| T avg | 190.03°C | $M_a{}^o$ | 38.497g | cat | 2.168g |
|---|---|---|---|---|---|
| | 463.18K | $M_w{}^o$ | 99.710g | $M_h{}^o$ | 0.006303moles |

| time (min) | T (°C) | P (psig) | $x_A$ | $x_W$ | $\alpha$ (moles) | Conv (%) |
|---|---|---|---|---|---|---|
| 0 | 190 | 263 | 0.10103 | 0.89897 | 0.00088 | 0.138 |
| 5 | 190 | 261 | 0.10111 | 0.89889 | 0.00040 | 0.062 |
| 10 | 189.5 | 261 | 0.10102 | 0.89898 | 0.00101 | 0.157 |
| 15 | 190.5 | 266 | 0.10100 | 0.89900 | 0.00100 | 0.156 |
| 20 | 190.5 | 266 | 0.10100 | 0.89900 | 0.00100 | 0.156 |
| 25 | 190 | 265 | 0.10094 | 0.89906 | 0.00137 | 0.214 |
| 30 | 190 | 264 | 0.10099 | 0.89901 | 0.00113 | 0.176 |
| 35 | 190 | 266 | 0.10090 | 0.89910 | 0.00162 | 0.253 |
| 40 | 189.5 | 264 | 0.10089 | 0.89911 | 0.00175 | 0.272 |
| 45 | 190.5 | 267 | 0.10096 | 0.89904 | 0.00125 | 0.194 |
| 50 | 190 | 264 | 0.10099 | 0.89901 | 0.00113 | 0.176 |
| 55 | 190 | 264 | 0.10099 | 0.89901 | 0.00113 | 0.176 |
| 60 | 190 | 265 | 0.10094 | 0.89906 | 0.00137 | 0.214 |
| 65 | 190 | 265 | 0.10094 | 0.89906 | 0.00137 | 0.214 |
| 70 | 190 | 264 | 0.10099 | 0.89901 | 0.00113 | 0.176 |
| 75 | 190 | 264 | 0.10099 | 0.89901 | 0.00113 | 0.176 |
| 80 | 190 | 264 | 0.10099 | 0.89901 | 0.00113 | 0.176 |
| 85 | 190 | 265 | 0.10094 | 0.89906 | 0.00137 | 0.214 |
| 90 | 190 | 264 | 0.10099 | 0.89901 | 0.00113 | 0.176 |

## Table A2.3 – Catalyst Screening Raw Data: Silicalite S-115 SiO$_2$ ExT.

| T avg | 190.16°C | Ma,° | 38.064g | cat | 2.184g |
|---|---|---|---|---|---|
| | 463.31K | Mw,° | 99.577g | Mh,o | 0.006823moles |

| time (min) | T (°C) | P (psig) | $x_A$ | $x_W$ | α (moles) | Conv (%) |
|---|---|---|---|---|---|---|
| 0 | 190 | 261 | 0.10025 | 0.89975 | 0.00003 | 0.005 |
| 5 | 189.5 | 260 | 0.10019 | 0.89981 | 0.00040 | 0.063 |
| 10 | 190 | 265 | 0.10007 | 0.89993 | 0.00101 | 0.160 |
| 15 | 191 | 277 | 0.09975 | 0.90025 | 0.00273 | 0.430 |
| 20 | 190 | 272 | 0.09977 | 0.90023 | 0.00275 | 0.434 |
| 25 | 190 | 274 | 0.09968 | 0.90032 | 0.00325 | 0.513 |
| 30 | 189.5 | 272 | 0.09967 | 0.90033 | 0.00338 | 0.533 |
| 35 | 189 | 270 | 0.09965 | 0.90035 | 0.00351 | 0.554 |
| 40 | 191 | 280 | 0.09962 | 0.90038 | 0.00347 | 0.548 |
| 45 | 189 | 271 | 0.09961 | 0.90039 | 0.00376 | 0.593 |
| 50 | 190.5 | 278 | 0.09960 | 0.90040 | 0.00361 | 0.570 |
| 55 | 190 | 276 | 0.09959 | 0.90041 | 0.00375 | 0.591 |
| 60 | 192 | 288 | 0.09947 | 0.90053 | 0.00417 | 0.658 |
| 65 | 190 | 282 | 0.09932 | 0.90068 | 0.00525 | 0.829 |
| 70 | 190 | 284 | 0.09923 | 0.90077 | 0.00575 | 0.908 |
| 75 | 191 | 285 | 0.09940 | 0.90060 | 0.00471 | 0.744 |
| 80 | 190.5 | 287 | 0.09920 | 0.90080 | 0.00586 | 0.925 |
| 85 | 190 | 287 | 0.09910 | 0.90090 | 0.00651 | 1.028 |
| 90 | 190 | 287 | 0.09910 | 0.90090 | 0.00651 | 1.028 |

## Table A2.4 – Catalyst Screening Raw Data: SAPO-5

| T avg | 190.18°C | Ma,° | 38.482g | cat | 2.184g |
|---|---|---|---|---|---|
| | 463.33K | Mw,° | 99.803g | Mh,° | 0.006792moles |

| time (min) | T (°C) | P (psig) | $x_A$ | $x_W$ | $\alpha$ (moles) | Conv (%) |
|---|---|---|---|---|---|---|
| 0 | 190 | 263 | 0.10100 | 0.89900 | 0.00039 | 0.061 |
| 5 | 190 | 262 | 0.10104 | 0.89896 | 0.00015 | 0.023 |
| 10 | 190.5 | 265 | 0.10101 | 0.89899 | 0.00026 | 0.041 |
| 15 | 191 | 270 | 0.10089 | 0.89911 | 0.00086 | 0.135 |
| 20 | 190 | 270 | 0.10070 | 0.89930 | 0.00211 | 0.329 |
| 25 | 190 | 269 | 0.10074 | 0.89926 | 0.00186 | 0.290 |
| 30 | 190 | 269 | 0.10074 | 0.89926 | 0.00186 | 0.290 |
| 35 | 190 | 269 | 0.10074 | 0.89926 | 0.00186 | 0.290 |
| 40 | 190 | 270 | 0.10070 | 0.89930 | 0.00211 | 0.329 |
| 45 | 190 | 270 | 0.10070 | 0.89930 | 0.00211 | 0.329 |
| 50 | 190 | 270 | 0.10070 | 0.89930 | 0.00211 | 0.329 |
| 55 | 190 | 270 | 0.10070 | 0.89930 | 0.00211 | 0.329 |
| 60 | 190 | 270 | 0.10070 | 0.89930 | 0.00211 | 0.329 |
| 65 | 190 | 271 | 0.10065 | 0.89935 | 0.00235 | 0.367 |
| 70 | 190 | 271 | 0.10065 | 0.89935 | 0.00235 | 0.367 |
| 75 | 190 | 271 | 0.10065 | 0.89935 | 0.00235 | 0.367 |
| 80 | 190 | 271 | 0.10065 | 0.89935 | 0.00235 | 0.367 |
| 85 | 190 | 270 | 0.10070 | 0.89930 | 0.00211 | 0.329 |
| 90 | 192 | 280 | 0.10066 | 0.89934 | 0.00205 | 0.319 |

## Table A2.5 – External Mass Transfer Raw Data: Stirrer Speed = 883 rpm

| stirrer speed | 883rpm | $Mw^o$ | 100.235g |
| --- | --- | --- | --- |
| cat. loading | 1.57wt % | $Ma^o$ | 38.06g |
| T avg | 463.13K | cat | 2.171g |

| time (min) | T (°C) | P (psig) | $x_W$ | $x_A$ | $\alpha$ (moles) |
| --- | --- | --- | --- | --- | --- |
| 0 | 189 | 269 | 0.90066 | 0.09934 | 0.00198 |
| 5 | 190 | 275 | 0.90072 | 0.09928 | 0.00222 |
| 10 | 191 | 285 | 0.90095 | 0.09905 | 0.00343 |
| 15 | 190 | 281 | 0.90098 | 0.09902 | 0.00371 |
| 20 | 190 | 285 | 0.90116 | 0.09884 | 0.00470 |
| 25 | 189.5 | 287 | 0.90135 | 0.09865 | 0.00585 |
| 30 | 190 | 291 | 0.90142 | 0.09858 | 0.00621 |
| 35 | 190 | 294 | 0.90156 | 0.09844 | 0.00696 |
| 40 | 190 | 298 | 0.90173 | 0.09827 | 0.00797 |
| 45 | 190 | 300 | 0.90182 | 0.09818 | 0.00848 |
| 50 | 190 | 301 | 0.90187 | 0.09813 | 0.00873 |
| 55 | 190 | 304 | 0.90200 | 0.09800 | 0.00950 |
| 60 | 190 | 306 | 0.90209 | 0.09791 | 0.01000 |
| 65 | 190 | 308 | 0.90218 | 0.09782 | 0.01052 |
| 70 | 190 | 312 | 0.90236 | 0.09764 | 0.01154 |
| 75 | 190 | 315 | 0.90250 | 0.09750 | 0.01232 |
| 80 | 190 | 318 | 0.90264 | 0.09736 | 0.01309 |
| 85 | 190 | 319 | 0.90268 | 0.09732 | 0.01335 |
| 90 | 190 | 321 | 0.90277 | 0.09723 | 0.01387 |
| 95 | 190 | 324 | 0.90291 | 0.09709 | 0.01465 |
| 100 | 190 | 326 | 0.90300 | 0.09700 | 0.01517 |
| 105 | 190 | 328 | 0.90310 | 0.09690 | 0.01569 |
| 110 | 190 | 331 | 0.90323 | 0.09677 | 0.01648 |
| 115 | 190 | 334 | 0.90337 | 0.09663 | 0.01727 |
| 120 | 190 | 339 | 0.90361 | 0.09639 | 0.01859 |
| 125 | 190 | 341 | 0.90370 | 0.09630 | 0.01912 |
| 130 | 190 | 343 | 0.90379 | 0.09621 | 0.01965 |
| 135 | 190 | 345 | 0.90389 | 0.09611 | 0.02019 |
| 140 | 190 | 347 | 0.90398 | 0.09602 | 0.02072 |
| 145 | 190 | 348 | 0.90403 | 0.09597 | 0.02099 |
| 150 | 190 | 350 | 0.90413 | 0.09587 | 0.02153 |

Table A2.6 – External Mass Transfer Raw Data: Stirrer Speed = 1004 rpm

| stirrer speed | 1004 rpm | $Mw^o$ | 100.67 g |
|---|---|---|---|
| cat. loading | 1.54 wt % | $Ma^o$ | 38.32 g |
| T avg | 463.17 K | cat | 2.146 g |

| time (min) | T (°C) | P (psig) | $x_W$ | $x_A$ | $\alpha$ (moles) |
|---|---|---|---|---|---|
| 0 | 190 | 269 | 0.90019 | 0.09981 | 0.00068 |
| 5 | 190 | 276 | 0.90050 | 0.09951 | 0.00239 |
| 10 | 190 | 280 | 0.90067 | 0.09933 | 0.00338 |
| 15 | 190 | 287 | 0.90097 | 0.09903 | 0.00511 |
| 20 | 190 | 293 | 0.90123 | 0.09877 | 0.00660 |
| 25 | 190 | 298 | 0.90145 | 0.09855 | 0.00785 |
| 30 | 190 | 304 | 0.90172 | 0.09828 | 0.00937 |
| 35 | 190 | 310 | 0.90199 | 0.09801 | 0.01089 |
| 40 | 190 | 316 | 0.90226 | 0.09774 | 0.01242 |
| 45 | 190 | 323 | 0.90257 | 0.09743 | 0.01422 |
| 50 | 190.5 | 330 | 0.90278 | 0.09722 | 0.01534 |
| 55 | 190 | 336 | 0.90317 | 0.09683 | 0.01760 |
| 60 | 190 | 342 | 0.90344 | 0.09656 | 0.01918 |
| 65 | 190 | 348 | 0.90372 | 0.09628 | 0.02077 |
| 70 | 190 | 354 | 0.90400 | 0.09600 | 0.02237 |
| 75 | 190 | 360 | 0.90429 | 0.09571 | 0.02398 |
| 80 | 190 | 364 | 0.90448 | 0.09552 | 0.02506 |
| 85 | 190 | 369 | 0.90472 | 0.09528 | 0.02641 |
| 90 | 189.5 | 373 | 0.90503 | 0.09497 | 0.02827 |
| 95 | 190 | 380 | 0.90525 | 0.09475 | 0.02943 |
| 100 | 190.5 | 386 | 0.90542 | 0.09459 | 0.03031 |
| 105 | 190 | 390 | 0.90574 | 0.09427 | 0.03220 |
| 110 | 190 | 394 | 0.90593 | 0.09407 | 0.03332 |
| 115 | 190 | 400 | 0.90623 | 0.09377 | 0.03501 |
| 120 | 190 | 405 | 0.90648 | 0.09352 | 0.03642 |
| 125 | 190 | 409 | 0.90668 | 0.09332 | 0.03756 |
| 130 | 190 | 414 | 0.90693 | 0.09307 | 0.03899 |
| 135 | 190 | 419 | 0.90718 | 0.09282 | 0.04043 |
| 140 | 190 | 423 | 0.90739 | 0.09261 | 0.04159 |
| 145 | 190 | 427 | 0.90759 | 0.09241 | 0.04276 |
| 150 | 190 | 431 | 0.90780 | 0.09220 | 0.04393 |

## Table A2.7 – External Mass Transfer Raw Data: Stirrer Speed = 1182 rpm

| stirrer speed | 1182rpm | $Mw^o$ | 100.284g |
|---|---|---|---|
| cat. loading | 1.57wt % | $Ma^o$ | 37.92g |
| T avg | 463.15K | cat | 2.175g |

| time (min) | T (°C) | P (psig) | $x_W$ | $x_A$ | $\alpha$ (moles) |
|---|---|---|---|---|---|
| 0 | 189 | 262 | 0.90074 | 0.09926 | 0.00031 |
| 5 | 190 | 275 | 0.90111 | 0.09889 | 0.00228 |
| 10 | 190.5 | 283 | 0.90136 | 0.09864 | 0.00363 |
| 15 | 190.5 | 289 | 0.90162 | 0.09838 | 0.00513 |
| 20 | 189.5 | 292 | 0.90196 | 0.09804 | 0.00718 |
| 25 | 190 | 298 | 0.90212 | 0.09788 | 0.00804 |
| 30 | 190 | 306 | 0.90248 | 0.09752 | 0.01008 |
| 35 | 190 | 313 | 0.90280 | 0.09720 | 0.01188 |
| 40 | 190.5 | 320 | 0.90301 | 0.09699 | 0.01300 |
| 45 | 190 | 327 | 0.90344 | 0.09656 | 0.01552 |
| 50 | 190 | 333 | 0.90372 | 0.09628 | 0.01709 |
| 55 | 190 | 338 | 0.90395 | 0.09605 | 0.01842 |
| 60 | 190 | 344 | 0.90424 | 0.09576 | 0.02001 |
| 65 | 190 | 349 | 0.90447 | 0.09553 | 0.02135 |
| 70 | 190 | 357 | 0.90485 | 0.09515 | 0.02351 |
| 75 | 190 | 364 | 0.90519 | 0.09481 | 0.02541 |
| 80 | 190 | 370 | 0.90548 | 0.09452 | 0.02706 |
| 85 | 190 | 377 | 0.90582 | 0.09418 | 0.02899 |
| 90 | 190 | 381 | 0.90602 | 0.09398 | 0.03011 |
| 95 | 190 | 386 | 0.90626 | 0.09374 | 0.03150 |
| 100 | 190 | 392 | 0.90656 | 0.09344 | 0.03319 |
| 105 | 190 | 398 | 0.90686 | 0.09314 | 0.03489 |
| 110 | 190 | 403 | 0.90712 | 0.09289 | 0.03632 |
| 115 | 190 | 408 | 0.90737 | 0.09263 | 0.03775 |
| 120 | 190 | 414 | 0.90767 | 0.09233 | 0.03949 |
| 125 | 190 | 419 | 0.90793 | 0.09207 | 0.04094 |
| 130 | 190 | 423 | 0.90814 | 0.09186 | 0.04211 |
| 135 | 190 | 428 | 0.90840 | 0.09160 | 0.04358 |
| 140 | 190 | 432 | 0.90861 | 0.09139 | 0.04476 |
| 145 | 190 | 436 | 0.90882 | 0.09118 | 0.04595 |
| 150 | 190 | 441 | 0.90908 | 0.09092 | 0.04745 |

### Table A2.8 – Internal Mass Transfer Raw Data: 90 - 150 μm Particle Diameters

particle size     100-170 mesh

| | | | | |
|---|---|---|---|---|
| stirrer speed | 1080rpm | $Mw^o$ | 100.537g |
| cat. loading | 1.58wt % | $Ma^o$ | 37.918g |
| T avg | 463.21K | cat | 2.186g |

| time (min) | T (°C) | P (psig) | $x_W$ | $x_A$ | α (moles) |
|---|---|---|---|---|---|
| 0 | 189.5 | 270 | 0.90121 | 0.09879 | 0.00169 |
| 5 | 191 | 284 | 0.90152 | 0.09848 | 0.00326 |
| 10 | 191 | 287 | 0.90166 | 0.09834 | 0.00400 |
| 15 | 190 | 292 | 0.90208 | 0.09792 | 0.00653 |
| 20 | 190 | 299 | 0.90239 | 0.09761 | 0.00830 |
| 25 | 190 | 304 | 0.90261 | 0.09739 | 0.00957 |
| 30 | 190 | 311 | 0.90292 | 0.09708 | 0.01136 |
| 35 | 190 | 317 | 0.90320 | 0.09680 | 0.01291 |
| 40 | 190 | 324 | 0.90352 | 0.09648 | 0.01472 |
| 45 | 190 | 330 | 0.90379 | 0.09621 | 0.01629 |
| 50 | 190.5 | 337 | 0.90400 | 0.09600 | 0.01742 |
| 55 | 190 | 342 | 0.90435 | 0.09565 | 0.01946 |
| 60 | 190 | 348 | 0.90464 | 0.09536 | 0.02106 |
| 65 | 190 | 354 | 0.90492 | 0.09508 | 0.02267 |
| 70 | 190 | 360 | 0.90520 | 0.09480 | 0.02429 |
| 75 | 190 | 366 | 0.90549 | 0.09451 | 0.02593 |
| 80 | 190 | 372 | 0.90578 | 0.09422 | 0.02757 |
| 85 | 190 | 378 | 0.90607 | 0.09393 | 0.02923 |
| 90 | 190 | 383 | 0.90632 | 0.09368 | 0.03062 |
| 95 | 190 | 389 | 0.90661 | 0.09339 | 0.03230 |
| 100 | 190 | 394 | 0.90686 | 0.09314 | 0.03371 |
| 105 | 190 | 399 | 0.90711 | 0.09289 | 0.03512 |
| 110 | 190 | 404 | 0.90736 | 0.09264 | 0.03655 |
| 115 | 190 | 408 | 0.90756 | 0.09244 | 0.03769 |
| 120 | 190 | 413 | 0.90782 | 0.09218 | 0.03913 |
| 125 | 190 | 418 | 0.90807 | 0.09193 | 0.04058 |
| 130 | 190 | 422 | 0.90828 | 0.09172 | 0.04175 |
| 135 | 190 | 426 | 0.90848 | 0.09152 | 0.04292 |
| 140 | 190 | 430 | 0.90869 | 0.09131 | 0.04410 |
| 145 | 190 | 434 | 0.90890 | 0.09110 | 0.04528 |
| 150 | 190 | 437 | 0.90906 | 0.09094 | 0.04617 |

## Table A2.9 – Internal Mass Transfer Raw Data: 595 - 850 μm Particle Diameters

| | | | | |
|---|---|---|---|
| particle size | 20-30 mesh | | |
| stirrer speed | 1080 rpm | $Mw^o$ | 100.459 g |
| cat. loading | 1.56 wt % | $Ma^o$ | 38.257 g |
| T avg | 463.17 K | cat | 2.158 g |

| time (min) | T (°C) | P (psig) | $x_W$ | $x_A$ | α (moles) |
|---|---|---|---|---|---|
| 0 | 189 | 268 | 0.90032 | 0.09968 | 0.00168 |
| 5 | 190 | 277 | 0.90051 | 0.09949 | 0.00265 |
| 10 | 190 | 285 | 0.90086 | 0.09914 | 0.00463 |
| 15 | 190.5 | 293 | 0.90111 | 0.09889 | 0.00598 |
| 20 | 190 | 300 | 0.90152 | 0.09848 | 0.00839 |
| 25 | 190 | 306 | 0.90188 | 0.09812 | 0.00990 |
| 30 | 189.5 | 312 | 0.90216 | 0.09784 | 0.01211 |
| 35 | 190 | 321 | 0.90246 | 0.09754 | 0.01375 |
| 40 | 190.5 | 330 | 0.90277 | 0.09723 | 0.01539 |
| 45 | 191 | 338 | 0.90302 | 0.09698 | 0.01676 |
| 50 | 190.5 | 346 | 0.90350 | 0.09650 | 0.01958 |
| 55 | 190 | 352 | 0.90390 | 0.09610 | 0.02190 |
| 60 | 190 | 358 | 0.90418 | 0.09582 | 0.02351 |
| 65 | 190 | 365 | 0.90452 | 0.09548 | 0.02540 |
| 70 | 190 | 372 | 0.90486 | 0.09514 | 0.02731 |
| 75 | 190 | 378 | 0.90515 | 0.09485 | 0.02896 |
| 80 | 190 | 384 | 0.90544 | 0.09456 | 0.03062 |
| 85 | 190 | 390 | 0.90573 | 0.09427 | 0.03230 |
| 90 | 190 | 396 | 0.90603 | 0.09397 | 0.03398 |
| 95 | 189.5 | 402 | 0.90646 | 0.09354 | 0.03649 |
| 100 | 190 | 409 | 0.90668 | 0.09332 | 0.03767 |
| 105 | 190 | 415 | 0.90699 | 0.09301 | 0.03940 |
| 110 | 190 | 421 | 0.90729 | 0.09271 | 0.04113 |
| 115 | 190 | 426 | 0.90755 | 0.09245 | 0.04259 |
| 120 | 190 | 432 | 0.90786 | 0.09214 | 0.04435 |
| 125 | 190 | 437 | 0.90812 | 0.09188 | 0.04583 |
| 130 | 190 | 441 | 0.90833 | 0.09167 | 0.04701 |
| 135 | 190 | 446 | 0.90874 | 0.09127 | 0.04939 |
| 140 | 190 | 451 | 0.90886 | 0.09114 | 0.05001 |
| 145 | 190 | 455 | 0.90907 | 0.09093 | 0.05122 |
| 150 | 190 | 458 | 0.90923 | 0.09077 | 0.05213 |

Table A2.10 – Temperature Dependence Raw Data: 463 K

| T avg | 189.98°C | Ma,° | 38.109g |
|---|---|---|---|
| | 463.13K | Mw,° | 100.173g |
| | | cat | 2.151g |
| | | Mh,° | 0.00806moles |

| time (min) | T (°C) | P (psig) | $x_A$ | $x_W$ | α (moles) | L (moles) | V (moles) | $C_A$ (moles/L) | $C_W$ (moles/L) |
|---|---|---|---|---|---|---|---|---|---|
| 0 | 189 | 263 | 0.09978 | 0.90022 | 0.00048 | 6.125 | 0.078 | 3.358 | 30.300 |
| 5 | 190 | 276 | 0.09941 | 0.90059 | 0.00245 | 6.124 | 0.081 | 3.342 | 30.275 |
| 10 | 190.5 | 285 | 0.09912 | 0.90088 | 0.00404 | 6.123 | 0.084 | 3.331 | 30.276 |
| 15 | 190.5 | 292 | 0.09881 | 0.90119 | 0.00579 | 6.122 | 0.086 | 3.324 | 30.314 |
| 20 | 190 | 298 | 0.09855 | 0.90145 | 0.00729 | 6.122 | 0.088 | 3.321 | 30.383 |
| 25 | 190 | 304 | 0.09817 | 0.90183 | 0.00947 | 6.122 | 0.091 | 3.313 | 30.430 |
| 30 | 189.5 | 310 | 0.09779 | 0.90221 | 0.01168 | 6.122 | 0.093 | 3.307 | 30.513 |
| 35 | 190 | 317 | 0.09758 | 0.90242 | 0.01281 | 6.121 | 0.095 | 3.299 | 30.504 |
| 40 | 190 | 324 | 0.09726 | 0.90274 | 0.01462 | 6.120 | 0.097 | 3.291 | 30.545 |
| 45 | 190 | 331 | 0.09694 | 0.90306 | 0.01645 | 6.119 | 0.100 | 3.283 | 30.586 |
| 50 | 190 | 338 | 0.09661 | 0.90339 | 0.01830 | 6.119 | 0.102 | 3.275 | 30.627 |
| 55 | 190 | 345 | 0.09629 | 0.90371 | 0.02016 | 6.118 | 0.105 | 3.268 | 30.669 |
| 60 | 190 | 352 | 0.09595 | 0.90405 | 0.02203 | 6.118 | 0.107 | 3.260 | 30.711 |
| 65 | 190 | 359 | 0.09562 | 0.90438 | 0.02392 | 6.117 | 0.110 | 3.252 | 30.754 |
| 70 | 190 | 365 | 0.09533 | 0.90467 | 0.02556 | 6.117 | 0.112 | 3.245 | 30.791 |
| 75 | 190 | 372 | 0.09499 | 0.90501 | 0.02748 | 6.116 | 0.114 | 3.236 | 30.834 |
| 80 | 190 | 378 | 0.09470 | 0.90530 | 0.02913 | 6.115 | 0.116 | 3.229 | 30.872 |
| 85 | 190 | 384 | 0.09440 | 0.90560 | 0.03080 | 6.115 | 0.119 | 3.222 | 30.910 |
| 90 | 190 | 390 | 0.09411 | 0.90589 | 0.03248 | 6.114 | 0.121 | 3.215 | 30.948 |
| 95 | 190 | 396 | 0.09381 | 0.90619 | 0.03418 | 6.114 | 0.123 | 3.208 | 30.986 |
| 100 | 190 | 402 | 0.09351 | 0.90649 | 0.03588 | 6.113 | 0.125 | 3.200 | 31.025 |
| 105 | 190 | 408 | 0.09320 | 0.90680 | 0.03760 | 6.113 | 0.128 | 3.193 | 31.065 |
| 110 | 190 | 414 | 0.09290 | 0.90710 | 0.03933 | 6.112 | 0.130 | 3.185 | 31.104 |
| 115 | 190 | 419 | 0.09264 | 0.90736 | 0.04078 | 6.112 | 0.132 | 3.179 | 31.138 |
| 120 | 190 | 424 | 0.09238 | 0.90762 | 0.04224 | 6.111 | 0.134 | 3.173 | 31.171 |
| 125 | 190 | 429 | 0.09212 | 0.90788 | 0.04371 | 6.111 | 0.136 | 3.166 | 31.205 |
| 130 | 190 | 433 | 0.09191 | 0.90809 | 0.04489 | 6.110 | 0.137 | 3.161 | 31.233 |
| 135 | 190 | 438 | 0.09165 | 0.90835 | 0.04638 | 6.110 | 0.139 | 3.155 | 31.267 |
| 140 | 190 | 442 | 0.09144 | 0.90856 | 0.04757 | 6.110 | 0.141 | 3.150 | 31.295 |
| 145 | 190 | 447 | 0.09117 | 0.90883 | 0.04907 | 6.109 | 0.143 | 3.143 | 31.329 |
| 150 | 190 | 451 | 0.09096 | 0.90904 | 0.05028 | 6.109 | 0.144 | 3.138 | 31.358 |

## Table A2.11 – Temperature Dependence Raw Data: 453 K

| T avg | 180.13°C | Ma,° | 38.19g |
|---|---|---|---|
| | 453.28K | Mw,° | 99.944g |
| | | cat | 2.175g |
| | | Mh,° | 0.00954 moles |

| time (min) | T (°C) | P (psig) | $x_A$ | $x_W$ | α (moles) | L (moles) | V (moles) | $C_A$ (moles/L) | $C_W$ (moles/L) |
|---|---|---|---|---|---|---|---|---|---|
| 0 | 180 | 222 | 0.10034 | 0.89966 | 0.00085 | 6.124 | 0.070 | 3.439 | 30.836 |
| 5 | 180.5 | 227 | 0.10020 | 0.89980 | 0.00156 | 6.123 | 0.071 | 3.432 | 30.821 |
| 10 | 180 | 227 | 0.10011 | 0.89989 | 0.00214 | 6.123 | 0.072 | 3.434 | 30.865 |
| 15 | 180 | 230 | 0.09997 | 0.90003 | 0.00292 | 6.123 | 0.073 | 3.430 | 30.882 |
| 20 | 181 | 235 | 0.09992 | 0.90008 | 0.00305 | 6.122 | 0.074 | 3.422 | 30.823 |
| 25 | 180 | 236 | 0.09970 | 0.90030 | 0.00448 | 6.123 | 0.075 | 3.424 | 30.916 |
| 30 | 180 | 237 | 0.09965 | 0.90035 | 0.00475 | 6.123 | 0.075 | 3.422 | 30.922 |
| 35 | 181 | 245 | 0.09946 | 0.90054 | 0.00561 | 6.121 | 0.077 | 3.411 | 30.880 |
| 40 | 180 | 244 | 0.09933 | 0.90067 | 0.00659 | 6.122 | 0.077 | 3.415 | 30.962 |
| 45 | 179.5 | 245 | 0.09919 | 0.90081 | 0.00745 | 6.123 | 0.078 | 3.415 | 31.012 |
| 50 | 181 | 252 | 0.09914 | 0.90086 | 0.00749 | 6.121 | 0.079 | 3.403 | 30.921 |
| 55 | 180 | 253 | 0.09891 | 0.90109 | 0.00898 | 6.122 | 0.080 | 3.404 | 31.015 |
| 60 | 180 | 254 | 0.09886 | 0.90114 | 0.00924 | 6.122 | 0.081 | 3.403 | 31.021 |
| 65 | 180 | 257 | 0.09872 | 0.90128 | 0.01005 | 6.121 | 0.082 | 3.400 | 31.038 |
| 70 | 180 | 259 | 0.09863 | 0.90137 | 0.01058 | 6.121 | 0.082 | 3.398 | 31.050 |
| 75 | 180 | 262 | 0.09849 | 0.90151 | 0.01139 | 6.121 | 0.083 | 3.394 | 31.068 |
| 80 | 180 | 265 | 0.09835 | 0.90165 | 0.01220 | 6.121 | 0.084 | 3.391 | 31.086 |
| 85 | 180 | 268 | 0.09820 | 0.90180 | 0.01301 | 6.121 | 0.085 | 3.387 | 31.104 |
| 90 | 180 | 270 | 0.09811 | 0.90189 | 0.01356 | 6.120 | 0.086 | 3.385 | 31.116 |
| 95 | 180 | 273 | 0.09796 | 0.90204 | 0.01437 | 6.120 | 0.087 | 3.381 | 31.134 |
| 100 | 180 | 275 | 0.09787 | 0.90213 | 0.01492 | 6.120 | 0.088 | 3.379 | 31.146 |
| 105 | 180.5 | 278 | 0.09782 | 0.90218 | 0.01510 | 6.119 | 0.088 | 3.374 | 31.120 |
| 110 | 180 | 281 | 0.09758 | 0.90242 | 0.01656 | 6.120 | 0.090 | 3.372 | 31.183 |
| 115 | 180 | 283 | 0.09748 | 0.90252 | 0.01712 | 6.120 | 0.090 | 3.369 | 31.195 |
| 120 | 180 | 285 | 0.09739 | 0.90261 | 0.01767 | 6.119 | 0.091 | 3.367 | 31.207 |
| 125 | 180 | 287 | 0.09729 | 0.90271 | 0.01822 | 6.119 | 0.092 | 3.365 | 31.220 |
| 130 | 180 | 290 | 0.09714 | 0.90286 | 0.01906 | 6.119 | 0.093 | 3.361 | 31.238 |
| 135 | 180.5 | 293 | 0.09720 | 0.90280 | 0.01856 | 6.118 | 0.093 | 3.359 | 31.199 |
| 140 | 180 | 295 | 0.09690 | 0.90310 | 0.02045 | 6.119 | 0.095 | 3.355 | 31.269 |
| 145 | 180 | 298 | 0.09675 | 0.90325 | 0.02129 | 6.118 | 0.096 | 3.351 | 31.288 |
| 150 | 180 | 299 | 0.09670 | 0.90330 | 0.02157 | 6.118 | 0.096 | 3.350 | 31.294 |

Table A2.12 – Temperature Dependence Raw Data: 444 K

| T avg | 170.95°C | Ma,° | 37.904g |
| | 444.10K | Mw,° | 100.708g |
| | | cat | 2.15g |
| | | Mh,° | 0.00779moles |

| time (min) | T (°C) | P (psig) | $x_A$ | $x_W$ | α (moles) | L (moles) | V (moles) | $C_A$ (moles/L) | $C_W$ (moles/L) |
|---|---|---|---|---|---|---|---|---|---|
| 0 | 170 | 177 | 0.09939 | 0.90061 | 0.00022 | 6.172 | 0.057 | 3.485 | 31.578 |
| 5 | 171 | 179 | 0.09944 | 0.90056 | -0.00028 | 6.171 | 0.057 | 3.480 | 31.511 |
| 10 | 170 | 178 | 0.09934 | 0.90066 | 0.00049 | 6.172 | 0.057 | 3.484 | 31.583 |
| 15 | 170 | 179 | 0.09930 | 0.90070 | 0.00075 | 6.172 | 0.058 | 3.483 | 31.589 |
| 20 | 171 | 180 | 0.09940 | 0.90060 | -0.00002 | 6.171 | 0.058 | 3.478 | 31.516 |
| 25 | 171 | 182 | 0.09931 | 0.90069 | 0.00052 | 6.171 | 0.058 | 3.476 | 31.528 |
| 30 | 171 | 183 | 0.09926 | 0.90074 | 0.00078 | 6.171 | 0.059 | 3.475 | 31.534 |
| 35 | 171 | 185 | 0.09917 | 0.90083 | 0.00132 | 6.171 | 0.059 | 3.473 | 31.545 |
| 40 | 171 | 186 | 0.09912 | 0.90088 | 0.00159 | 6.171 | 0.060 | 3.471 | 31.551 |
| 45 | 171 | 187 | 0.09908 | 0.90092 | 0.00186 | 6.171 | 0.060 | 3.470 | 31.557 |
| 50 | 171 | 189 | 0.09898 | 0.90102 | 0.00240 | 6.171 | 0.061 | 3.468 | 31.569 |
| 55 | 171 | 190 | 0.09894 | 0.90106 | 0.00266 | 6.171 | 0.061 | 3.467 | 31.574 |
| 60 | 171 | 191 | 0.09889 | 0.90111 | 0.00293 | 6.170 | 0.061 | 3.466 | 31.580 |
| 65 | 171 | 192 | 0.09884 | 0.90116 | 0.00320 | 6.170 | 0.062 | 3.465 | 31.586 |
| 70 | 171 | 193 | 0.09880 | 0.90120 | 0.00347 | 6.170 | 0.062 | 3.463 | 31.592 |
| 75 | 171 | 194 | 0.09875 | 0.90125 | 0.00375 | 6.170 | 0.062 | 3.462 | 31.598 |
| 80 | 171 | 195 | 0.09870 | 0.90130 | 0.00402 | 6.170 | 0.063 | 3.461 | 31.604 |
| 85 | 171 | 197 | 0.09861 | 0.90139 | 0.00456 | 6.170 | 0.063 | 3.459 | 31.616 |
| 90 | 171 | 198 | 0.09856 | 0.90144 | 0.00483 | 6.170 | 0.064 | 3.457 | 31.622 |
| 95 | 171 | 200 | 0.09847 | 0.90153 | 0.00538 | 6.170 | 0.064 | 3.455 | 31.634 |
| 100 | 171 | 201 | 0.09842 | 0.90158 | 0.00565 | 6.170 | 0.065 | 3.454 | 31.640 |
| 105 | 171 | 202 | 0.09837 | 0.90163 | 0.00592 | 6.170 | 0.065 | 3.453 | 31.646 |
| 110 | 171 | 204 | 0.09828 | 0.90172 | 0.00647 | 6.170 | 0.066 | 3.450 | 31.658 |
| 115 | 171 | 205 | 0.09823 | 0.90177 | 0.00674 | 6.170 | 0.066 | 3.449 | 31.663 |
| 120 | 171 | 206 | 0.09818 | 0.90182 | 0.00702 | 6.170 | 0.066 | 3.448 | 31.669 |
| 125 | 171 | 208 | 0.09809 | 0.90191 | 0.00757 | 6.169 | 0.067 | 3.446 | 31.682 |
| 130 | 171.5 | 209 | 0.09812 | 0.90188 | 0.00728 | 6.169 | 0.067 | 3.443 | 31.647 |
| 135 | 171 | 210 | 0.09804 | 0.90196 | 0.00784 | 6.169 | 0.067 | 3.444 | 31.688 |
| 140 | 172 | 212 | 0.09806 | 0.90194 | 0.00755 | 6.168 | 0.068 | 3.438 | 31.624 |
| 145 | 171 | 211 | 0.09795 | 0.90205 | 0.00839 | 6.169 | 0.068 | 3.442 | 31.700 |
| 150 | 171 | 213 | 0.09785 | 0.90215 | 0.00895 | 6.169 | 0.069 | 3.440 | 31.712 |

## Table A2.13 − Temperature Dependence Raw Data: 434 K

| | | | | | | | |
|---|---|---|---|---|---|---|---|
| T avg | 160.94°C | Ma,° | 37.802g | | | | |
| | 434.09K | Mw,° | 99.963g | | | | |
| | | cat | 2.168g | | | | |
| | | Mh,° | 0.00757moles | | | | |

| time (min) | T (°C) | P (psig) | $x_A$ | $x_W$ | α (moles) | L (moles) | V (moles) | $C_A$ (moles/L) | $C_W$ (moles/L) |
|---|---|---|---|---|---|---|---|---|---|
| 0 | 160 | 140 | 0.10013 | 0.89987 | 0.00018 | 6.138 | 0.048 | 3.568 | 32.066 |
| 5 | 161 | 142 | 0.10016 | 0.89984 | -0.00020 | 6.137 | 0.048 | 3.563 | 32.006 |
| 10 | 161 | 142 | 0.10016 | 0.89984 | -0.00020 | 6.137 | 0.048 | 3.563 | 32.006 |
| 15 | 161 | 143 | 0.10011 | 0.89989 | 0.00008 | 6.137 | 0.049 | 3.561 | 32.012 |
| 20 | 161 | 143 | 0.10011 | 0.89989 | 0.00008 | 6.137 | 0.049 | 3.561 | 32.012 |
| 25 | 161 | 143 | 0.10011 | 0.89989 | 0.00008 | 6.137 | 0.049 | 3.561 | 32.012 |
| 30 | 161 | 143 | 0.10011 | 0.89989 | 0.00008 | 6.137 | 0.049 | 3.561 | 32.012 |
| 35 | 161 | 143 | 0.10011 | 0.89989 | 0.00008 | 6.137 | 0.049 | 3.561 | 32.012 |
| 40 | 161 | 144 | 0.10007 | 0.89993 | 0.00036 | 6.137 | 0.049 | 3.560 | 32.018 |
| 45 | 161 | 144 | 0.10007 | 0.89993 | 0.00036 | 6.137 | 0.049 | 3.560 | 32.018 |
| 50 | 161 | 145 | 0.10002 | 0.89998 | 0.00064 | 6.137 | 0.049 | 3.559 | 32.024 |
| 55 | 161 | 145 | 0.10002 | 0.89998 | 0.00064 | 6.137 | 0.049 | 3.559 | 32.024 |
| 60 | 161 | 146 | 0.09997 | 0.90003 | 0.00092 | 6.137 | 0.050 | 3.558 | 32.030 |
| 65 | 161 | 145 | 0.10002 | 0.89998 | 0.00064 | 6.137 | 0.049 | 3.559 | 32.024 |
| 70 | 161 | 147 | 0.09992 | 0.90008 | 0.00120 | 6.137 | 0.050 | 3.556 | 32.036 |
| 75 | 162 | 147 | 0.10005 | 0.89995 | 0.00024 | 6.136 | 0.050 | 3.553 | 31.963 |
| 80 | 161 | 147 | 0.09992 | 0.90008 | 0.00120 | 6.137 | 0.050 | 3.556 | 32.036 |
| 85 | 161 | 147 | 0.09992 | 0.90008 | 0.00120 | 6.137 | 0.050 | 3.556 | 32.036 |
| 90 | 161 | 147 | 0.09992 | 0.90008 | 0.00120 | 6.137 | 0.050 | 3.556 | 32.036 |
| 95 | 161 | 147 | 0.09992 | 0.90008 | 0.00120 | 6.137 | 0.050 | 3.556 | 32.036 |
| 100 | 161 | 148 | 0.09987 | 0.90013 | 0.00148 | 6.137 | 0.050 | 3.555 | 32.042 |
| 105 | 161 | 148 | 0.09987 | 0.90013 | 0.00148 | 6.137 | 0.050 | 3.555 | 32.042 |
| 110 | 161 | 148 | 0.09987 | 0.90013 | 0.00148 | 6.137 | 0.050 | 3.555 | 32.042 |
| 115 | 161 | 149 | 0.09982 | 0.90018 | 0.00176 | 6.137 | 0.051 | 3.554 | 32.048 |
| 120 | 161 | 149 | 0.09982 | 0.90018 | 0.00176 | 6.137 | 0.051 | 3.554 | 32.048 |
| 125 | 161 | 149 | 0.09982 | 0.90018 | 0.00176 | 6.137 | 0.051 | 3.554 | 32.048 |
| 130 | 161 | 150 | 0.09978 | 0.90022 | 0.00205 | 6.137 | 0.051 | 3.553 | 32.054 |
| 135 | 160 | 150 | 0.09964 | 0.90036 | 0.00301 | 6.137 | 0.051 | 3.556 | 32.128 |
| 140 | 160 | 150 | 0.09964 | 0.90036 | 0.00301 | 6.137 | 0.051 | 3.556 | 32.128 |
| 145 | 161 | 151 | 0.09973 | 0.90027 | 0.00233 | 6.137 | 0.051 | 3.551 | 32.061 |
| 150 | 161 | 151 | 0.09973 | 0.90027 | 0.00233 | 6.137 | 0.051 | 3.551 | 32.061 |

## Table A2.14 – Concentration Dependence Raw Data: 8 mol % Initial 2-Propanol/Water Concentration in the Feed at 463 K

T avg   190.06°C   $x_a^0$   0.0811   $Mh,^o$   0.00722 moles

          463.21 K   $Ma,^o$   31.786g   cat   2.156g

                       $Mw,^o$   107.93g

| time (min) | T (°C) | P (psig) | $x_A$ | $x_W$ | α (moles) | L (moles) | V (moles) | $C_A$ (moles/L) | $C_W$ (moles/L) |
|---|---|---|---|---|---|---|---|---|---|
| 0 | 190 | 258 | 0.07874 | 0.92126 | 0.00193 | 6.452 | 0.077 | 2.823 | 33.026 |
| 5 | 191 | 269 | 0.07847 | 0.92153 | 0.00348 | 6.451 | 0.080 | 2.809 | 32.992 |
| 10 | 190 | 270 | 0.07824 | 0.92176 | 0.00497 | 6.452 | 0.081 | 2.809 | 33.097 |
| 15 | 190.5 | 279 | 0.07796 | 0.92204 | 0.00664 | 6.451 | 0.083 | 2.799 | 33.102 |
| 20 | 191 | 287 | 0.07772 | 0.92228 | 0.00806 | 6.450 | 0.086 | 2.789 | 33.100 |
| 25 | 190 | 290 | 0.07740 | 0.92260 | 0.01012 | 6.450 | 0.087 | 2.787 | 33.218 |
| 30 | 190 | 297 | 0.07710 | 0.92290 | 0.01195 | 6.450 | 0.090 | 2.779 | 33.261 |
| 35 | 189 | 300 | 0.07677 | 0.92323 | 0.01406 | 6.450 | 0.091 | 2.776 | 33.380 |
| 40 | 190 | 309 | 0.07658 | 0.92342 | 0.01512 | 6.449 | 0.094 | 2.764 | 33.336 |
| 45 | 189.5 | 314 | 0.07625 | 0.92375 | 0.01713 | 6.449 | 0.096 | 2.759 | 33.418 |
| 50 | 190 | 320 | 0.07609 | 0.92391 | 0.01806 | 6.448 | 0.097 | 2.751 | 33.405 |
| 55 | 191 | 331 | 0.07582 | 0.92418 | 0.01963 | 6.446 | 0.100 | 2.738 | 33.373 |
| 60 | 190 | 332 | 0.07556 | 0.92444 | 0.02131 | 6.447 | 0.101 | 2.737 | 33.482 |
| 65 | 190 | 338 | 0.07529 | 0.92471 | 0.02295 | 6.447 | 0.104 | 2.729 | 33.521 |
| 70 | 189.5 | 340 | 0.07509 | 0.92491 | 0.02412 | 6.447 | 0.104 | 2.727 | 33.586 |
| 75 | 191 | 349 | 0.07502 | 0.92498 | 0.02453 | 6.445 | 0.107 | 2.716 | 33.490 |
| 80 | 192 | 358 | 0.07483 | 0.92517 | 0.02554 | 6.444 | 0.109 | 2.705 | 33.443 |
| 85 | 189 | 355 | 0.07429 | 0.92571 | 0.02913 | 6.446 | 0.110 | 2.708 | 33.738 |
| 90 | 189 | 359 | 0.07411 | 0.92589 | 0.03026 | 6.446 | 0.112 | 2.703 | 33.765 |
| 95 | 189.5 | 363 | 0.07404 | 0.92596 | 0.03065 | 6.445 | 0.113 | 2.698 | 33.740 |
| 100 | 191 | 375 | 0.07382 | 0.92618 | 0.03179 | 6.443 | 0.116 | 2.683 | 33.663 |
| 105 | 190 | 375 | 0.07359 | 0.92641 | 0.03332 | 6.444 | 0.117 | 2.683 | 33.770 |
| 110 | 189.5 | 378 | 0.07333 | 0.92667 | 0.03495 | 6.444 | 0.118 | 2.678 | 33.843 |
| 115 | 189.5 | 382 | 0.07314 | 0.92686 | 0.03611 | 6.444 | 0.120 | 2.673 | 33.871 |
| 120 | 190 | 386 | 0.07307 | 0.92693 | 0.03649 | 6.443 | 0.121 | 2.668 | 33.846 |
| 125 | 190 | 391 | 0.07283 | 0.92717 | 0.03794 | 6.443 | 0.123 | 2.661 | 33.881 |
| 130 | 190 | 395 | 0.07264 | 0.92736 | 0.03911 | 6.442 | 0.124 | 2.656 | 33.910 |
| 135 | 190 | 398 | 0.07250 | 0.92750 | 0.03999 | 6.442 | 0.125 | 2.652 | 33.931 |
| 140 | 190 | 401 | 0.07235 | 0.92765 | 0.04087 | 6.442 | 0.126 | 2.648 | 33.952 |
| 145 | 190 | 403 | 0.07225 | 0.92775 | 0.04146 | 6.442 | 0.127 | 2.645 | 33.967 |
| 150 | 190 | 406 | 0.07211 | 0.92789 | 0.04235 | 6.441 | 0.128 | 2.641 | 33.988 |

## Table A2.15 – Concentration Dependence Raw Data: 6 mol % Initial 2-Propanol/Water Concentration in the Feed at 463 K

| T avg | 189.97°C | $x_a^0$ | 0.06 | $M_h,^0$ | 0.00707 moles |
| | 463.12K | $M_a,^0$ | 25.06g | cat | 2.169g |
| | | $M_w,^0$ | 117.7g | | |

| time (min) | T (°C) | P (psig) | $x_A$ | $x_W$ | α (moles) | L (moles) | V (moles) | $C_A$ (moles/L) | $C_W$ (moles/L) |
|---|---|---|---|---|---|---|---|---|---|
| 0 | 189 | 233 | 0.05844 | 0.94156 | 0.00023 | 6.888 | 0.069 | 2.245 | 36.180 |
| 5 | 189 | 237 | 0.05828 | 0.94172 | 0.00124 | 6.888 | 0.071 | 2.241 | 36.205 |
| 10 | 191 | 251 | 0.05808 | 0.94192 | 0.00247 | 6.886 | 0.074 | 2.226 | 36.096 |
| 15 | 190 | 252 | 0.05787 | 0.94213 | 0.00390 | 6.886 | 0.075 | 2.224 | 36.201 |
| 20 | 189.5 | 256 | 0.05763 | 0.94237 | 0.00552 | 6.887 | 0.076 | 2.219 | 36.276 |
| 25 | 190 | 261 | 0.05753 | 0.94247 | 0.00621 | 6.886 | 0.078 | 2.213 | 36.258 |
| 30 | 190 | 266 | 0.05733 | 0.94267 | 0.00751 | 6.886 | 0.079 | 2.207 | 36.290 |
| 35 | 190 | 271 | 0.05714 | 0.94286 | 0.00881 | 6.885 | 0.081 | 2.201 | 36.322 |
| 40 | 190 | 275 | 0.05698 | 0.94302 | 0.00985 | 6.885 | 0.082 | 2.196 | 36.348 |
| 45 | 190 | 279 | 0.05682 | 0.94318 | 0.01090 | 6.885 | 0.083 | 2.191 | 36.374 |
| 50 | 190 | 284 | 0.05662 | 0.94338 | 0.01222 | 6.884 | 0.085 | 2.185 | 36.406 |
| 55 | 190 | 288 | 0.05646 | 0.94354 | 0.01328 | 6.884 | 0.086 | 2.180 | 36.433 |
| 60 | 190 | 292 | 0.05630 | 0.94370 | 0.01435 | 6.884 | 0.088 | 2.175 | 36.459 |
| 65 | 190 | 297 | 0.05610 | 0.94390 | 0.01568 | 6.884 | 0.089 | 2.169 | 36.492 |
| 70 | 190 | 300 | 0.05598 | 0.94402 | 0.01649 | 6.883 | 0.090 | 2.165 | 36.512 |
| 75 | 190 | 304 | 0.05582 | 0.94418 | 0.01757 | 6.883 | 0.092 | 2.160 | 36.539 |
| 80 | 190 | 308 | 0.05565 | 0.94435 | 0.01865 | 6.883 | 0.093 | 2.155 | 36.566 |
| 85 | 190 | 311 | 0.05553 | 0.94447 | 0.01947 | 6.883 | 0.094 | 2.151 | 36.586 |
| 90 | 190 | 315 | 0.05537 | 0.94463 | 0.02056 | 6.882 | 0.095 | 2.146 | 36.613 |
| 95 | 190 | 319 | 0.05520 | 0.94480 | 0.02163 | 6.882 | 0.097 | 2.141 | 36.641 |
| 100 | 190 | 322 | 0.05508 | 0.94492 | 0.02248 | 6.882 | 0.098 | 2.137 | 36.661 |
| 105 | 192 | 329 | 0.05518 | 0.94482 | 0.02166 | 6.880 | 0.099 | 2.132 | 36.501 |
| 110 | 190 | 327 | 0.05487 | 0.94513 | 0.02386 | 6.882 | 0.100 | 2.130 | 36.696 |
| 115 | 189.5 | 327 | 0.05477 | 0.94523 | 0.02455 | 6.882 | 0.100 | 2.129 | 36.748 |
| 120 | 189.5 | 329 | 0.05469 | 0.94531 | 0.02510 | 6.882 | 0.100 | 2.127 | 36.762 |
| 125 | 190 | 332 | 0.05466 | 0.94534 | 0.02525 | 6.881 | 0.101 | 2.124 | 36.731 |
| 130 | 190 | 335 | 0.05454 | 0.94546 | 0.02608 | 6.881 | 0.102 | 2.120 | 36.752 |
| 135 | 190 | 337 | 0.05445 | 0.94555 | 0.02664 | 6.881 | 0.103 | 2.117 | 36.766 |
| 140 | 189.5 | 336 | 0.05439 | 0.94561 | 0.02706 | 6.881 | 0.103 | 2.117 | 36.811 |
| 145 | 190 | 338 | 0.05441 | 0.94559 | 0.02692 | 6.881 | 0.103 | 2.116 | 36.773 |
| 150 | 190 | 339 | 0.05437 | 0.94563 | 0.02720 | 6.881 | 0.104 | 2.115 | 36.780 |

## Table A2.16 – Concentration Dependence Raw Data: 4 mol % Initial 2-Propanol/Water Concentration in the Feed at 463 K

| | | | | | | |
|---|---|---|---|---|---|---|
| T avg | 189.98°C | $x_a^0$ | 0.039 | $M_h,^0$ | 0.00431 moles |
| | 463.13K | $M_a,^0$ | 17.113g | cat | 2.178g |
| | | $M_w,^0$ | 126.38g | | |

| time (min) | T (°C) | P (psig) | $x_A$ | $x_W$ | α (moles) | L (moles) | V (moles) | $C_A$ (moles/L) | $C_W$ (moles/L) |
|---|---|---|---|---|---|---|---|---|---|
| 0 | 190 | 209 | 0.03803 | 0.96197 | -0.00041 | 7.240 | 0.064 | 1.568 | 39.675 |
| 5 | 190 | 215 | 0.03781 | 0.96219 | 0.00115 | 7.240 | 0.065 | 1.561 | 39.716 |
| 10 | 190 | 216 | 0.03777 | 0.96223 | 0.00141 | 7.240 | 0.066 | 1.559 | 39.723 |
| 15 | 189.5 | 219 | 0.03759 | 0.96241 | 0.00276 | 7.240 | 0.067 | 1.554 | 39.792 |
| 20 | 190 | 223 | 0.03752 | 0.96248 | 0.00324 | 7.240 | 0.068 | 1.550 | 39.771 |
| 25 | 190 | 225 | 0.03744 | 0.96256 | 0.00377 | 7.239 | 0.069 | 1.548 | 39.785 |
| 30 | 190 | 228 | 0.03733 | 0.96267 | 0.00456 | 7.239 | 0.070 | 1.544 | 39.806 |
| 35 | 190 | 232 | 0.03718 | 0.96282 | 0.00562 | 7.239 | 0.071 | 1.538 | 39.834 |
| 40 | 190 | 234 | 0.03711 | 0.96289 | 0.00616 | 7.239 | 0.071 | 1.536 | 39.848 |
| 45 | 190 | 237 | 0.03700 | 0.96300 | 0.00696 | 7.239 | 0.072 | 1.532 | 39.869 |
| 50 | 190 | 240 | 0.03689 | 0.96311 | 0.00776 | 7.239 | 0.073 | 1.528 | 39.890 |
| 55 | 190 | 242 | 0.03681 | 0.96319 | 0.00829 | 7.239 | 0.074 | 1.525 | 39.905 |
| 60 | 190 | 245 | 0.03670 | 0.96330 | 0.00910 | 7.238 | 0.075 | 1.521 | 39.926 |
| 65 | 190 | 247 | 0.03662 | 0.96338 | 0.00964 | 7.238 | 0.076 | 1.518 | 39.940 |
| 70 | 190 | 249 | 0.03655 | 0.96345 | 0.01018 | 7.238 | 0.076 | 1.516 | 39.955 |
| 75 | 190 | 251 | 0.03647 | 0.96353 | 0.01072 | 7.238 | 0.077 | 1.513 | 39.969 |
| 80 | 190 | 253 | 0.03640 | 0.96360 | 0.01126 | 7.238 | 0.078 | 1.510 | 39.983 |
| 85 | 190 | 255 | 0.03632 | 0.96368 | 0.01181 | 7.238 | 0.078 | 1.507 | 39.998 |
| 90 | 190 | 256 | 0.03628 | 0.96372 | 0.01208 | 7.238 | 0.079 | 1.506 | 40.005 |
| 95 | 190 | 257 | 0.03624 | 0.96376 | 0.01235 | 7.238 | 0.079 | 1.505 | 40.012 |
| 100 | 190 | 259 | 0.03617 | 0.96383 | 0.01290 | 7.238 | 0.080 | 1.502 | 40.027 |
| 105 | 190 | 260 | 0.03613 | 0.96387 | 0.01317 | 7.238 | 0.080 | 1.501 | 40.034 |
| 110 | 190 | 261 | 0.03609 | 0.96391 | 0.01344 | 7.237 | 0.080 | 1.499 | 40.041 |
| 115 | 190 | 262 | 0.03605 | 0.96395 | 0.01372 | 7.237 | 0.081 | 1.498 | 40.049 |
| 120 | 190 | 263 | 0.03601 | 0.96399 | 0.01399 | 7.237 | 0.081 | 1.496 | 40.056 |
| 125 | 190 | 263.5 | 0.03600 | 0.96400 | 0.01413 | 7.237 | 0.081 | 1.496 | 40.060 |
| 130 | 190 | 263 | 0.03601 | 0.96399 | 0.01399 | 7.237 | 0.081 | 1.496 | 40.056 |
| 135 | 190 | 264 | 0.03598 | 0.96402 | 0.01427 | 7.237 | 0.081 | 1.495 | 40.063 |
| 140 | 190 | 264 | 0.03598 | 0.96402 | 0.01427 | 7.237 | 0.081 | 1.495 | 40.063 |
| 145 | 190 | 264.5 | 0.03596 | 0.96404 | 0.01440 | 7.237 | 0.081 | 1.494 | 40.067 |
| 150 | 190 | 265 | 0.03594 | 0.96406 | 0.01454 | 7.237 | 0.082 | 1.494 | 40.071 |

## Table A2.17 — Catalyst Reusability Raw Data: Used Catalyst at 463 K

T  190°C  xa$^0$  0.1026  Mh,$^°$  0.009 moles
   463.2K  Ma,$^°$  38.149g  cat  1.825g
        Mw,$^°$  100.07g

| time (min) | T (°C) | P (psig) | $x_A$ | $x_W$ | α (moles) | L (moles) | V (moles) | $C_A$ (moles/L) | $C_W$ (moles/L) |
|---|---|---|---|---|---|---|---|---|---|
| 0 | 190 | 274 | 0.10002 | 0.89998 | 0.00005 | 6.120 | 0.079 | 3.356 | 30.199 |
| 5 | 190 | 282 | 0.09967 | 0.90033 | 0.00202 | 6.119 | 0.082 | 3.348 | 30.242 |
| 10 | 190.5 | 289 | 0.09947 | 0.90053 | 0.00311 | 6.118 | 0.084 | 3.339 | 30.232 |
| 15 | 190 | 291 | 0.09928 | 0.90072 | 0.00425 | 6.118 | 0.085 | 3.339 | 30.291 |
| 20 | 190 | 296 | 0.09906 | 0.90094 | 0.00550 | 6.118 | 0.086 | 3.334 | 30.319 |
| 25 | 189.5 | 300 | 0.09878 | 0.90122 | 0.00716 | 6.118 | 0.088 | 3.331 | 30.390 |
| 30 | 190 | 309 | 0.09848 | 0.90152 | 0.00878 | 6.117 | 0.091 | 3.320 | 30.392 |
| 35 | 190 | 314 | 0.09825 | 0.90175 | 0.01006 | 6.116 | 0.092 | 3.315 | 30.420 |
| 40 | 190 | 320 | 0.09798 | 0.90202 | 0.01159 | 6.116 | 0.094 | 3.308 | 30.454 |
| 45 | 190 | 326 | 0.09771 | 0.90229 | 0.01314 | 6.116 | 0.096 | 3.302 | 30.489 |
| 50 | 190 | 332 | 0.09743 | 0.90257 | 0.01470 | 6.115 | 0.098 | 3.295 | 30.523 |
| 55 | 190 | 339 | 0.09711 | 0.90289 | 0.01654 | 6.114 | 0.101 | 3.287 | 30.564 |
| 60 | 190 | 346 | 0.09678 | 0.90322 | 0.01838 | 6.114 | 0.103 | 3.279 | 30.606 |
| 65 | 190.5 | 355 | 0.09648 | 0.90352 | 0.02005 | 6.113 | 0.106 | 3.268 | 30.609 |
| 70 | 190 | 360 | 0.09612 | 0.90388 | 0.02212 | 6.113 | 0.108 | 3.264 | 30.690 |
| 75 | 189.5 | 365 | 0.09576 | 0.90424 | 0.02422 | 6.113 | 0.110 | 3.259 | 30.771 |
| 80 | 189 | 370 | 0.09540 | 0.90460 | 0.02634 | 6.113 | 0.112 | 3.254 | 30.852 |
| 85 | 189.5 | 378 | 0.09513 | 0.90487 | 0.02779 | 6.112 | 0.115 | 3.244 | 30.852 |
| 90 | 189 | 383 | 0.09476 | 0.90524 | 0.02995 | 6.112 | 0.117 | 3.238 | 30.934 |
| 95 | 190 | 391 | 0.09462 | 0.90538 | 0.03062 | 6.110 | 0.119 | 3.227 | 30.882 |
| 100 | 191 | 402 | 0.09433 | 0.90567 | 0.03211 | 6.108 | 0.123 | 3.213 | 30.848 |
| 105 | 191 | 407 | 0.09408 | 0.90592 | 0.03351 | 6.108 | 0.125 | 3.207 | 30.880 |
| 110 | 190.5 | 413 | 0.09365 | 0.90635 | 0.03603 | 6.108 | 0.127 | 3.200 | 30.971 |
| 115 | 190.5 | 419 | 0.09334 | 0.90666 | 0.03774 | 6.107 | 0.129 | 3.193 | 31.011 |
| 120 | 190 | 424 | 0.09295 | 0.90705 | 0.04002 | 6.107 | 0.132 | 3.187 | 31.097 |
| 125 | 190 | 428 | 0.09275 | 0.90725 | 0.04119 | 6.107 | 0.133 | 3.182 | 31.124 |
| 130 | 190 | 433 | 0.09249 | 0.90751 | 0.04265 | 6.106 | 0.135 | 3.175 | 31.157 |
| 135 | 190.5 | 436 | 0.09247 | 0.90753 | 0.04268 | 6.106 | 0.136 | 3.171 | 31.124 |
| 140 | 190 | 437 | 0.09228 | 0.90772 | 0.04383 | 6.106 | 0.137 | 3.170 | 31.185 |
| 145 | 189 | 436 | 0.09206 | 0.90794 | 0.04526 | 6.107 | 0.137 | 3.172 | 31.285 |
| 150 | 190 | 443 | 0.09197 | 0.90803 | 0.04561 | 6.105 | 0.139 | 3.163 | 31.226 |

## Table A2.18 – Catalyst Loading Raw Data: 0.762 wt %

| T | 189.95°C | Ma,° | 38.128g | cat | 1.053g |
|---|----------|------|---------|-----|--------|
|   | 463.10K  | Mw,° | 100.09g | Mh,° | 0.00807 moles |

| time (min) | T (°C) | P (psig) | $x_A$ | $x_W$ | α (moles) | L (moles) | V (moles) | $C_A$ (moles/L) | $C_W$ (moles/L) |
|---|---|---|---|---|---|---|---|---|---|
| 0 | 189 | 263 | 0.09990 | 0.90010 | 0.00051 | 6.121 | 0.078 | 3.361 | 30.285 |
| 5 | 189 | 268 | 0.09968 | 0.90032 | 0.00174 | 6.121 | 0.079 | 3.356 | 30.312 |
| 10 | 190 | 275 | 0.09958 | 0.90042 | 0.00223 | 6.120 | 0.081 | 3.346 | 30.254 |
| 15 | 189.5 | 275 | 0.09948 | 0.90052 | 0.00285 | 6.120 | 0.081 | 3.339 | 30.231 |
| 20 | 190 | 278 | 0.09944 | 0.90056 | 0.00297 | 6.119 | 0.082 | 3.339 | 30.235 |
| 25 | 190 | 281 | 0.09931 | 0.90069 | 0.00371 | 6.119 | 0.083 | 3.340 | 30.287 |
| 30 | 190 | 283 | 0.09923 | 0.90077 | 0.00421 | 6.119 | 0.084 | 3.338 | 30.298 |
| 35 | 190 | 285 | 0.09914 | 0.90086 | 0.00471 | 6.119 | 0.084 | 3.335 | 30.309 |
| 40 | 190 | 288 | 0.09900 | 0.90100 | 0.00546 | 6.119 | 0.085 | 3.332 | 30.326 |
| 45 | 190 | 291 | 0.09887 | 0.90113 | 0.00621 | 6.118 | 0.086 | 3.329 | 30.342 |
| 50 | 190 | 293 | 0.09878 | 0.90122 | 0.00672 | 6.118 | 0.087 | 3.327 | 30.354 |
| 55 | 190 | 296 | 0.09865 | 0.90135 | 0.00747 | 6.118 | 0.088 | 3.324 | 30.370 |
| 60 | 190 | 299 | 0.09852 | 0.90148 | 0.00823 | 6.118 | 0.089 | 3.321 | 30.387 |
| 65 | 190 | 302 | 0.09838 | 0.90162 | 0.00899 | 6.117 | 0.090 | 3.318 | 30.404 |
| 70 | 190 | 305 | 0.09825 | 0.90175 | 0.00976 | 6.117 | 0.091 | 3.314 | 30.421 |
| 75 | 190 | 308 | 0.09811 | 0.90189 | 0.01052 | 6.117 | 0.092 | 3.311 | 30.438 |
| 80 | 190 | 311 | 0.09797 | 0.90203 | 0.01129 | 6.117 | 0.093 | 3.308 | 30.455 |
| 85 | 190.5 | 315 | 0.09790 | 0.90210 | 0.01164 | 6.116 | 0.094 | 3.302 | 30.429 |
| 90 | 190.5 | 317 | 0.09781 | 0.90219 | 0.01216 | 6.116 | 0.095 | 3.300 | 30.440 |
| 95 | 190 | 319 | 0.09761 | 0.90239 | 0.01336 | 6.116 | 0.096 | 3.299 | 30.501 |
| 100 | 190 | 322 | 0.09747 | 0.90253 | 0.01414 | 6.116 | 0.097 | 3.296 | 30.518 |
| 105 | 190 | 324 | 0.09738 | 0.90262 | 0.01466 | 6.116 | 0.097 | 3.294 | 30.530 |
| 110 | 190 | 327 | 0.09724 | 0.90276 | 0.01544 | 6.115 | 0.098 | 3.290 | 30.548 |
| 115 | 190 | 329 | 0.09715 | 0.90285 | 0.01596 | 6.115 | 0.099 | 3.288 | 30.559 |
| 120 | 190 | 332 | 0.09701 | 0.90299 | 0.01675 | 6.115 | 0.100 | 3.285 | 30.577 |
| 125 | 190 | 334 | 0.09692 | 0.90308 | 0.01728 | 6.115 | 0.101 | 3.283 | 30.589 |
| 130 | 190 | 337 | 0.09678 | 0.90322 | 0.01807 | 6.115 | 0.102 | 3.279 | 30.606 |
| 135 | 190 | 340 | 0.09664 | 0.90336 | 0.01887 | 6.114 | 0.103 | 3.276 | 30.624 |
| 140 | 190 | 343 | 0.09650 | 0.90350 | 0.01966 | 6.114 | 0.104 | 3.273 | 30.642 |
| 145 | 190 | 346 | 0.09635 | 0.90365 | 0.02046 | 6.114 | 0.105 | 3.269 | 30.660 |
| 150 | 190 | 349 | 0.09621 | 0.90379 | 0.02127 | 6.114 | 0.106 | 3.266 | 30.678 |

### Table A2.19 - Catalyst Loading Raw Data: 1.106 wt %

T      190.06°C    $Ma,^o$    38.153g    cat    1.106g
       463.21K    $Mw,^o$    100.58g    $Mh,^o$    0.00804moles

| time (min) | T (°C) | P (psig) | $x_A$ | $x_W$ | α (moles) | L (moles) | V (moles) | $C_A$ (moles/L) | $C_W$ (moles/L) |
|---|---|---|---|---|---|---|---|---|---|
| 0 | 189 | 265 | 0.09945 | 0.90055 | 0.00103 | 6.149 | 0.078 | 3.351 | 30.341 |
| 5 | 191 | 281 | 0.09915 | 0.90085 | 0.00247 | 6.146 | 0.082 | 3.328 | 30.236 |
| 10 | 191 | 283 | 0.09907 | 0.90093 | 0.00296 | 6.146 | 0.083 | 3.326 | 30.247 |
| 15 | 190.5 | 285 | 0.09888 | 0.90112 | 0.00408 | 6.147 | 0.084 | 3.325 | 30.306 |
| 20 | 190.5 | 290 | 0.09866 | 0.90134 | 0.00532 | 6.146 | 0.085 | 3.320 | 30.333 |
| 25 | 190 | 294 | 0.09838 | 0.90162 | 0.00697 | 6.146 | 0.087 | 3.318 | 30.404 |
| 30 | 190 | 298 | 0.09821 | 0.90179 | 0.00798 | 6.146 | 0.088 | 3.313 | 30.426 |
| 35 | 190 | 302 | 0.09803 | 0.90197 | 0.00899 | 6.146 | 0.090 | 3.309 | 30.448 |
| 40 | 190 | 306 | 0.09785 | 0.90215 | 0.01000 | 6.145 | 0.091 | 3.305 | 30.471 |
| 45 | 189.5 | 310 | 0.09756 | 0.90244 | 0.01169 | 6.145 | 0.092 | 3.294 | 30.471 |
| 50 | 190 | 315 | 0.09745 | 0.90255 | 0.01230 | 6.145 | 0.094 | 3.295 | 30.522 |
| 55 | 190 | 320 | 0.09722 | 0.90278 | 0.01359 | 6.144 | 0.096 | 3.290 | 30.550 |
| 60 | 190 | 325 | 0.09699 | 0.90301 | 0.01488 | 6.144 | 0.097 | 3.284 | 30.579 |
| 65 | 190.5 | 330 | 0.09687 | 0.90313 | 0.01549 | 6.143 | 0.099 | 3.278 | 30.559 |
| 70 | 190 | 335 | 0.09653 | 0.90347 | 0.01749 | 6.143 | 0.101 | 3.273 | 30.638 |
| 75 | 190 | 339 | 0.09635 | 0.90365 | 0.01855 | 6.143 | 0.102 | 3.269 | 30.661 |
| 80 | 190 | 343 | 0.09616 | 0.90384 | 0.01961 | 6.142 | 0.103 | 3.265 | 30.685 |
| 85 | 190 | 348 | 0.09593 | 0.90407 | 0.02093 | 6.142 | 0.105 | 3.259 | 30.715 |
| 90 | 190 | 353 | 0.09569 | 0.90431 | 0.02227 | 6.141 | 0.107 | 3.253 | 30.745 |
| 95 | 190 | 357 | 0.09550 | 0.90450 | 0.02335 | 6.141 | 0.108 | 3.249 | 30.769 |
| 100 | 190 | 361 | 0.09531 | 0.90469 | 0.02444 | 6.141 | 0.110 | 3.244 | 30.793 |
| 105 | 190 | 365 | 0.09512 | 0.90488 | 0.02551 | 6.140 | 0.111 | 3.240 | 30.817 |
| 110 | 190 | 370 | 0.09488 | 0.90512 | 0.02687 | 6.140 | 0.113 | 3.234 | 30.848 |
| 115 | 190 | 375 | 0.09464 | 0.90536 | 0.02824 | 6.140 | 0.115 | 3.228 | 30.879 |
| 120 | 190 | 379 | 0.09445 | 0.90555 | 0.02935 | 6.139 | 0.116 | 3.223 | 30.904 |
| 125 | 190 | 383 | 0.09425 | 0.90575 | 0.03045 | 6.139 | 0.118 | 3.218 | 30.929 |
| 130 | 190 | 387 | 0.09405 | 0.90595 | 0.03157 | 6.139 | 0.119 | 3.214 | 30.955 |
| 135 | 190 | 391 | 0.09386 | 0.90614 | 0.03269 | 6.138 | 0.121 | 3.209 | 30.980 |
| 140 | 190 | 395 | 0.09366 | 0.90634 | 0.03381 | 6.138 | 0.122 | 3.204 | 31.006 |
| 145 | 190 | 399 | 0.09346 | 0.90654 | 0.03494 | 6.137 | 0.124 | 3.199 | 31.031 |
| 150 | 190 | 402 | 0.09331 | 0.90669 | 0.03579 | 6.137 | 0.125 | 3.196 | 31.051 |